Markus Grimming, Dipl.-Ing. BSc

Displacement analysis in tunnels in terms of dry and undrained conditions

Master's Thesis

Submitted in fulfilment of the requirements for the degree of

Diplom-Ingenieur

Master's programme Civil Engineering, Geotechnics and Hydraulics

at

Graz University of Technology

Supervisor

O.Univ.-Prof. Dipl.-Ing. Dr.mont. Wulf Schubert

Institute of Rock Mechanics and Tunnelling

Graz University of Technology

Additional Supervisor

Dipl.-Ing. Gerold Lenz

Graz, Juni 2018

Eidesstattliche Erklärung

Affidavit

Ich erkläre an Eides statt, dass ich die vorliegende Arbeit selbstständig verfasst, andere als die angegebenen Quellen/Hilfsmittel nicht benutzt, und die den benutzten Quellen wörtlich und inhaltlich entnommenen Stellen als solche kenntlich gemacht habe. Das in TUGRAZonline hochgeladene Textdokument ist mit der vorliegenden Masterarbeit identisch.

I declare that I have authored this thesis independently, that I have not used other than the declared sources/resources, and that I have explicitly marked all material which has been quoted either literally or by content from the used sources. The text document uploaded to TUGRAZonline is identical to the present master‘s thesis.

Datum / Date

Unterschrift / Signature

Acknowledgment

Lots of thanks to Professor Wulf Schubert for enabling me to write this master's thesis at the Institute of Rock Mechanics and Tunnelling. He referred me to Dipl.-Ing. Gerold Lenz, my immediate supervisor. Gerold, I am deeply grateful for your help and support during the last few months. Your practical on-site experience made assessments much easier. Furthermore, a huge thank-you to Dipl.-Ing. Alexander Kluckner for essential numerical inputs. Sincere thanks to Dipl.-Ing. Michael Henzinger for teaching me the basics of the software in the early stage of the thesis. I really appreciate the excellent environment of the "Beton- und Holzbau Zeichensaal" - I spent five years of my life in such a great community and do not regret one single day - you guys are marvelous and I will attempt to participate our "Veteranenbier-abend" every year. Thanks to all friends I have met during my studies. According to the saying "No money, no music" - thanks to site manager Dipl.-Ing. Markus Prumetz for giving me the opportunity to time my work flexibly. Last, but most important, cordial thanks to my entire family and my girlfriend for respecting, understanding and loving me. To them I dedicate this thesis.

Abstract

Pore water pressure changes the ground behaviour significantly. This thesis aims to investigate the impact of pore water pressure on the displacement development in tunnels due to excavation. Analytical and numerical analysis in terms of dry and undrained ground conditions are performed to show differences in radial displacements referred to the procedure proposed by Vlachopoulos & Diederichs (2009). Based on a deep, circular tunnel with homogeneous ground conditions, the Mohr-Coulomb failure criterion is applied. Without considering time, the undrained analysis leads to smaller radial displacements but ends up with a increased plastic radius compared to dry ground conditions. Longitudinal Displacement Profiles (LDP) of dry and undrained analysis clearly verify the differences in radial displacements. Furthermore, the stiffness of the undrained rock mass may impacts the depth of plastic zone around the tunnel significantly.

Kurzfassung

Das mechanische Verhalten von Fels wird vom Porenwasserdruck stark beeinflusst. Ziel dieser Masterarbeit ist es, den Einfluss des Porenwasserdrucks auf die Entwicklung der Tunnelverschiebungen während des Ausbruches zu untersuchen. Dazu werden analytische und numerische Berechnungen durchgeführt. Das Radialverschiebungsverhalten wird jeweils im trockenen und undränierten Fels bestimmt und mit dem Verfahren nach Vlachopoulos & Diederichs (2009) verglichen. Dazu wird ein tiefliegender, runder Tunnel im homogenen, isotropen Gebirge nach dem Mohr-Coulomb Bruchkriterium untersucht. Zeitliche Einflüsse werden nicht berücksichtigt. Im undränierten Gebirge kommt es einerseits zu höheren Verschiebungen und andererseits ist der undränierte plastische Radius höher, verglichen zu trockenen Bedingungen. Die Radialverschiebungsverteilung in Tunnellängsrichtung (LDP) zeigt das unterschiedliche Verschiebungsverhalten sehr gut. Außerdem kann die Steifigkeit des undränierten Gebirges die plastische Zone um den Tunnel stark beeinflussen.

Contents

List of Figures

List of Tables

Abbreviations

CCM	.....	Convergence confinement method
GCC	.....	Ground characteristic curve
SCC	.....	Support characteristic curve
LDP	.....	Longitudinal displacement curve
p_{crit}	.....	Critical support pressure
r_t	.....	Tunnel radius
r_{pl}	.....	Plastic radius
u_0	.....	Face displacement
u_{max}	.....	Maximal displacement
D	.....	Tunnel diameter
E	.....	Young's Modulus

1 Introduction

In tunneling water has a major impact on the rock mass behaviour. To which extent the pore water pressure affects the displacements due to tunnel excavation, is investigated in this thesis. The Convergence Confinement Method (CCM), a conventional established approach to assume the rock mass behaviour, does not consider water. Therefore a comparable analytical and numerical study is done in this thesis.

1.1 Aim of work

The main goal of this thesis is to study the undrained ground behaviour and show the differences in radial displacements compared to dry ground behaviour. Numerical methods are used for analysis. Influence of time dependent behaviour is neglected for sake of simplicity. Furthermore, a comparison of the undrained results with analytical closed-form solutions is done - especially by applying the relationship proposed by Vlachopoulos & Diederichs (2009).

1.2 Methodology

First of all the analytical solutions in displacements with approaches according to Sulem et al. (1987), Anagnostou (2009) and Vlachopoulos & Diederichs (2009) are calculated in a spread sheet. Several parameter sets were defined, varying tunnel radius, rock mass parameters and stress level. Further on, two numerical models are established using the software $FLAC^{3D}$ (Itasca, 2016) to model the short-term behaviour; one for dry conditions and the other one for fully saturated and undrained conditions. The models are checked for plausibility in respect to stress and deformation with the analytical solutions. Subsequently, all calculations for the previous defined input parameter sets were done. The final step contains the analysis and interpretation of the results between dry and undrained ground conditions.

2 Effects of groundwater in tunneling

2.1 General

Dealing with groundwater in tunneling is complex and multifaceted. During tunnel excavation through water-bearing ground, seepage flow towards the opening occurs. The pressure at the excavation boundary is atmospheric in general and for this reason drainage through the tunnel is provided. This leads to a draw-down of the water-level close to the tunnel and therefore to a consolidation-process of the ground.
Concerning the mechanical action, water can affect the deformations and the stability of the tunnel by changing the effective stress and consequently the shearing resistance. According to Anagnostou (2006): "The interactions between seepage flow and equilibrium, porewater pressure and stress field around a tunnel constitute perhaps the most important coupled process in geotechnical engineering."

2.2 Principal of effective stresses

Pore water pressure can essentially affect the behaviour of the rock mass. According to the theory of Terzaghi (1936) all measurable effects of changes in stress can be ascribed to changes in effective stress[1]. Deformation can occur if total stresses remain constant and the pore water pressure is changing. The mentioned theory is based on fundamental knowledge in soil mechanics and results are confirmed due to lab tests and field observations (e.g. Vogelhuber, 2007).

[1] *Terzaghi* explains the principal as follow: "All the measurable effects of a change of stress, such as compression, distortion and a change of shearing resistance, are exclusively due to changes in the effective stresses."

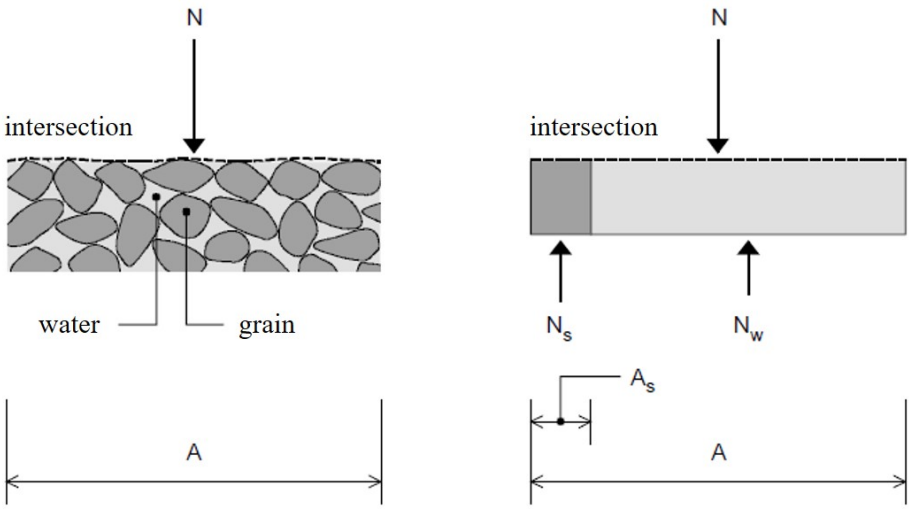

with:

N	Normal force	$[MN]$
N_s	Related strength of grains	$[MN]$
N_w	Related strength of water	$[MN]$
A	Total area	$[m^2]$
A_s	Related area of grains	$[m^2]$

Figure 2.1: Microscopic consideration of effective normal stress (modified after Vogelhuber, 2007).

In everyday language effective stresses are known as grain pressure (German: "Korn zu Korn Spannung"). By expressing equilibrium related to the intersection of figure 2.1, effective stress under consideration of the pore water pressure p can be written as (Vogelhuber, 2007):

$$\sigma^* = \sigma - p \times \left\{1 - \frac{A_s}{A}\right\} \tag{2.1}$$

with:

σ^*	Effective stress	$[MPa]$
σ	Total stress	$[MPa]$
A_s	Related area of grains	$[m^2]$
A	Total area	$[m^2]$
p	Pore water pressure	$[MPa]$

Generally, the rock substance (A_s) takes a small part related to the total area A. Therefore, grain contact in selective points is assumed ($A_s/A = 0$) and leads to the following formula:

$$\sigma^* = \sigma - p \tag{2.2}$$

This theory assumes a high stiffness of water and grains compared to the total matrix. Due to lab tests in rock mechanics, deviations from the theory of Terzaghi (1936) were noticed. For this reason further research was done by e.g. Biot (1941), Skempton (1954) and others. They observed that the compressibility of water and grains has an impact on the effective stress. Therefore Biot (1941) defined the effective stress as equation 2.3 with Biot's coefficient β, which considers the ratio in compressibility of water and dry rock. (Alam et al., 2010)

$$\sigma^* = \sigma - \beta p \tag{2.3}$$

2.3 Change in stress and pore pressure

Due to problems in the design of earth dams concerning the undrained shear strength of soils, it is common to check the change in pore pressure Δu. This occurs by changing the principal stresses $\Delta\sigma_1$ and $\Delta\sigma_3$ in combination with pore pressure coefficients A and B, by equation 2.4 according to Skempton (1954).

$$\Delta u = B \times [\Delta\sigma_3 + A \times (\Delta\sigma_1 - \Delta\sigma_3)] \tag{2.4}$$

The coefficients A and B are measured in the undrained triaxial test, whereby A is determined experimentally and depends on the volume change of the ground due to shearing loads. Generally, the change in pore pressure can be expressed as equation 2.5.

$$\Delta u = B \times \Delta\sigma \tag{2.5}$$

Basically the coefficient B depends on the porosity and the relationship in compression between water and the grains of the ground (see equation 2.6). The conversion between the Young's modulus E and the Compression modulus C is described in equation 2.7.

$$B = \frac{1}{1 + \frac{n \times C}{C_w}} \tag{2.6}$$

with: B Pore pressure coefficient B $[-]$
n Porosity $[-]$
C Bulk modulus of the ground $[MPa]$
C_w Bulk modulus of water $[\sim 2e6\ MPa\, at\ 20°C]$

$$C = \frac{E}{3 \times (1 - 2\nu)} \tag{2.7}$$

with: C Bulk modulus $[MPa]$
E Young's modulus $[MPa]$
ν Poisson's ratio $[-]$

For saturated soils it is assumed that the compressibility of water is negligible compared to the soil structures. Therefore the compressibility of the grains is neglected. Consequently the pore pressure coefficient B is assumed as $B = 1$ (Skempton, 1954). However, the compressibility of the solid grains is not neglected for rocks. Thus the pore pressure coefficient B can deceed the value of 1. If the compressibilities of the solid grains and the rock mass are equal, any influence of pore water pressure disappears. Therefore, in terms of small porosity in an extreme case only the total stresses may remain equal to effective stresses. (e.g. Vogelhuber, 2007)

2.4 Pore water pressure in squeezing rock

In zones of cohesive materials with low strength and large deformability, tunnel engineering is faced with new challenges. In tunneling such grounds are characterized as "squeezing rock". According to Radoncic (2011) "squeezing" is used to describe such ground conditions, when the secondary stresses are much higher than the ground strength. Common suggestions are the "critical strength ratio" and the notation of a "critical strain" to verify "squeezing conditions". Detailed explanations can found in the doctoral thesis of Radoncic (2011). Normally, squeezing develops slowly and therefore the deforming process takes place over a long period of time. Somewhere from a couple of days to months. Regarding the mechanism of deformation development during tunneling, three forms can be traced back (Anagnostou, 2006):

a) Redistribution of stresses around the working face in 3D. With this mechanism long-term rock deformations cannot be explained, because it occurs close to the tunnel face.

b) Rheological properties of the ground like "creep" for instance. Creeping is evident in highly stressed rock as the failure state approaches.

c) Tunnel excavation triggers a transient seepage flow in saturated rock. Therefore, the pore water pressure and subsequently the effective stresses are changing with time. The more impermeable the rock, the slower will the process occur and the time dependent deformation becomes more important.

In reality these mechanisms interfere with each other. For better understanding and a rough separation of the mechanisms, Anagnostou (2009) differs between short- and long-term behaviour in his research. Figure 2.2 shows the Ground Characteristic Curve GCC (also Ground Reaction Curve GRC) of a short-term behaviour at time $t = 0$ and the long-term behaviour at $t = \infty$. The present thesis focuses on the short-term behaviour.

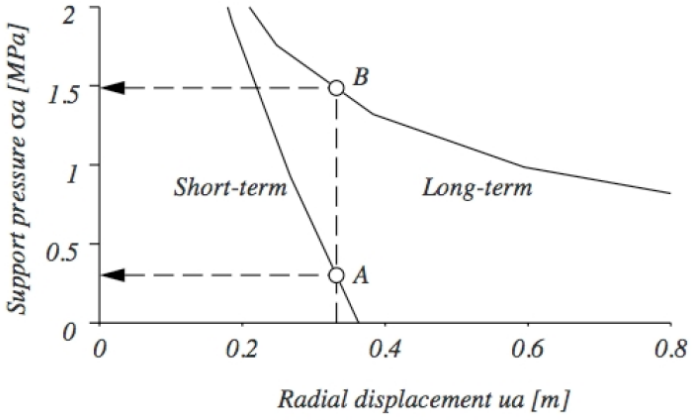

Figure 2.2: Ground Characteristic Curve GCC of short- and long-term behavior (Anagnostou, 2006).

2.5 Short term behaviour

The short-term behaviour represents the performance of the rock mass in the vicinity of the tunnel face during excavation. Considerable support may be required close to the working face to stabilize the ground (Anagnostou, 2009). The impact of pre-consolidation is not con-

sidered in the thesis at hand, as it is targeting the ground behaviour without any support or drainage measures.

The closed-form solution for the short-term behaviour of undrained ground is derived from the Ground Characteristic Curve GCC. It is assumed that the saturated ground is incompressible, which means that no volumetric strains are allowed. For modeling the short-term behaviour either the ground is considered as a single phase frictionless medium (friction angle $\phi = 0$) by analyzing in total stresses, or considered as a saturated, porous medium analyzing the effective stresses. An analysis with total stresses is simpler, but does not take into account the pore pressure distribution (Anagnostou, 2009). For this reason, this thesis deals only with effective stress analysis.

The increase of pore volume in a ground with low permeability can not happen immediately. As a consequence, negative pore pressures start to develop, occurring only in the plastic zone. The pore pressure in the surrounding elastic zone remains equal to the initial pore pressure p_0. Thus, the solution according to *Kirsch* is valid by replacing the total stresses with the effective stresses (formula 2.8) (Anagnostou, 2009).

$$u_p = \frac{1+\nu}{E} \times p \times (\sigma_0^{'} - \sigma_p^{'}) \tag{2.8}$$

with:

p	Certain radius of interest in the elastic zone $\left[m\right]$
u_p	Displacement at $r(p) = p$ in the elastic zone $\left[m\right]$
ν	Poisson's ratio $\left[-\right]$
E	Young's modulus $\left[MPa\right]$
$\sigma_0^{'}$	Initial effective stress $\left[MPa\right]$
$\sigma_p^{'}$	Initial effective stress at $r(p) = p$ $\left[MPa\right]$

The elastic and plastic volumetric strains in the plastic zone are zero. By considering the classic plain-strain problem of a deep, rotationally symmetric and circular tunnel, figure 2.3 shows the development of total and effective stresses and the pore pressure around the tunnel.

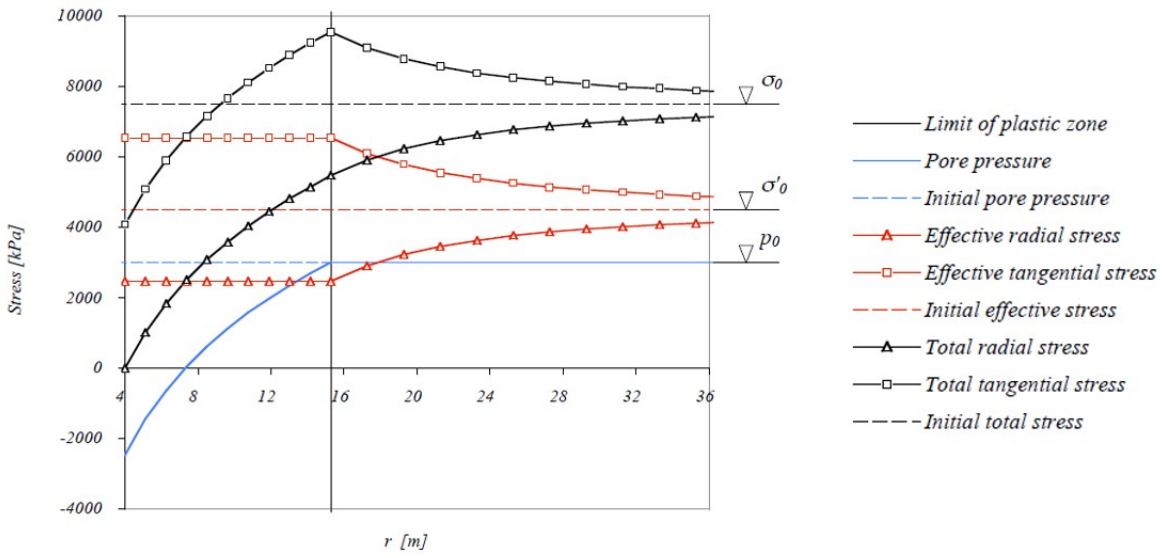

Figure 2.3: Short-term distribution of pore pressure p_0, total and effective stresses of the ground (Anagnostou, 2009).

According to the research work of *Anagnostou* the expression for the radial plastic displacements can be written as formula 2.9. The entire derivation of the formula can be found in the original paper of Anagnostou (2009).

$$\frac{u_a}{a} = \frac{1+\nu}{E} \times s_u \times e^{\frac{\sigma_0 - \sigma_a}{s_u} - 1} \tag{2.9}$$

with:

a	Certain radius of interest in the elastic zone	$[m]$
u_a	Displacement at tunnel surface	$[m]$
s_u	Shear strength of the ground	$[MPa]$
ν	Poisson's ratio	$[-]$
E	Young's modulus	$[MPa]$
σ_0	Initial total stress	$[MPa]$
σ_a	Initial effective stress at tunnel surface	$[MPa]$

2.6 Long term behaviour

In general deformations of the long-term behaviour include changes in pore volume and changes in water content. The development of the deformation depends on the seepage

flow velocity and on the permeability of the rock mass. During the excavation of tunnels, excess pore pressures are generated. Due to a hydraulic gradient between the tunnel surface and the far field, seepage flow starts to evolve. In this system the tunnel acts as a drain. This phenomenon is limited by the steady state pore water pressure distribution. Thus, the excess pore pressures dissipate over time, leading to a increase of the effective stresses. This effect describes the time-dependent ground behaviour known as consolidation until the steady state is reached. At the same time the displacements will continue until the steady state development is reached (Anagnostou, 2009). Figure 2.2 shows that the short-term behaviour is more favorable than the long-term behaviour (Anagnostou, 2006).

3 Analysis of ground and system behaviour in water-bearing rock mass

According to the Austrian Society of Geomechanics (OEGG, 2010) the ground behaviour is defined as: "Reaction of the ground to the excavation of the full profile without consideration of sequential excavation and support". Whereas the system behaviour is the result from the interaction between ground, excavation and support.

3.1 Convergence Confinement Method - State of the art

With the convergence confinement method the ground system and behaviour is described in a analytical-graphical way - see figure 3.1. The convergence confinement method is composed of three characteristic curves:

- Ground Characteristic Curve GCC / Ground Reaction Curve GRC
- Support Characteristic Curve SCC
- Longitudinal Displacement Profile LDP

A combination of GCC and SCC can be used to estimate required support measures. If these curves (GCC and SCC) intersect, equilibrium between loading forces of the rock mass and sustaining forces of supporting elements is reached. For considering the place and time of the installation of supporting elements the Longitudinal Displacement Profile LDP is added to a three dimensional system. The LDP shows the development of radial displacements in the tunnel, related to the direction of the tunnel axis.

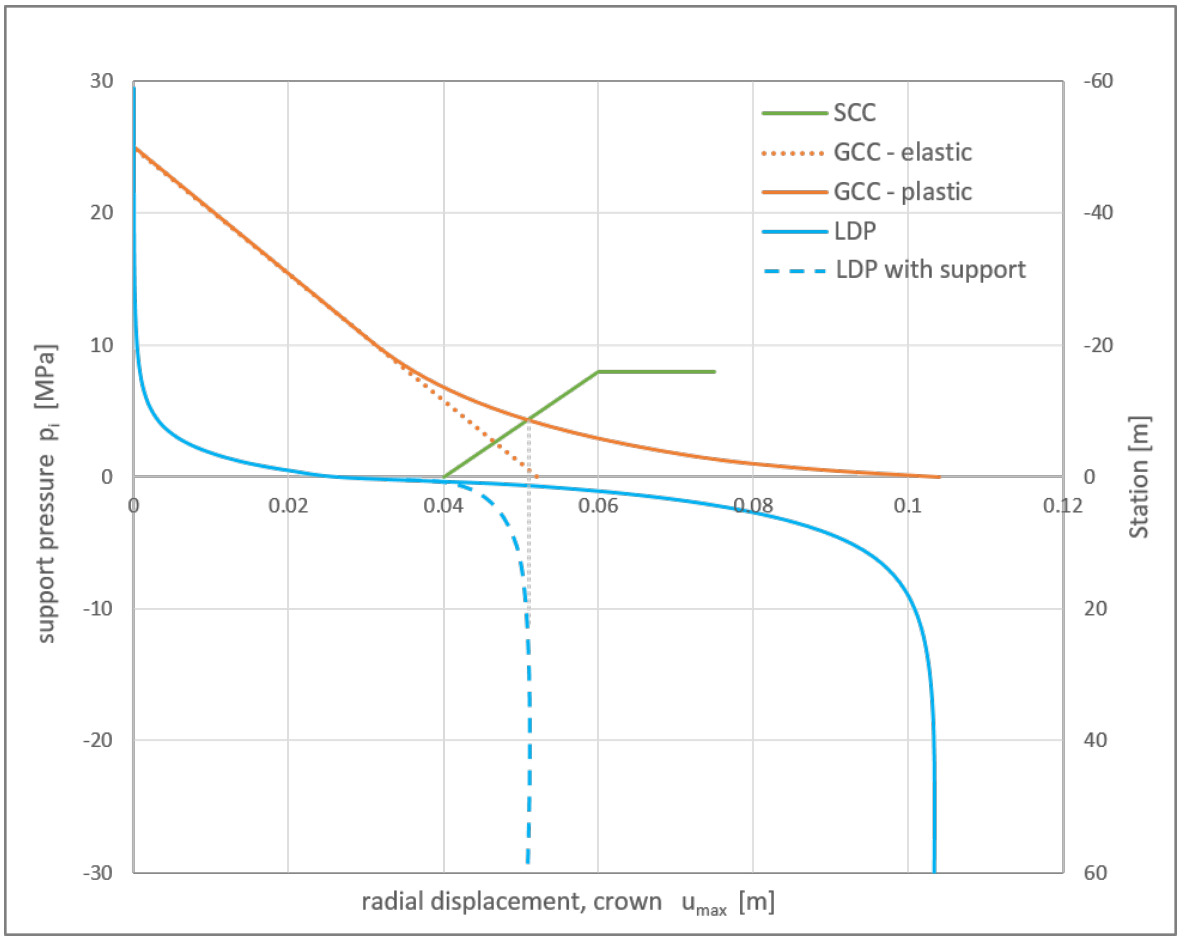

Figure 3.1: Convergence confinement method: GCC, SCC, LDP (scheme)

3.1.1 Development

Kirsch provided 1898 the theoretical stress distributions around an infinite plate with a circular hole. In 1949, *Kastner* extended the theory of *Kirsch* with plastic material behaviour. At the end of the seventies many researchers dealt with different theories in stress and displacement distributions. Established names in this business are Egger, Feder, Fenner, Hoek, Kastner, Lombardi, Müller, Panet, Pacher, Rabcewicz, Salencon, Sulem in alphabetical order. For a comprehensive chronology see Gschwandtner (2010).

3.1.2 Basics and assumptions

The convergence confinement method is typically applied for deep tunnels and also for tunnels where displacements play a major role (Kainrath et al., 2009). This method is not recommended for shallow tunnels in loose ground (Oreste, 2009).

The convergence confinement method belongs to the rational approaches in using analytical calculation and supposes the following assumptions:

- Two-dimensional plate of infinite extension
- Plate with circular opening
- Homogeneous rock mass
- Side pressure coefficient of $K_0 = 1$ (except the theory of Feder & Arwanitakis (1976): $K_0 \neq 1$)

Most of the models (summarized in Gschwandtner (2010)) contain the listed assumptions, except of the model delivered by *Feder* for instance. Therefore, he provides the model with limitations for any state of primary stress and cavity geometry (Feder & Arwanitakis, 1976). Usually a planar deformation state is assumed, whereby the component of deformation in tunnel axis direction is set zero. Concerning the determination of the deformation distribution all assumptions, simplifications and integration constants lead to inaccuracies in the model. Additionally, the Young's modulus and Shear modulus are stress dependent. These stress dependent stiffnesses are not considered in most of the models, which can affect the results seriously.

3.1.3 Ground characteristic/reaction curve - GCC/GRC

The ground characteristic curve represents the development of displacements at the excavation surface. Thereby the relationship between a fictitious reduction of support pressure to the radial increase of deformation is illustrated. The support pressure of the rock mass itself is reduced and starts from the primary stress state, while the rock mass behaves elastically (linear progression) until the critical support pressure p_{crit} is achieved. At this stage the defined failure criterion is reached and plastic material behaviour occurs with further reduction of the support pressure. The transition from elastic to plastic behaviour is defined at the plastic radius r_{pl} - see figure 3.2. Figure 3.3 shows the elastic and plastic progression of the GCC.

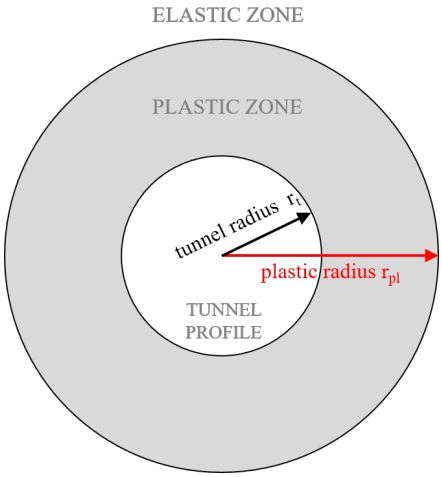

Figure 3.2: Definition of the plastic radius as the transition of the elastic to the plastic zone (scheme).

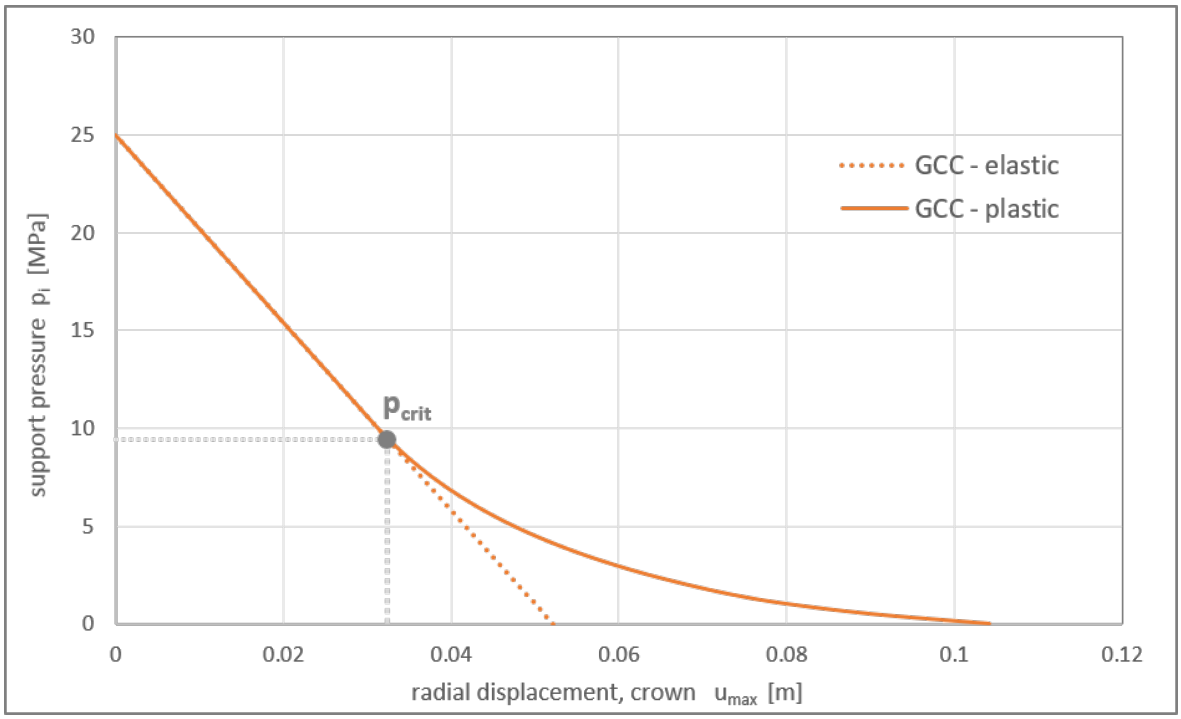

Figure 3.3: Ground characteristic curve with elastic and plastic progression.

3.1.4 Support characteristic curve - SCC

All support measures are implemented in the support characteristic curve. The SCC can be described mathematically with material parameters of stiffness and the maximum sustainable

stress and strain. A simplified material model for shotcrete or rock bolts is for instance the ideal-elastic, linear-plastic one. The resisting forces of the support measures have to be as big as the loading forces of the rock mass to reach equilibrium (Kainrath et al., 2009).

3.1.5 Longitudinal displacement curve - LDP

The LDP considers the sequences and location for the installation of support measures. Figure 3.4 shows the relationship between the plain strain analysis (2D) and a 3D-model. Panet & Guenot (1982) developed the first correlation of the radial deformation along the tunnel axis. They considered only the elastic component of deformation in their formulas. Further theories involve also the plastic component as well, depending on the size of the plastic zone (Kainrath et al., 2009).

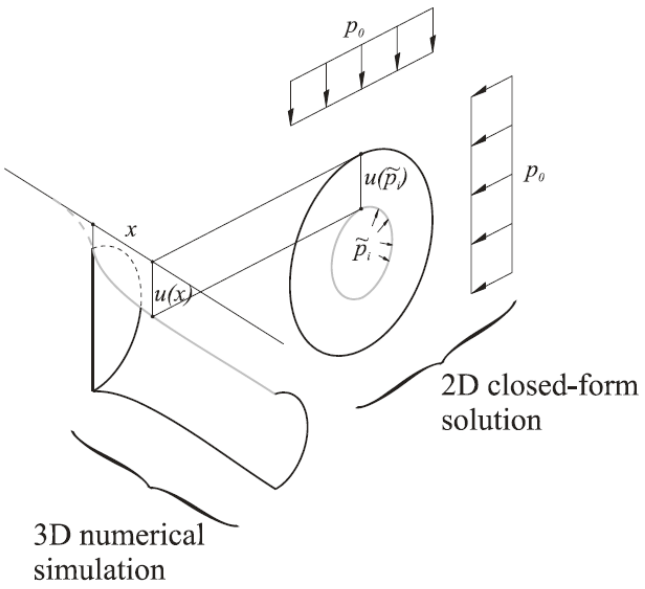

Figure 3.4: Relationship between the LDP from the 3D numerical model to the 2D closed-from solution and fictitious support pressure (Radoncic et al., 2009).

Many researchers have proposed various analytical approaches for LDP calculations. The different approaches produce quite varying solutions in deformations. All the further research of this thesis is referred to the approach of Vlachopoulos & Diederichs (2009).

3.1.6 LDP according to *Vlachopoulus and Diederichs*

In 2009 *Vlachopoulus and Diederichs* developed a new formulation to calculate LDP profiles based on the size of the plastic yield zone. There is no interaction between the plastic yield zone at the tunnel face and around the tunnel, if the plastic yield zone is smaller than twice the tunnel radius. Beyond this range the formulation of Panet & Guenot (1982) is not acceptable anymore. Figure 3.5 shows the different cases with and without interaction of the plastic zones.

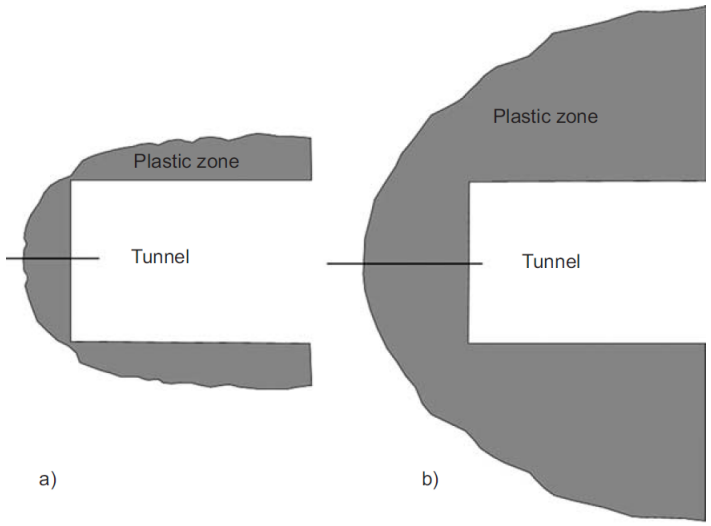

Figure 3.5: Case a): plastic yield zone is smaller than twice the tunnel radius ($r_p < 2 \times r_0$) - formulation of Panet & Guenot (1982) is valid, case b): plastic yield zone is larger than twice the tunnel radius ($r_P > 2 \times r_0$) - formulation of Panet & Guenot (1982) is not acceptable (Vlachopoulos & Diederichs, 2009).

Based on numerical calculations a direct correlation was found between the normalized radial displacement ($u^* = u_r/u_{r,max}$) and the normalized maximal plastic zone ($R^* = r_p/r_0$). The relationship between u^* and R^* is shown in figure 3.6. The relationship suggested by *Unlu & Gercek* (2003) correctly demonstrates that the rock mass behaviour ahead ($X < 0$ into the rock mass) and behind ($X > 0$ in the tunnel) the tunnel face does not follow the same distribution. Formula 3.1, 3.2 and 3.3 illustrate the distribution of radial displacements (Vlachopoulos & Diederichs, 2009).

$$u_0^* = \frac{u_{r,0}}{u_{r,max}} = \frac{1}{3} e^{-0.15R^*} \tag{3.1}$$

$$u^* = \frac{u}{u_{max}} = u_0^* \times e^{X^*} \quad \text{for } X^* \leqslant 0 \text{ (into the rock mass)} \tag{3.2}$$

$$u^* = 1 - (1 - u_0^*) \times e^{-\frac{3X^*}{2R^*}} \quad \text{for } X^* \geqslant 0 \text{ (in the tunnel)} \tag{3.3}$$

If axisymmetrical or full 3D-models are used for determining the LDP relationship, the excavation step size is very important and has to be considered (Vlachopoulos & Diederichs, 2009).

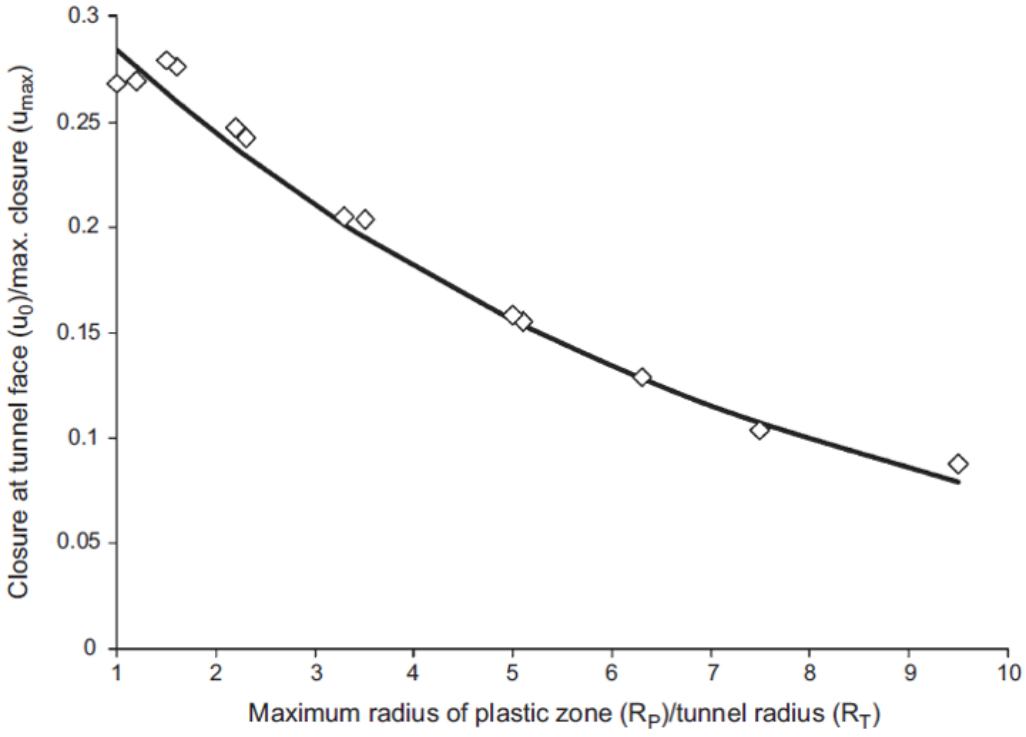

Figure 3.6: Correlation between $u^* = u_r/u_{r,max}$ and $R^* = r_p/r_0$ (Vlachopoulos & Diederichs, 2009).

3.2 Numerical methods - State of the art

Numerical simulations have become state of the art. Of particular importance are numerical simulations in cases of complex geometries or interaction with other structures. Besides the many benefits, numerical simulations can be time-consuming, produces high amounts of data and the determination of influential design parameters is mostly unknown. The following

numerical methods are available:

- Finite Element Method (FEM)
- Finite Different Method (FDM)
- Boundary Element Method (BEM)
- Discrete Element Method (DEM)

All different numerical methods allow analysis including the impact of water, known as an coupled analysis. In rock mechanics DEM is probably most appropriate and used in the actual thesis. FEM does have some limitations for instance is not suitable for blocky structures and discontinua respectively. BEM contains only surface discretization for 3D and constitutes a feasible alternative in terms of shorter calculation times (Schwaiger, 2016).

4 Implemented analytical and numerical calculations

4.1 Setup considerations

4.1.1 Input parameters

All numerical calculation carried out for this thesis use the Mohr-Coulomb failure criterion. This ensures the comparability of the analytical results. As a positive side effect the Mohr-Coulomb failure criterion is based on solely five input parameters. Following is a list of the used input parameters:

a) Fixed parameters:
   - Poisson's ratio
   - Dilatancy angle is set to zero

b) Changing parameters:
   - Friction angle
   - Cohesion
   - Young's modulus

Furthermore, the Mohr-Coulomb failure criterion simplifies the real rock mass behaviour. The friction angle remains constant and no stress depended stiffness is considered. This may lead to inaccuracies in stress and deformation. The dilatancy angle is set to zero, otherwise according to figure 4.1 infinite stresses would be generated leading to an overestimate in displacements (Schwaiger, 2016).

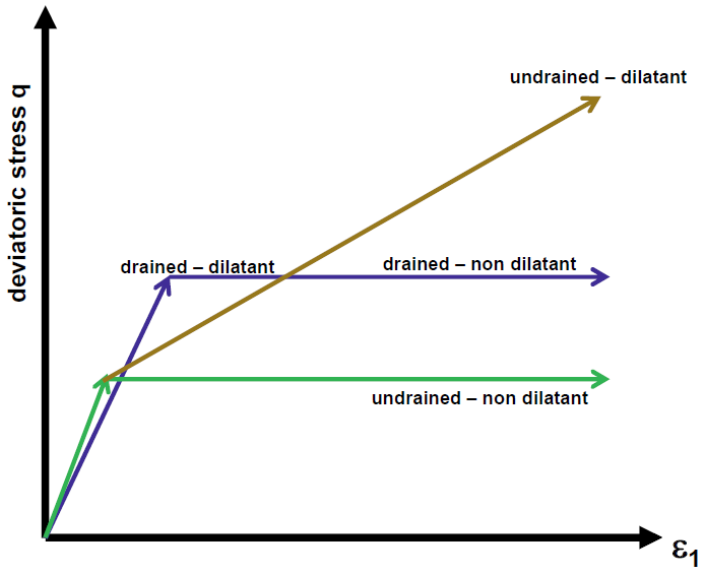

Figure 4.1: Stress-strain diagram of a triaxial test by using the MC-model for drained and undrained conditions (scheme) (Schwaiger, 2016).

The input parameters for the simulations are listed in table 4.1.

Position and abbreviation		1	2	3	4	5
Tunnel radius - R	[m]	3	5	7		
Overburden - OB	[m]	50	100	200	500	1000
(Primary stress σ_0)	[MPa]	(1.25)	(2.5)	(5)	(12.5)	(25)
Friction angle - P	[°]	23	29	35		
Young's modulus - E	[GPa]	1	3	10		
Cohesion - C	[MPa]	0.1	0.5	1.5	3	
Poisson's ratio	$\nu = 0.25$ for all calculations					
Dilatancy angle	set to zero for all calculations					
Lateral pressure coefficient	$K_0 = 1$ for all calculations					

Table 4.1: Input parameters for numerical analysis

For all simulations, the development of a plastic zone has been considered. The analytical approach for dry conditions has been used to verify this. Hence all combinations are checked by using the analytical approach for dry conditions (see chapter 4.2). Therefore, the criterion to reach plasticity constitutes the lower boundary while the upper boundary is limited

with the plastic radius of 20 m. This is done to obtain reasonable results with respect to the limited model geometry. The strength and deformation parameters, i.e. Young's modulus and friction angle are considered to be correlated, which means that high Young's moduli are used in combination with high values of shear strength, and vice versa.

	model	R - radius [m]	OB - overburden [m]	P - friction angle [°]	E - young's modulus [GPa]	C - shear strength [MPa]
Radius 3 m	R3_OB50_P23_E1_C0.1	3	50	23	1	0.1
	R3_OB50_P29_E3_C1.5	3	50	29	3	1.5
	R3_OB100_P29_E3_C1.5	3	100	29	3	1.5
	R3_OB200_P29_E3_C1.5	3	200	29	3	1.5
	R3_OB1000_P29_E3_C1.5	3	1000	29	3	1.5
	R3_OB500_P29_E3_C3	3	500	29	3	3
	R3_OB500_P35_E10_C3	3	500	29	10	3
	R3_OB1000_P35_E10_C3	3	1000	29	10	3
Radius 5 m	R5_OB100_P29_E3_C0.5	5	100	29	3	0.5
	R5_OB200_P29_E3_C0.5	5	200	29	3	0.5
	R5_OB500_P29_E3_C0.5	5	500	29	3	0.5
	R5_OB200_P29_E3_C1.5	5	200	29	3	1.5
	R5_OB500_P29_E3_C1.5	5	500	29	3	1.5
	R5_OB1000_P29_E3_C1.5	5	1000	29	3	1.5
	R5_OB500_P29_E3_C3	5	500	29	3	3
	R5_OB1000_P29_E3_C3	5	1000	29	3	3
	R5_OB500_P35_E10_C3	5	500	35	10	3
	R5_OB1000_P35_E10_C3	5	1000	35	10	3
Radius 7 m	R7_OB50_P29_E3_C0.5	7	50	29	3	0.5
	R7_OB100_P29_E3_C0.5	7	100	29	3	0.5
	R7_OB200_P29_E3_C1.5	7	200	29	3	1.5
	R7_OB500_P29_E3_C3	7	500	29	3	3
	R7_OB1000_P29_E3_C3	7	1000	29	3	3
	R7_OB1000_P35_E10_C3	7	1000	35	10	3

Table 4.2: Model parameters for dry and undrained conditions

In order to maintain the overview of all calculations and to provide a clear structure for quick understanding, the models are designated with abbreviations and single parameters

referenced to table 4.1. Altogether 48 different calculations are performed, divided in 24 calculations for dry conditions and 24 calculations for undrained conditions. Table 4.2 shows the different models classified by the tunnel radius.

4.2 Analytical analysis

The formulas according to Sulem et al. (1987) are used for the analytical analysis for dry conditions. In the following, all formulas are listed, which are applied in the analytical calculations.

4.2.1 Used equations

$$\sigma_{ucs} = \frac{2 \times c \times cos(\varphi)}{1 - sin(\varphi)} \tag{4.1}$$

with:
- σ_{ucs} **Uniaxial compressive strength [MPa]**
- c Cohesion $[MPa]$
- φ Friction angle $[^{\circ}]$

$$k = tan^2\left(45 + \frac{\varphi}{2}\right) = \frac{1 + sin(\varphi)}{1 - sin(\varphi)} \tag{4.2}$$

with:
- **k** **Lateral pressure coefficient (passive) [-]**
- φ Friction angle $[^{\circ}]$

$$p_i^{cr} = \frac{2 \times p_0 - \sigma_{ucs}}{1 + k} \tag{4.3}$$

with:
- p_i^{cr} **Critical support pressure [MPa]**
- p_i Support pressure $[MPa]$
- p_0 Primary stress $[MPa]$
- k Lateral pressure coefficient (passive) $[-]$
- σ_{ucs} Uniaxial compressive strength $[MPa]$

$$r_p = r_0 \times \left(\frac{2 \times (k-1) \times p_0 + \sigma_{ucs}}{(k+1) \times (k-1) \times p_i + \sigma_{ucs}} \right)^{\frac{1}{k-1}} \tag{4.4}$$

with:

r_p	**Plastic radius** [**m**]
r_0	Tunnel radius $[m]$
p_i	Support pressure $[MPa]$
p_0	Primary stress $[MPa]$
k	Lateral pressure coefficient (passive) $[-]$
σ_{ucs}	Uniaxial compressive strength $[MPa]$

$$\sigma_{t,el} = p_0 + (p_0 - p_i^{cr}) \times \left(\frac{r_p}{r} \right)^2 \tag{4.5}$$

with:

$\sigma_{t,el}$	**Tangential stress in the elastic zone** [**MPa**]
r	Control variable in tunnel radius direction $[m]$
r_p	Plastic radius $[m]$
p_i^{cr}	Critical support pressure $[MPa]$
σ_{ucs}	Uniaxial compressive strength $[MPa]$

$$\sigma_{t,pl} = -\frac{\sigma_{ucs}}{k-1} + k \times \left(p_i + \frac{\sigma_{ucs}}{k-1} \right) \times \left(\frac{r}{r_0} \right)^{k-1} \tag{4.6}$$

with:

$\sigma_{t,pl}$	**Tangential stress in the plastic zone** [**MPa**]
r_0	Tunnel radius $[m]$
r_p	Plastic radius $[m]$
k	Lateral pressure coefficient (passive) $[-]$
p_i^{cr}	Critical support pressure $[MPa]$
σ_{ucs}	Uniaxial compressive strength $[MPa]$

$$\sigma_{r,el} = p_0 - (p_0 - p_i^{cr}) \times \left(\frac{r_p}{r}\right)^2 \tag{4.7}$$

with:

$\sigma_{r,el}$	**Radial stress in the elastic zone [MPa]**
r	Control variable in tunnel radius direction $[m]$
r_p	Plastic radius $[m]$
p_i^{cr}	Critical support pressure $[MPa]$
σ_{ucs}	Uniaxial compressive strength $[MPa]$

$$\sigma_{r,pl} = -\frac{\sigma_{ucs}}{k-1} + \left(p_i + \frac{\sigma_{ucs}}{k-1}\right) \times \left(\frac{r}{r_0}\right)^{k-1} \tag{4.8}$$

with:

$\sigma_{r,pl}$	**Radial stress in the plastic zone [MPa]**
r_0	Tunnel radius $[m]$
r_p	Plastic radius $[m]$
k	Lateral pressure coefficient (passive) $[-]$
p_i^{cr}	Critical support pressure $[MPa]$
σ_{ucs}	Uniaxial compressive strength $[MPa]$

$$u_{r,el} = (p_0 - p_i^{cr}) \times \frac{r_p}{2 \times G} \times \left(\frac{r_p}{r}\right) \tag{4.9}$$

with:

$u_{r,el}$	**Radial displacement in the elastic zone [m]**
r	Control variable in tunnel radius direction $[m]$
r_p	Plastic radius $[m]$
p_i^{cr}	Critical support pressure $[MPa]$
p_0	Primary stress $[MPa]$
G	Shear modulus $[MPa]$

$$u_{r,el} = (p_0 - p_i) \times \frac{r_0}{2 \times G} \times \left(\frac{r_0}{r}\right) \tag{4.10}$$

with:

$u_{r,el}$	**Radial displacement if no plastic zone develops** [**m**]
r	Control variable in tunnel radius direction $[m]$
r_0	Tunnel radius $[m]$
p_i	Support pressure $[MPa]$
p_0	Primary stress $[MPa]$
G	Shear modulus $[MPa]$

$$u_{r,pl} = \lambda \times r_0 \times \frac{p_0}{2 \times G} \times \left(\frac{r_p}{r_0}\right)^2 ; \lambda = \frac{1}{k+1} \times \left(k - 1 + \frac{\sigma_{ucs}}{p_0}\right) \tag{4.11}$$

with:

$u_{r,pl}$	**Radial displacement in the plastic zone** [**m**]
σ_{ucs}	Uniaxial compressive strength $[MPa]$
r_0	Tunnel radius $[m]$
r_p	Plastic radius $[m]$
p_0	Primary stress $[MPa]$
G	Shear modulus $[MPa]$
k	Lateral pressure coefficient (passive) $[-]$

To calculate the undrained radial displacements equations 2.8 and 2.8 are applied. Additional information concerning the undrained analytical analysis can be found in the original paper of Anagnostou (2009).

4.3 Numerical analysis

For the numerical part of this thesis the software $FLAC^{3D}$ (Itasca, 2016) is used. Two types of models are coded: one for dry ground behaviour and an additional one considering undrained conditions.

4.3.1 Model

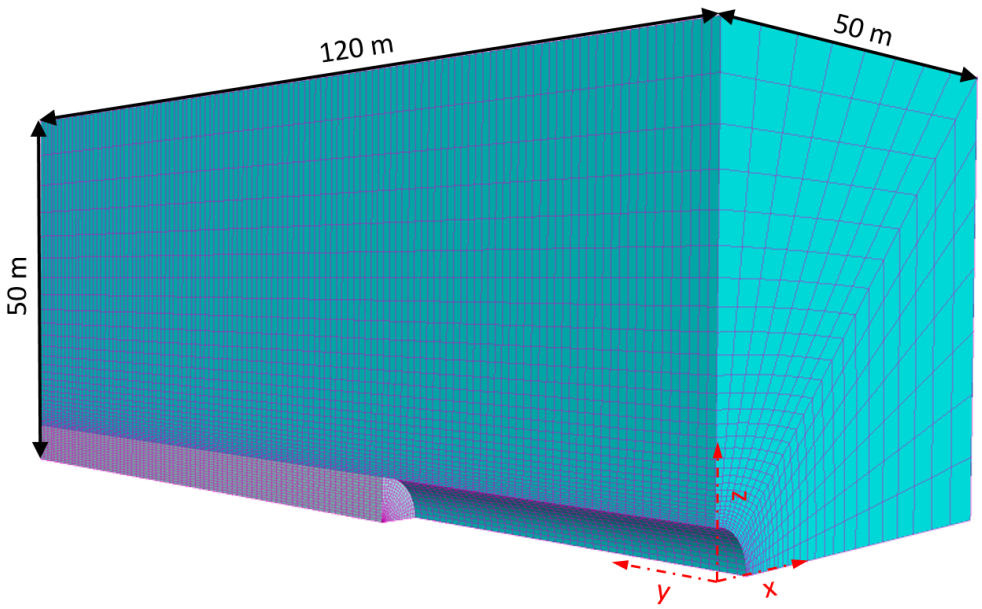

Figure 4.2: Model geometry

The mechanical behaviour of the rock mass is modeled using a linear-elastic and perfectly plastic model according to the Mohr-Coulomb failure criterion, which is characterized by the five material constants mentioned in chapter 4.1.1. The model represents an axisymmetric, deep, cylindrical tunnel with homogeneous and isotropic ground conditions. The model is 50 m high, 50 m wide and has a depth of 120 m. The tunnel radius varies between 3 m and 7 m and the stress state of the rock mass depends on the overburden of the tunnel. All input parameters are listed in tabel 4.1. The model with a radius of 5 m is shown in figure 4.2. The length of one excavation step is 1 m, which leads to 120 steps in total.

4.3.2 Influence of mesh properties

The originally defined mesh properties of the calculated models are shown on the left side in figure 4.3. The consideration is to get an accurate plastic radius by using fine mesh properties in radial direction by simultaneously allowing for reasonable calculation time. The single elements of the original mesh properties look like "plates". Thus, the mesh discretization in radial direction is small compared to the length in y-direction, which is as long as one excavation step (1 m).

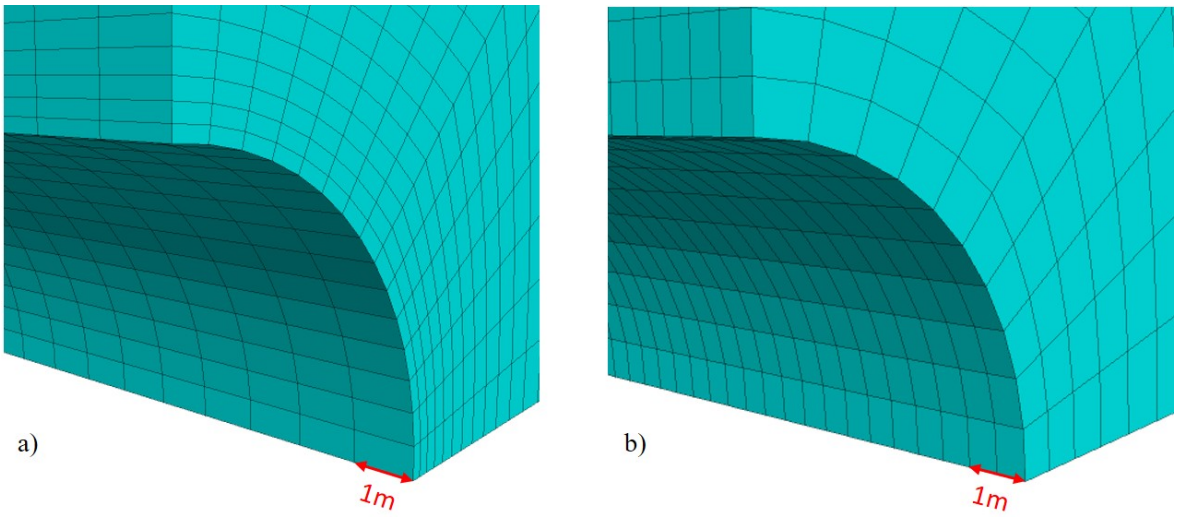

Figure 4.3: "Original mesh" properties (a) and "treated mesh" properties (b)

The analysis of the results shows that deviations in radial displacements occur. A plain-strain mesh study with the software $Phase^2$ and studies with different element lengths in the 3D model show that a different element shape leads to significant differences in the normalized radial displacements $u^* = u_r/u_{r,max}$. For this reason the element properties are modified to "cubical" elements. The so called "treated mesh" is shown in figure 4.3 (b). More details are given in chapter 5.

4.3.3 Ground water

Water affects the mechanical ground behaviour by reducing the total stresses to effective stresses. The short term behaviour and undrained analysis respectively (no flow) is considered according to the $FLAC^{3D}$ manual (Itasca, 2016): "No real time will be involved in the numerical simulation (i.e., $t_s <<< t_c$), but the pore pressure will change due to volumetric straining if the fluid modulus (M or K_f) is given a realistic value." The fluid modulus is set to 2000 MPa. The water density is 1000 kg/m^3. The porosity of the rock mass is assumed as 0.2.

In the thesis at hand, the pore pressure is directly linked to the overburden of the tunnel, which means that the entire overburden is fully saturated. When the excavation starts, a negative pore water pressure develops at the tunnel surface. This is caused by the positive volumetric strain into the tunnel. The tunnel deforms and becomes smaller in radius, while at the same time suction increases. In the excavated part of the tunnel atmospheric pressure

is assumed and consequently negative pore pressure is confined at the tunnel surface. That means that the negative pore pressure cannot be infinite. Therefore, the fluid tension is limited according to Amann et al. (2014) as -2.0 MPa at the tunnel surface.

4.3.4 Output

With numerical analysis a lot of data is produced and hence a lot of storage is needed. It is thus not possible to save each excavation step. Due to high amount of data, $FLAC^{3D}$ enables to code separate output-files as simple, low-data text-files. Actually, two different output-files of each calculation are created, which include the radial displacements on the one hand and the effective stresses on the other hand. Both, the displacements and the effective stresses are logged at the grid-point in the crown of tunnel-station 60 (half the tunnel-length) of each excavation step (figure 4.4). Figure 4.5 shows a cutout of such an output-file of displacements in x-, y- and z-direction.

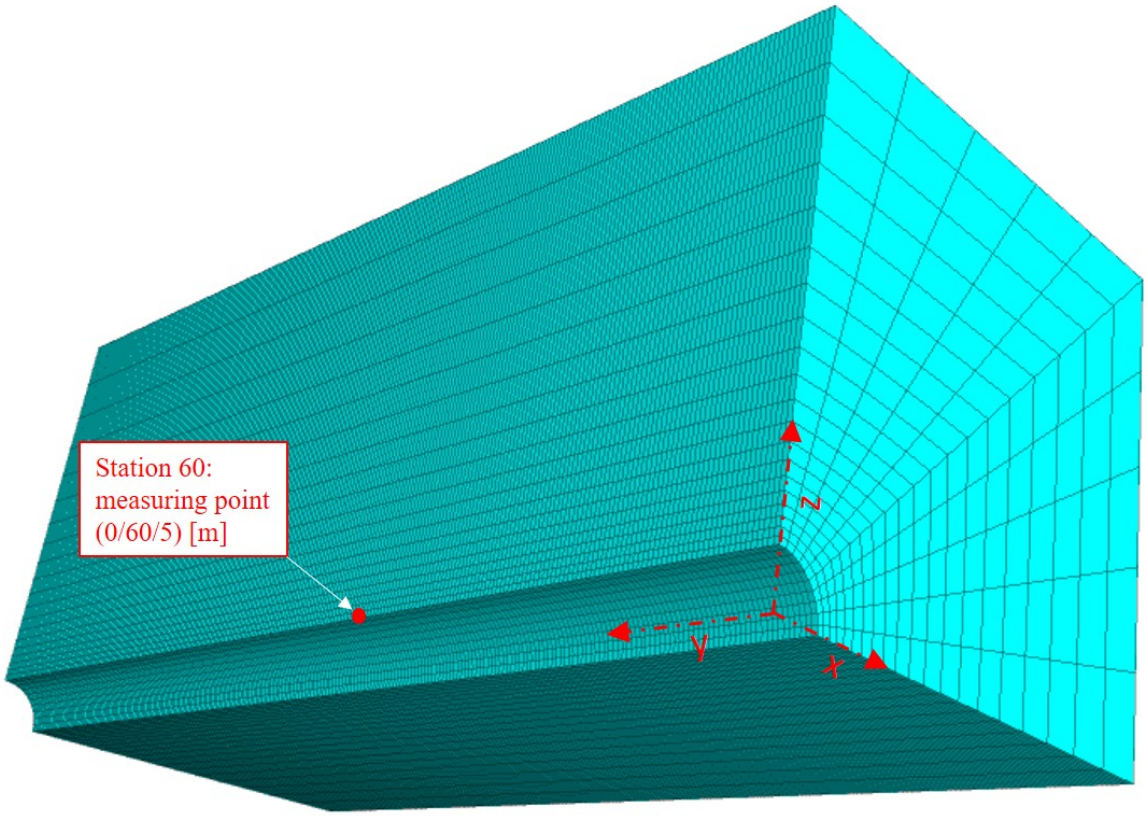

Figure 4.4: Location of the measuring point for stresses and displacements.

```
***DEFORMATIONS ROCK MASS - ROOF***
============================================================
model parameter:          R5_OB500_P29_E3_C3_sat

tunnel radius: 5 m
model overburden: 500 m
friction angle: 29 Grad
elastic modulus: 3e+09 Pa
cohesion: 3e+06 Pa
============================================================
station  x_disp              y_disp               z_disp
1          0          -0.000125352            -6.28246e-06
2          0          -0.000176696            -8.81249e-06
3          0          -0.000212299            -9.08808e-06
```

Figure 4.5: Output-file of displacements from station 1 until station 3

4.3.5 Convergence criterion

For the numerical calculation a convergence criterion is required, which defines the accuracy of the iteration steps and therefore the calculation time. If the convergence criterion is set very small, the calculation takes a lot of time. The convergence criterion for the dry ground is set to 10E-5 and gives adequate results. Concerning the undrained case the convergence criterion of 10E-5 is inaccurate, which can be shown in figure 4.6 - there are continuous settlements until station 120 is reached. As seen, lowering the convergence ratio to 10E-6 leads to more adequate results and is used for all undrained calculations.

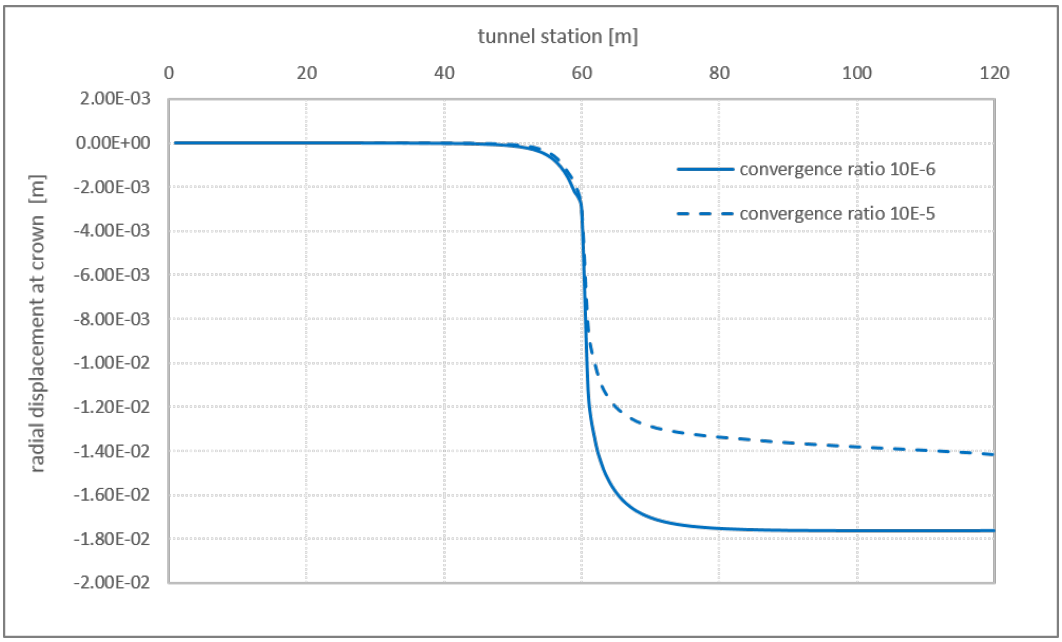

Figure 4.6: Impact on LDP of different convergence criteria for undrained conditions.

5 Results

This chapter represents the results of analytical and numerical analysis. For better understanding the interpretations of the results are provided in chapter 6.

5.1 Ground reaction curve for dry and undrained conditions

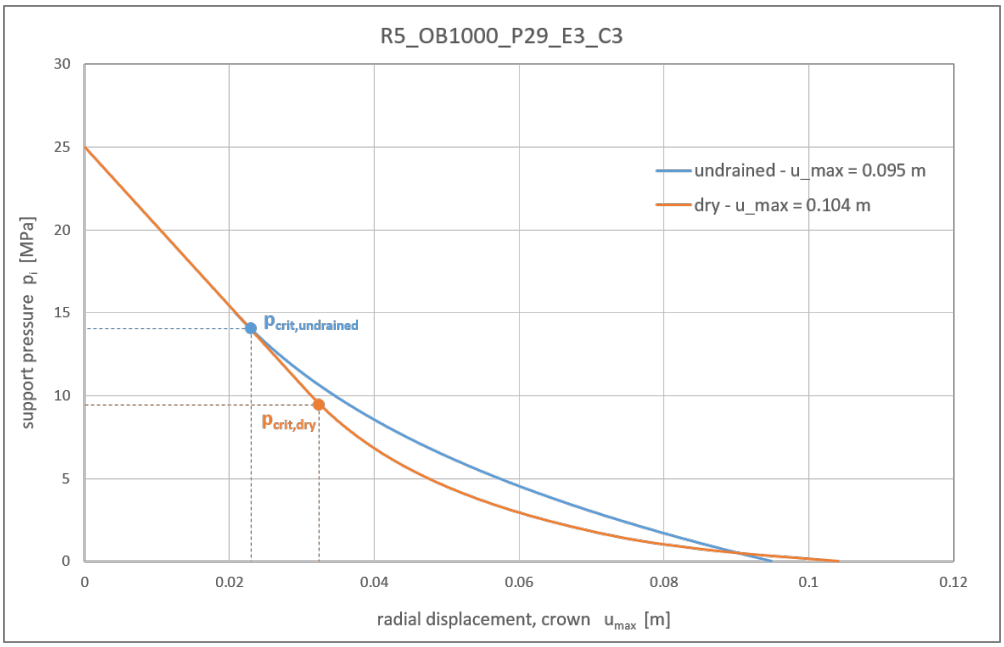

Figure 5.1: Analytical GRC of the model "R5_OB1000_P29_E3_C3" for dry and undrained conditions.

To calculate the radial displacements the formulas of chapter 4.2.1 for the dry case and equation 2.9 to determine the undrained case are used. Figure 5.1 represents the GRC of the model "R5_OB1000_P29_E3_C3" in terms of dry and undrained conditions. The radial displacement for the undrained case is lower (0.095 m) than for the dry case (0.104 m). Furthermore plasticity ($p_{crit,undrained}$) is reached earlier for undrained conditions.

5.2 Longitudinal displacement profiles (LDP)

5.2.1 Undrained vs. dry LDP of numerical analysis

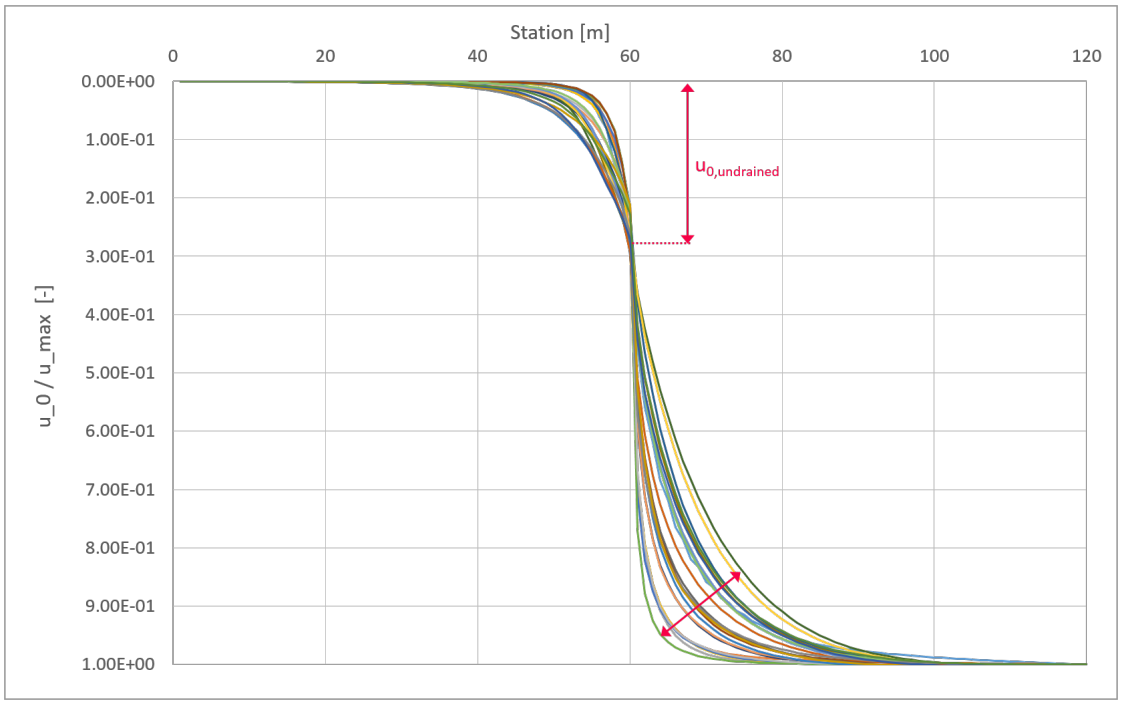

Figure 5.2: LDP's of all undrained calculations.

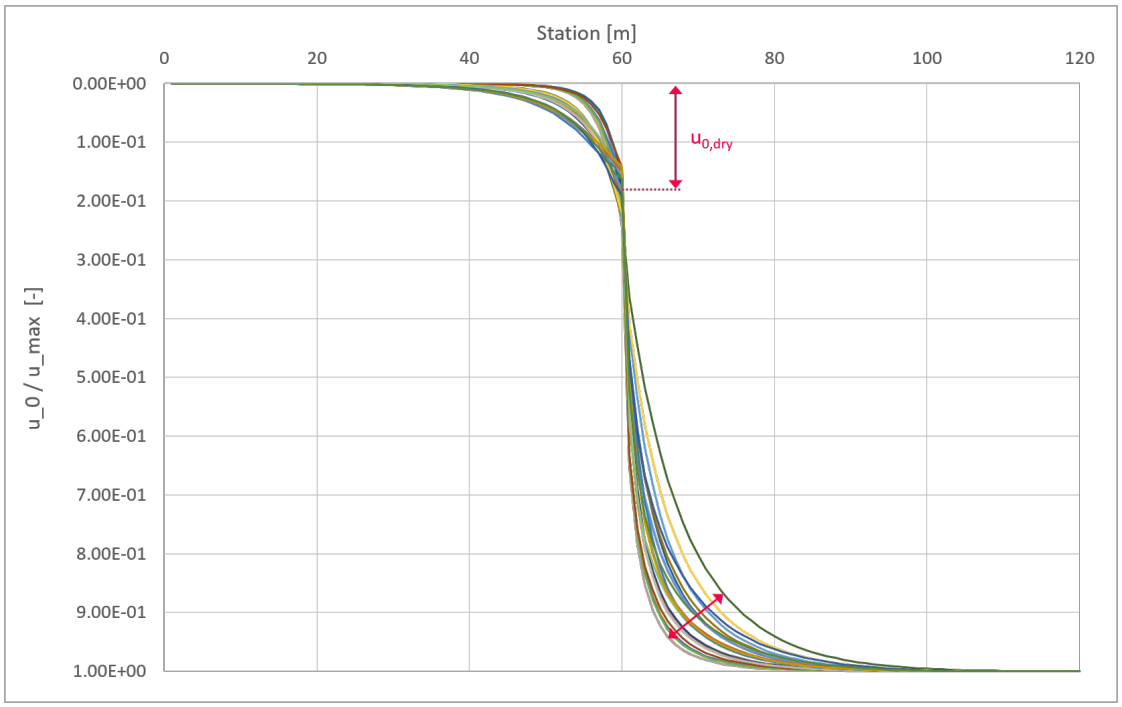

Figure 5.3: LDP's of all dry calculations.

The LDP's of all numerical model-sets in table 4.2 are plotted for dry and undrained conditions respectively. The y-axis represents the normalized radial displacements and the x-axis the tunnel meter with the face position at 60 m. Figure 5.2 shows all undrained models and figure 5.3 includes all dry models. Both, the models in figure 5.2 and the models in figure 5.3 are calculated with the "original mesh" properties. By comparing the undrained with the dry LDP's, three statements are remarkable:

- At the tunnel face the undrained normalized radial displacements are higher than the dry normalized radial displacements.
- The displacement trend behind the face varies more for the undrained case.
- The progression of pre-displacements (in front of the tunnel face) is similar in both cases.

The differences in radial displacements for dry and undrained conditions are shown in figure 5.4. The model parameters are set to "R5_OB1000_P29_E3_C3" by using the "treated mesh" properties. For the undrained ground the radial displacements at the face u_0 are higher, but the final radial displacements remain smaller than for the dry case.

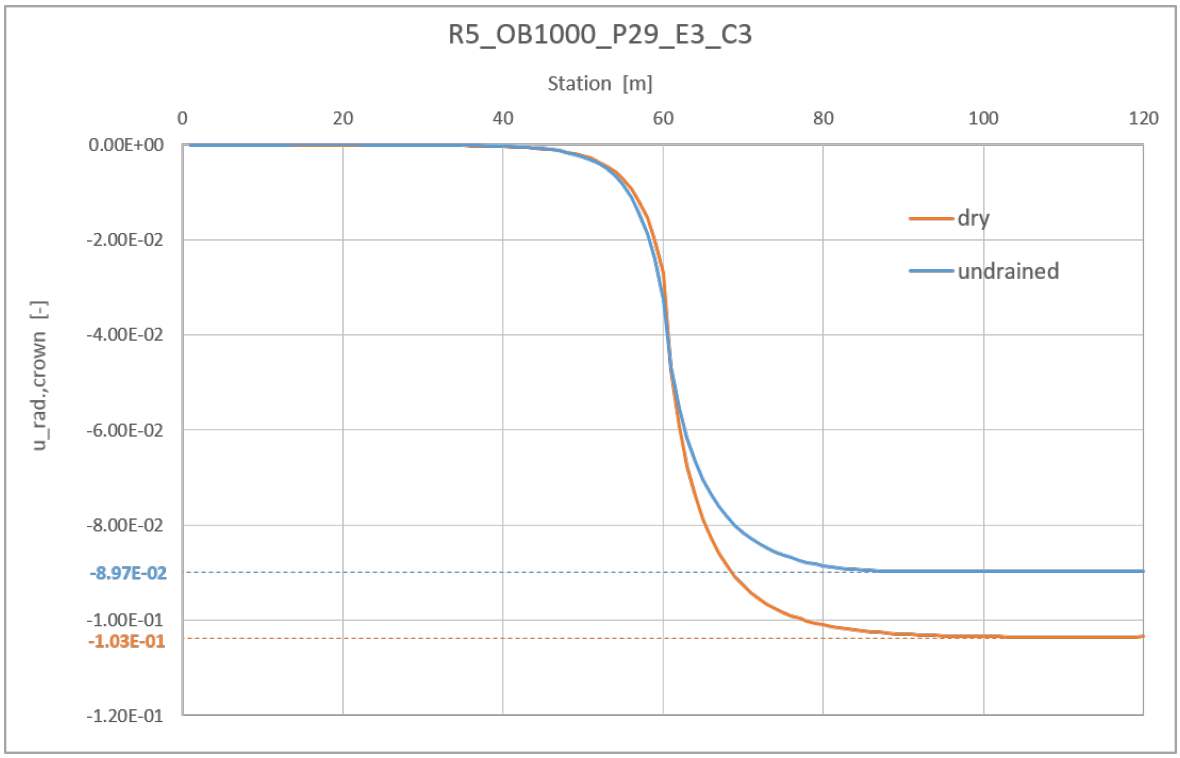

Figure 5.4: Dry and undrained LDP for the model "R5_OB1000_P29_E3_C3".

5.2.2 Undrained LDP with various tunnel radii

In this thesis the tunnel radius was varied between 3 and 7 m. To evaluate the influence of different tunnel radii on the radial displacements, only the tunnel radius is changed while the remaining input parameters are fixed. Figure 5.5 shows the LDP's for the parameter set "R-var._OB500_P29_E3_C3", while the x-axis is normalized to the tunnel radius. The obtained LDP's look similar.

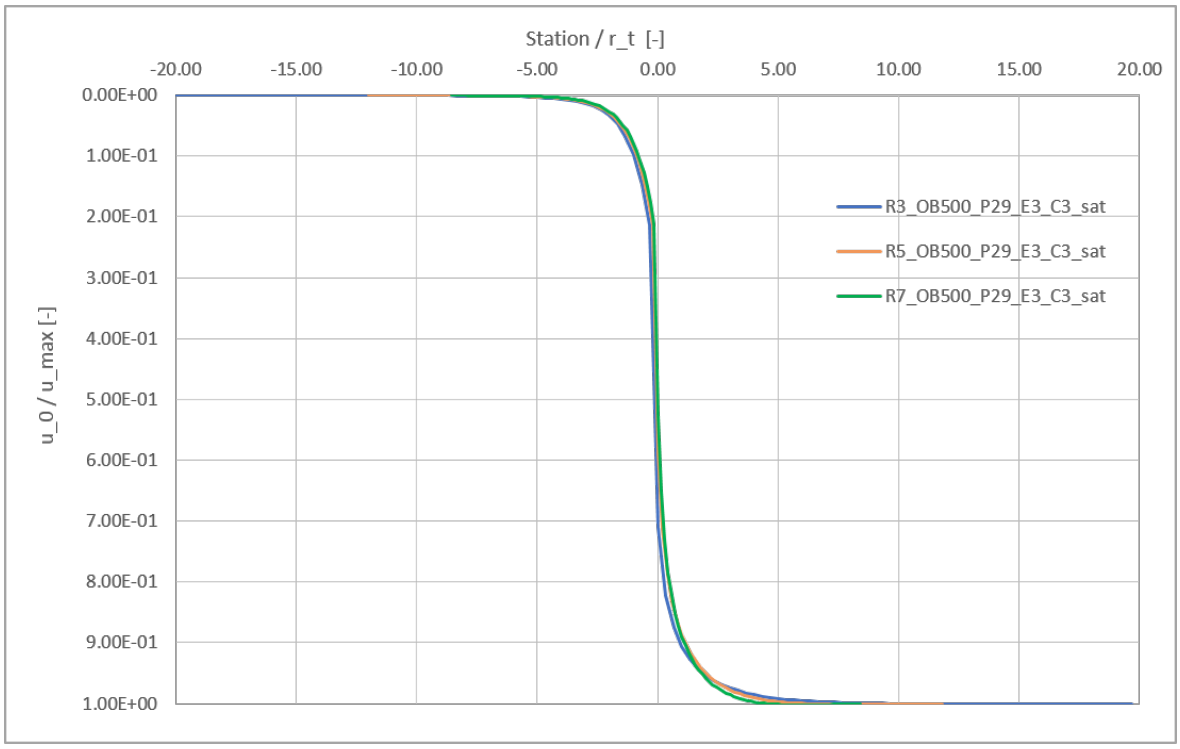

Figure 5.5: Undrained LDP's of the model sets "R-var._OB500_P29_E3_C3" with various tunnel radii.

5.2.3 Undrained LDP for varying cohesion

To evaluate the influence of a varying cohesion, analyses for values from 0,5 to 3 MPa are carried out. The LDP's in figure 5.6 are obtained. The remaining parameter sets are the same and belong to "R5_OB500_P29_E3_C-var.". It can be noticed that a varying cohesion has more impact in normalized displacements behind than in front of the face. Furthermore the displacements at the face are higher when the cohesion is low.

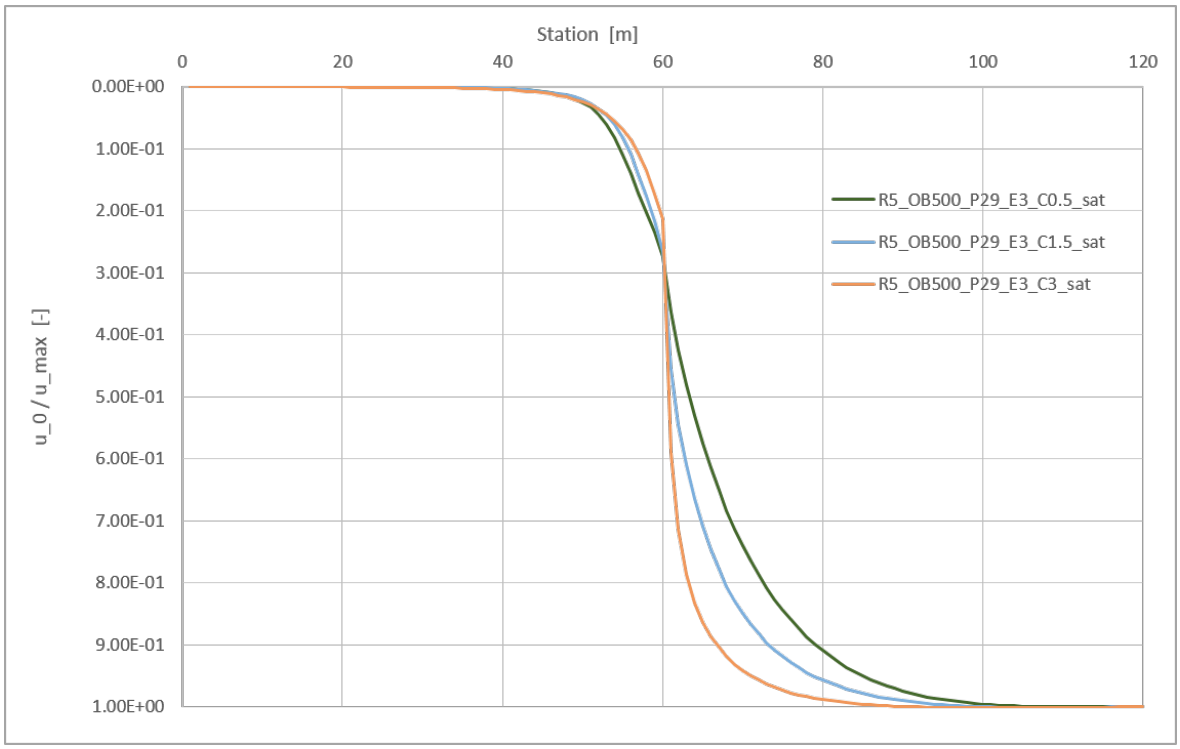

Figure 5.6: Undrained LDP's with varying cohesion of the model "R5_OB500_P29_E3_C-var.".

5.2.4 LDP with different mesh properties

Concerning deviations in radial displacements, a significant impact of different mesh properties (chapter 4.3.2) can be identified. Due to different shapes of discretized elements ("plates" vs. "cubes"), the "original mesh" (with "plates" at excavation boundary) leads to approximately 20 % higher radial displacements. Figure 5.7 illustrates the impact of the mesh. The analytical solution confirms the radial displacements using the "treated mesh". The displacements at the face (u_0) of the analytical solution and the solution with the "treated mesh" are roughly the same, which is shown in table 5.1.

	u_0/u_{max}
Original mesh	0.180
Treated mesh	0.260
Analytical solution - Vlachopoulos	0.256

Table 5.1: Ratio of pre-displacement to max. displacement referenced to figure 5.7

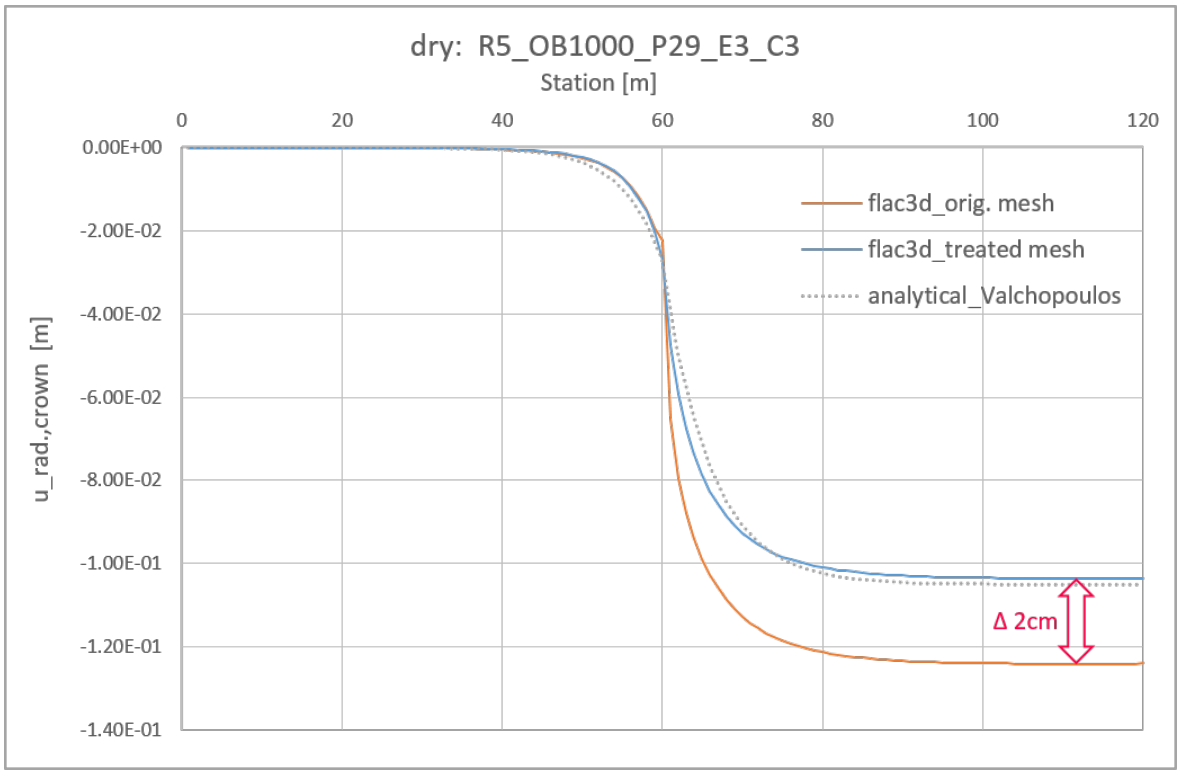

Figure 5.7: LDP's of the dry model "R5_OB1000_P29_E3_C3" with "original" and "treated mesh" properties and also the analytical LDP according to Vlachopoulos & Diederichs (2009).

5.3 Plastic radii

The development of plastic radii for undrained conditions is a significant output of the current thesis. All analytical and numerical calculated plastic radii presented in figure 5.8 are computed with the "original mesh" properties. The dry analytically determined plastic radii are consistent with the dry numerically analyzed plastic radii. All plastic radii of undrained conditions (only numerically analyzed) are higher when compared to the analysis for dry conditions.

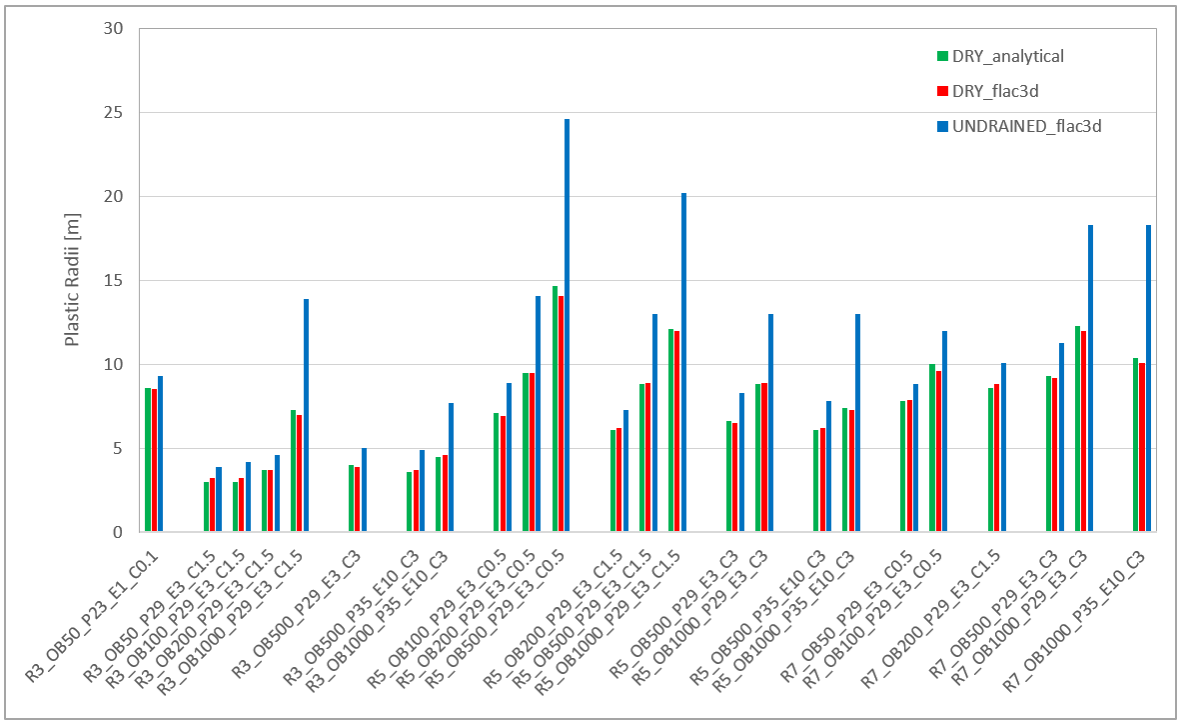

Figure 5.8: Plastic radii of all dry and undrained calculations

5.3.1 Plastic radii for different mesh properties

The influence of the different mesh properties (”original mesh” compared to the ”treated mesh”) on the plastic radius is shown in figure 5.9. The plastic radius for the parameter set ”R5_OB1000_P29_E3_C3” in both, the ”original mesh” and the ”treated mesh” is approximately the same. The ”treated mesh” contains less elements in the radial direction compared to the ”original mesh” properties. This may lead to inaccuracies, when models with large plastic radii are analyzed.

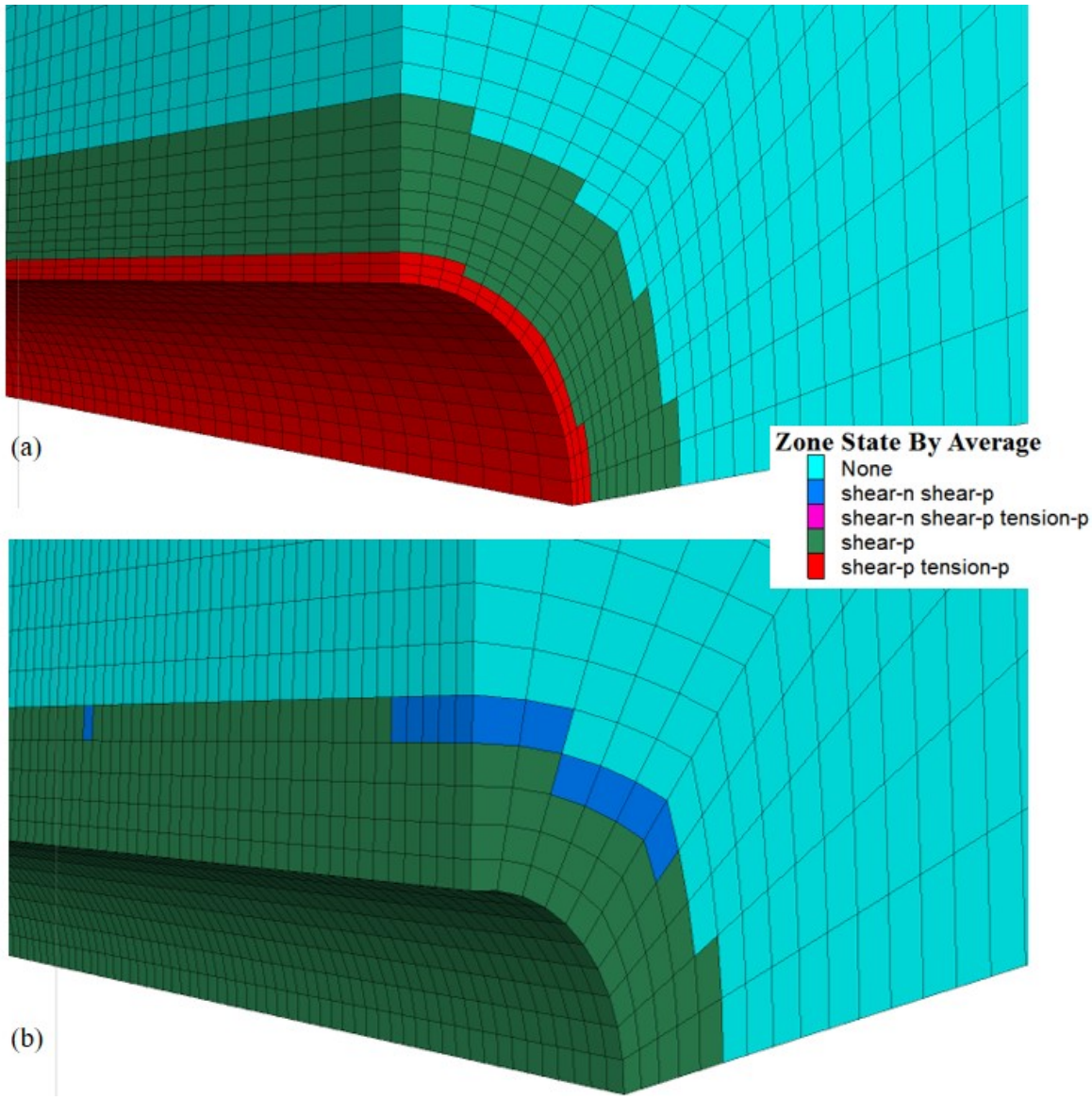

Figure 5.9: Plastic radii of various mesh properties - "original mesh" properties (a) and "treated mesh" properties (b).

5.3.2 Plastic radii for varying cohesion

Due to the fact that the plastic radii appear to be higher for undrained conditions than for dry ones, the relationship of the plastic radii for different conditions is investigated. The models with the parameter sets "R5_OB-var._P29_E3_C0.5" and "R5_OB-var._P29_E3_C1.5" (both with varying overburden) are analyzed to show the development of the plastic radius for different conditions. Figure 6.2 shows that the lower the cohesion, the higher the normalized plastic radii are for dry and undrained conditions.

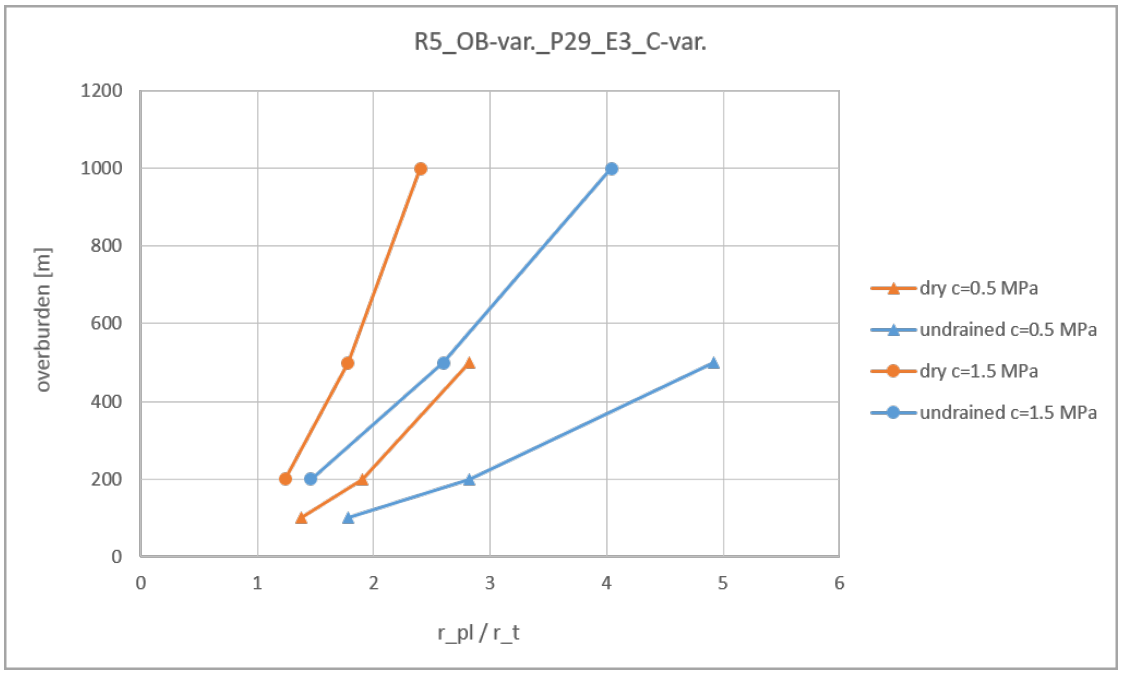

Figure 5.10: Normalized plastic radii for parameter sets "R5_OB-var._P29_E3_C-var." with varying overburden and shear strength.

5.3.3 Plastic radii for varying tunnel radii

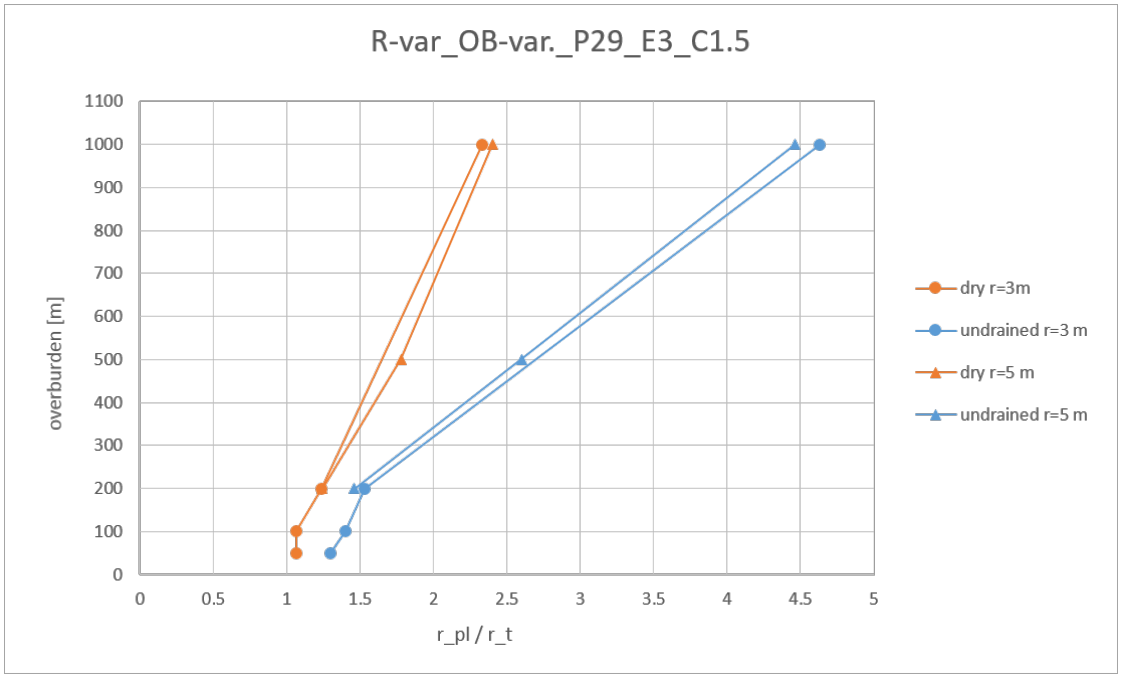

Figure 5.11: Normalized plastic radii vs. overburden for parameter sets "R-var._OB-var._P29_E3_C1.5" with varying tunnel radius and overburden.

Figure 5.11 illustrates the development of the normalized plastic radii versus the overburden, respectively the effective stress state. The model "R-var._OB-var._P29_E3_C1.5" with varying tunnel radius and overburden is analyzed for dry and undrained conditions. It is observed that a varying tunnel radius of 3 and 5 m does not lead to a significant difference in the normalized plastic radius for dry and undrained conditions.

5.3.4 Plastic radii for varying stiffness

In figure 5.12 the dry normalized plastic radii are plotted versus the undrained normalized plastic radii. For the parameter sets of "R-var._OB-var._P29_E3_C-var." the trend is linear. Figure 5.12 shows that various friction angles respectively Young's moduli give different normalized plastic radii for dry and undrained conditions. Higher friction angles and stiffness lead to significantly higher normalized plastic radii. In a further step additional investigations regarding the impact of the Young's modulus have been carried out.

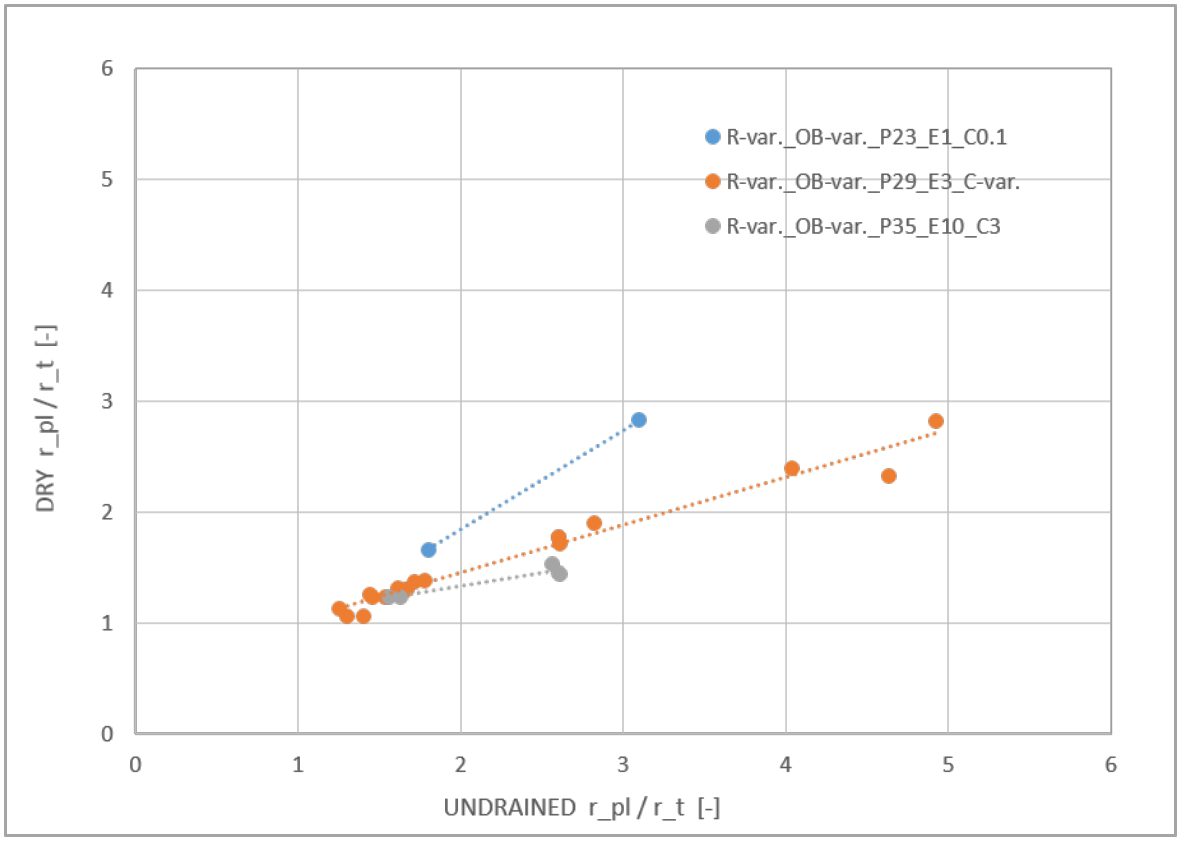

Figure 5.12: Normalized plastic radii for dry and undrained conditions.

The influence of different Young's moduli on the plastic radii is presented in figure 5.13.

The input parameters are referred to "R5_OB-var._P29_E-var._C3" by varying the Young's modulus and the overburden. The undrained normalized plastic radius is higher for $E = 10000\,MPa$ compared to $E = 3000\,MPa$ for the same overburden. While the dry normalized plastic radius does not change, whether $E = 3000\,MPa$ or $E = 10000\,MPa$.

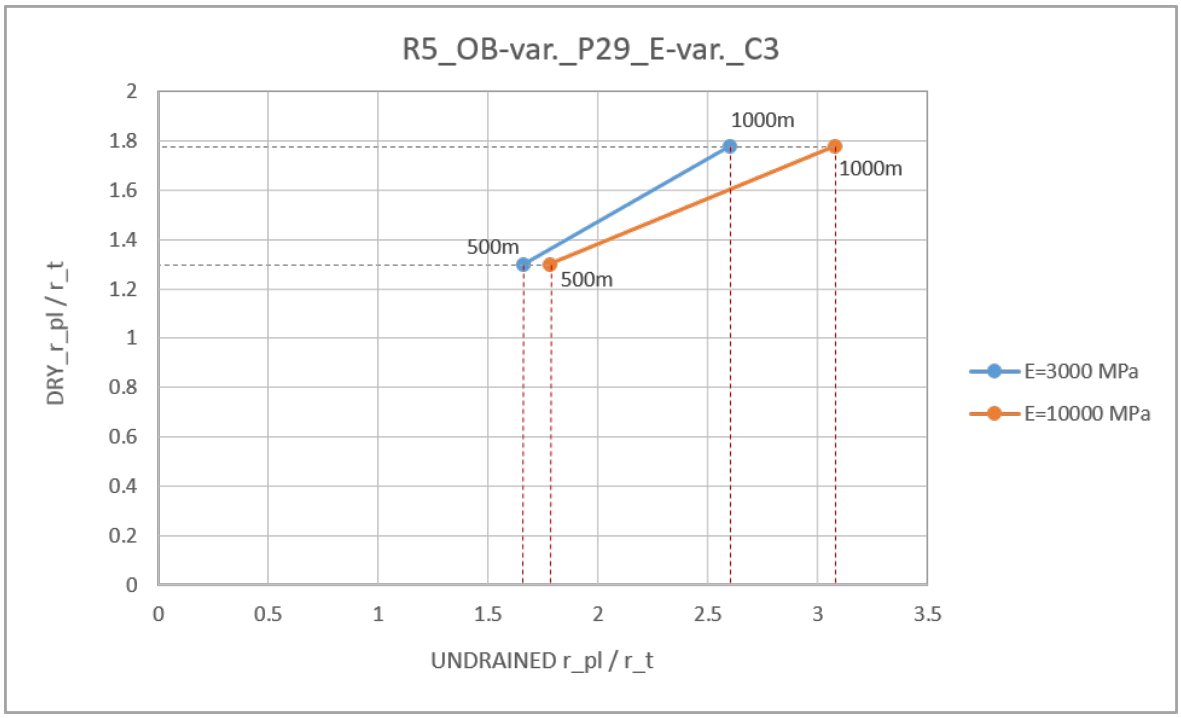

Figure 5.13: Development of normalized plastic radii for dry and undrained cases due to different Young's moduli.

5.4 Normalized radial displacements vs. normalized plastic radii

Vlachopoulos & Diederichs (2009) compared the normalized radial displacements against the normalized plastic radii - depicted in figure 3.6. This is done for all calculations of the current thesis as well, illustrated in figure 5.14. It is observed that the numerical calculations with dry conditions do not follow the trend according to Vlachopoulos & Diederichs (2009). While the results are mostly below the trend of *Vlachopoulos and Diederichs*, the results of the simulations for undrained conditions are generally higher.

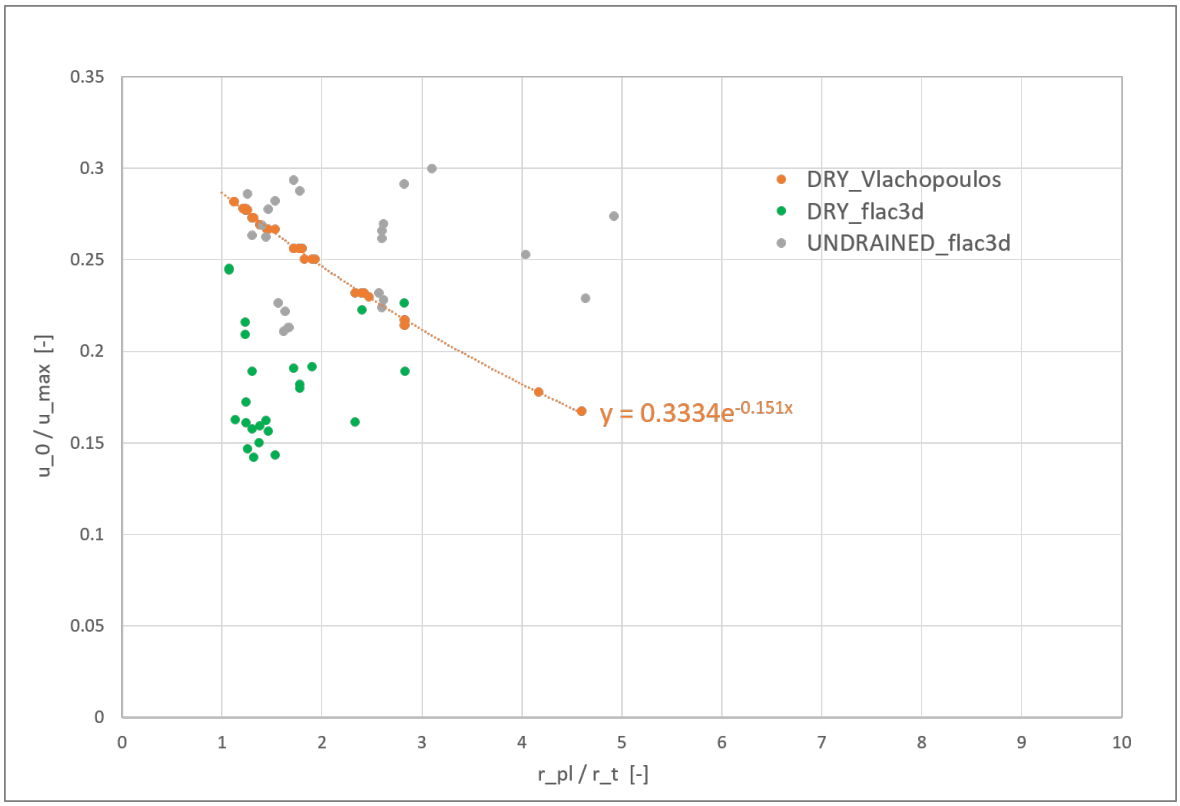

Figure 5.14: Normalized radial displacements vs. normalized plastic radii of numerical analysis compared to the analytical approaches of Vlachopoulos & Diederichs (2009).

5.4.1 Normalized radial displacements with varying mesh properties

The deviations in figure 5.14 show that the mesh properties affect the dry normalized displacements. A comparative analysis is done with the "treated mesh" properties (shown in figure 5.15). It can be shown that the impact of mesh properties affects the normalized displacements by a factor of approximately 1.44 for dry and 1.4 for undrained analysis.

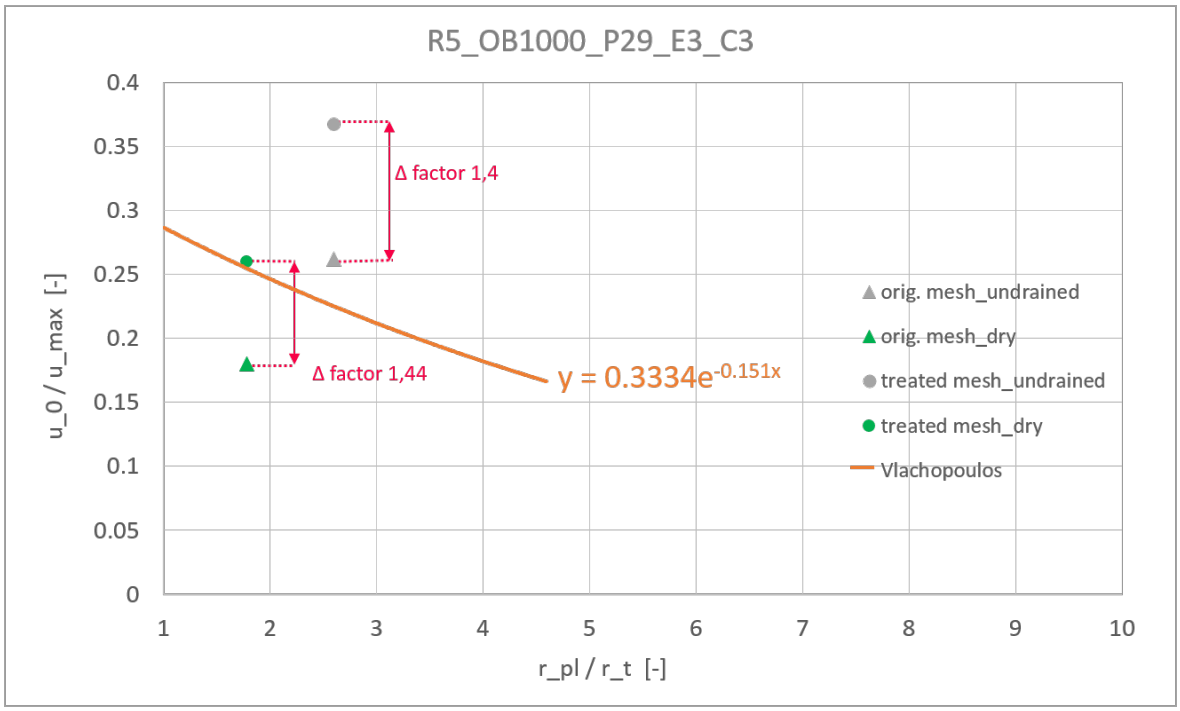

Figure 5.15: Deviation between the "original mesh" properties and the "treated mesh" properties

5.4.2 Analysis of normalized radial displacements

No obvious trend regarding the normalized radial displacements vs. the normalized plastic radii of the undrained results are recognized (figure 5.14). Hence, an intense analysis of related models is done. In table 5.2 all performed calculations are listed and ordered by analysis schemes, if minimal two models with comparable input parameters exist. Then each analysis scheme is investigated in terms of the normalized undrained plastic radii and finally the following combinations could be made:

- "AS 1" and "AS 4"
- "AS 2" and "AS 6"
- "AS 3" and "AS 7"
- "AS 5" and "AS 8"

The stiffness and strength parameters are equal within the combinations, although the tunnel radius and the overburden respectively the stress state are varying.

	model	analysis scheme [AS]
Radius 3 m	R3_OB50_P23_E1_C0.1	
	R3_OB50_P29_E3_C1.5	AS 1
	R3_OB100_P29_E3_C1.5	
	R3_OB200_P29_E3_C1.5	
	R3_OB1000_P29_E3_C1.5	
	R3_OB500_P29_E3_C3	
	R3_OB500_P35_E10_C3	AS 2
	R3_OB1000_P35_E10_C3	
Radius 5 m	R5_OB100_P29_E3_C0.5	AS 3
	R5_OB200_P29_E3_C0.5	
	R5_OB500_P29_E3_C0.5	
	R5_OB200_P29_E3_C1.5	AS 4
	R5_OB500_P29_E3_C1.5	
	R5_OB1000_P29_E3_C1.5	
	R5_OB500_P29_E3_C3	AS 5
	R5_OB1000_P29_E3_C3	
	R5_OB500_P35_E10_C3	AS 6
	R5_OB1000_P35_E10_C3	
Radius 7 m	R7_OB50_P29_E3_C0.5	AS 7
	R7_OB100_P29_E3_C0.5	
	R7_OB200_P29_E3_C1.5	
	R7_OB500_P29_E3_C3	AS 8
	R7_OB1000_P29_E3_C3	
	R7_OB1000_P35_E10_C3	

Table 5.2: Overview of the analyzed undrained models and classification in analysis scheme.

The following figures 5.16, 5.17, 5.18 and 5.19 show the different combinations according to the parameter sets of table 5.2. All combinations show that the trend proceeds more or less horizontally. Figure 5.19 also contains the analysis with the ”treated mesh” properties for the model sets ”R5_OB500_P29_E-var._C3” and ”R5_OB1000_P29_E-var._C3” with higher normalized radial displacements compared to the ”original mesh” properties.

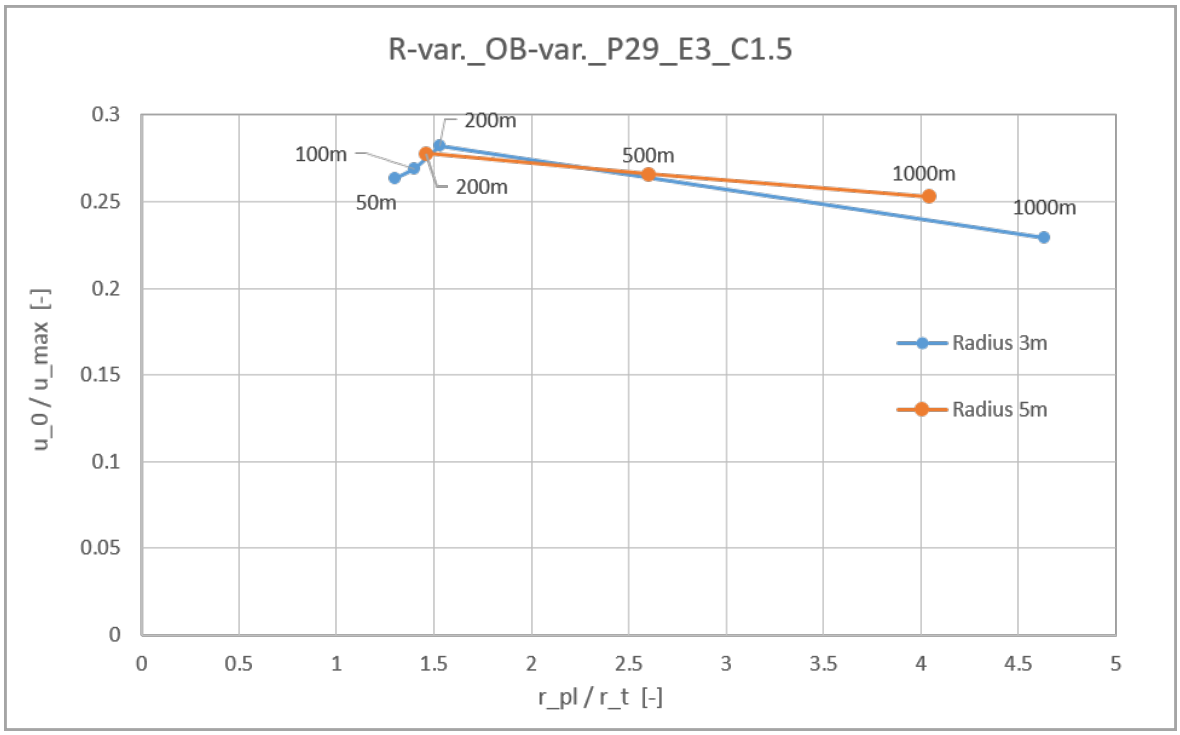

Figure 5.16: Undrained normalized displacements - combination of "AS 1" and "AS 4"

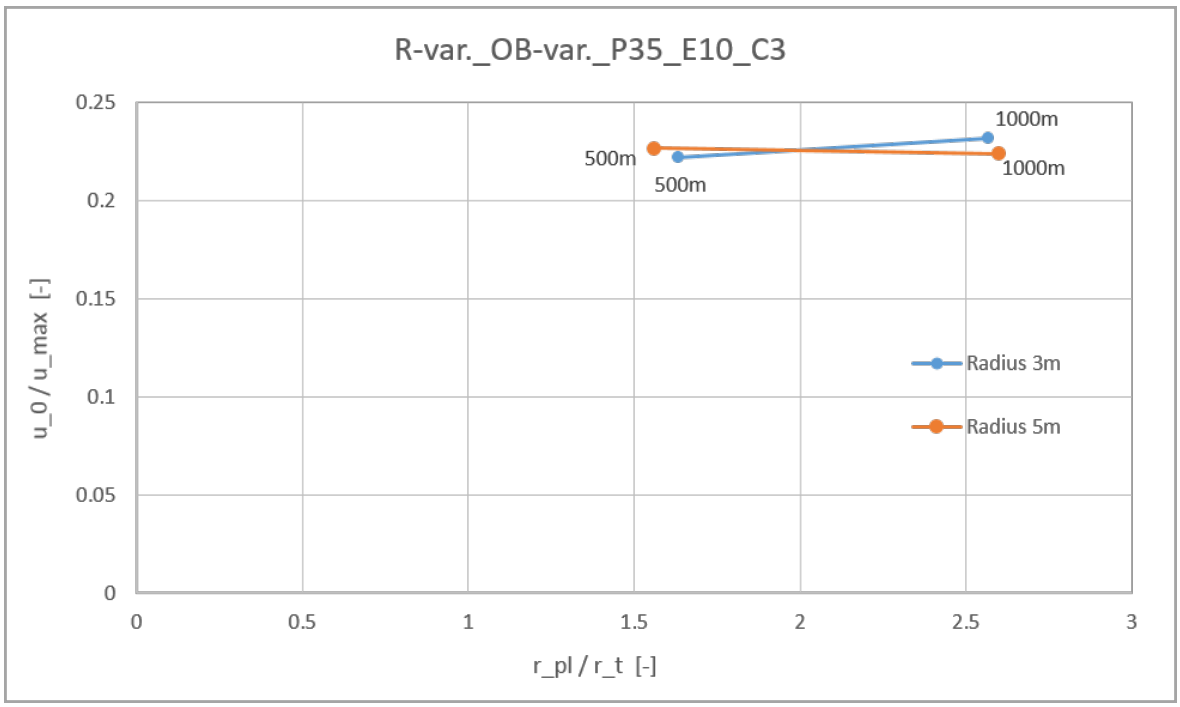

Figure 5.17: Undrained normalized displacements - combination of "AS 2" and "AS 6"

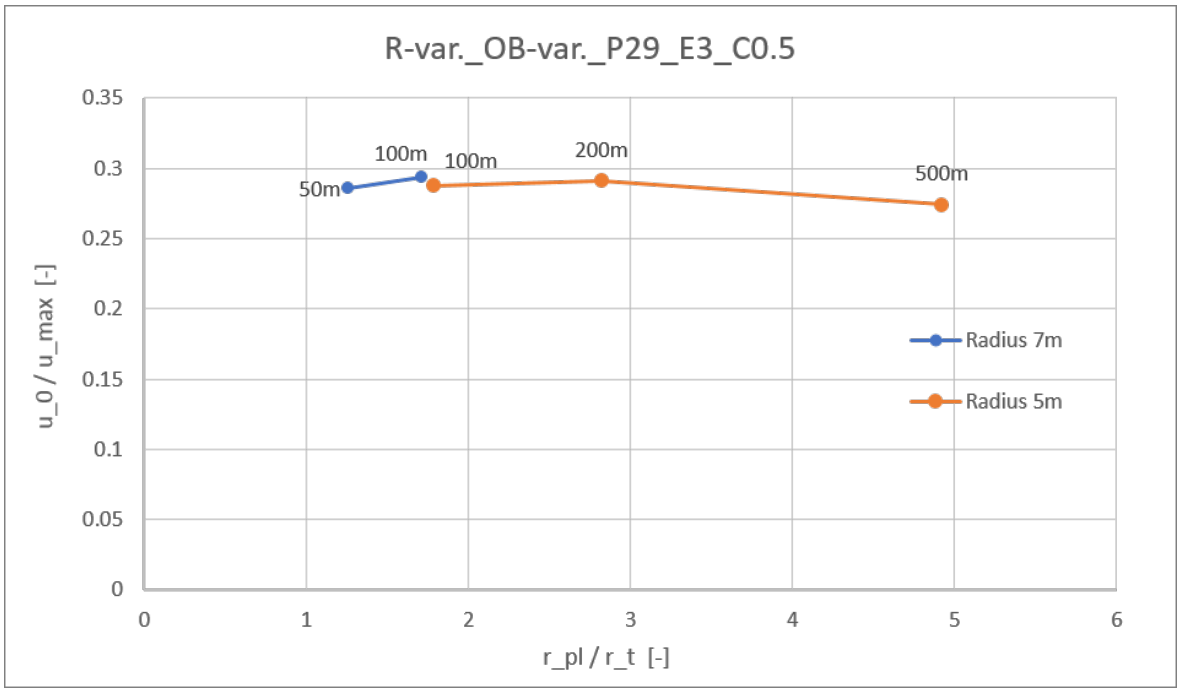

Figure 5.18: Undrained normalized displacements - combination of "AS 3" and "AS 7"

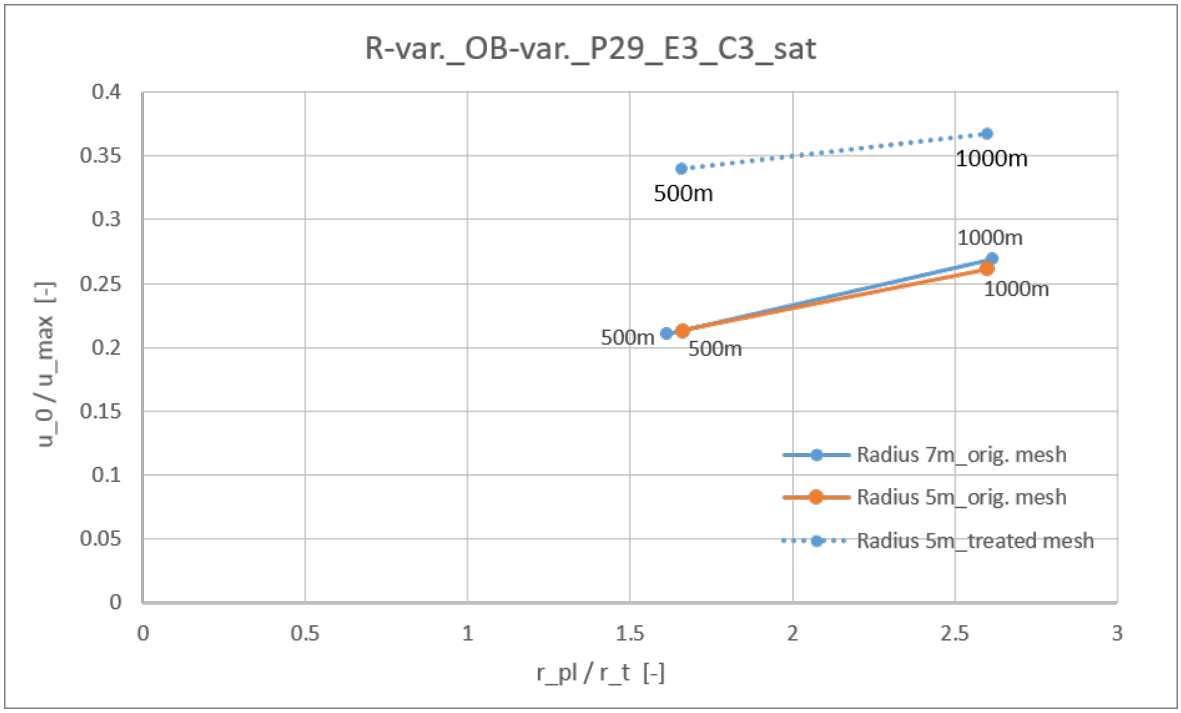

Figure 5.19: Undrained normalized displacements - combination of "AS 5" and "AS 8"

6 Discussion

6.1 Comparison of radial displacements from analytical and numerical analysis

The parameter set "R5_OB1000_P29_E3_C3" is used to compare the radial displacements of the analytical and the numerical calculations for dry and undrained conditions (figures 5.1 and 5.4). The "treated mesh" properties have been applied for the numerical simulations. The analytical and numerical results in radial displacements are summarized in table 6.1. It can be shown that the analytical radial displacements correspond with the numerical ones for dry and undrained conditions. This confirms the correctness of the "treated mesh" properties of the numerical model. By using the "original mesh" properties the radial displacements are overestimated (figure 5.7).

radial displacements $[m]$		
	dry	undrained
Analytical results	0.104	0.095
Numerical results	0.103	0.090

Table 6.1: Comparison of the analytical and numerical analysis for radial displacements in [m] by using the "treated mesh" properties.

6.2 Longitudinal displacement profile

The LDP's for undrained conditions show approximately 40 % higher ratios of displacement at the face (u_0/u_{max}) compared to dry conditions (figure 5.2 and 5.3). Due to the higher plastic radii in undrained conditions, the displacements occur earlier around of the face. This

means that in the undrained GCC plasticity is reached at a higher internal pressure compared to the dry GCC (figure 5.1). Therefore the normalized radial displacements at the face (u_0/u_{max}) are higher for undrained conditions.

In the undrained LDP's, the range of various radial displacements behind the face is much greater than for dry conditions (figure 5.2 and 5.3). Larger plastic radii lead to an extended influence length of the excavation. This is valid for dry and undrained ground conditions.

Both, in dry and undrained ground conditions the pre-displacements start approximately at station 40 (∼2D ahead of the face), whereas about from station 50 higher pre-displacements of the undrained ground are achieved (figure 5.4). Three different trends can be noticed by investigating the development of pre-displacements (figure 5.2 and 5.3). This is caused by the different tunnel radii. The smaller the tunnel radius, the closer to the face the pre-displacements develop. If the x-axis of the LDP is referred to the tunnel radius (figure 5.5) a uniform development of the LDP is achieved. This means that there is a linear correlation between tunnel radius and displacement for undrained conditions.

The influence of a varying cohesion on the results is investigated (figure 5.6). By fixing all other input parameters the development of the LDP's is different. A higher cohesion leads to smaller pre-displacements ahead of the face. Hence, different displacement developments start approximately 10 m ahead of the face and lead to smaller normalized displacements at the face if the cohesion is higher. With higher shear strength the influence length is shorter behind the face. Therefore the maximal normalized displacements are achieved earlier, which means closer to the face. This phenomenon in displacement development is as similar behind the face for dry and undrained ground, as the mentioned displacement developments of various tunnel radii in this chapter previously.

Different mesh properties influence the radial displacements (figure 5.7). Vlachopoulos & Diederichs (2009) also published the significant impact of the modeled excavation length on radial displacements. For this reason the excavation length (set to 1 m) is sufficient small for the performed analyses. However the relationship between excavation length and the single element length may also have a significant impact on the face displacements. Thus the

"treated mesh" contains two elements each excavation step, while the element length corresponds to each excavation length for the "original mesh" (figure 4.3). Figure 6.1 demonstrates the impact of face displacements for different mesh properties in detail. Just ahead of the face the displacement development with "original mesh" properties (orange) is drifting off and results in smaller face displacements. This leads to distortions of the normalized displacements.

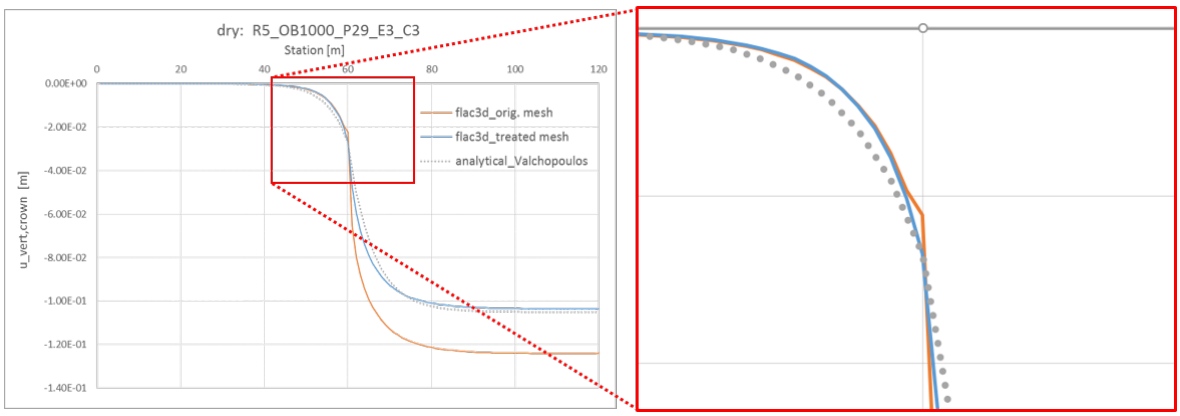

Figure 6.1: Differences of the "original" vs. the "treated mesh" properties - referred to figure 5.7

6.3 Plastic radii

The plastic zone develops larger in undrained ground (figure 5.8). Due to the reduction of the total stresses (equation 2.8), the resistance against shear stress is reduced. Therefore the undrained plastic radii are generally higher than under dry conditions. There are no changes in plastic radii when changing the mesh properties (figure 5.9). Consequently all analyzed plastic radii of dry and undrained ground behaviour are not affected by the changed mesh properties.

Generally, the higher the shear strength, the lower is the plastic radius (figure 5.10). If the overburden increases, the difference in plastic radii between dry and undrained conditions is becoming larger. Thus the relationship of normalized plastic radii for dry and undrained conditions is investigated. By considering the formulas of the uniaxial compression strength and the plastic radius for dry conditions (equations 4.1 and 4.4), a linear influence of the cohesion on the dry plastic radii is established. In figure 6.2 the ratios of $\mathbf{a}/\mathbf{b}$ and $\mathbf{c}/\mathbf{d}$ are equivalent. Therefore the impact of shear strength on the normalized plastic radii remains linear for both, dry and undrained ground behaviour.

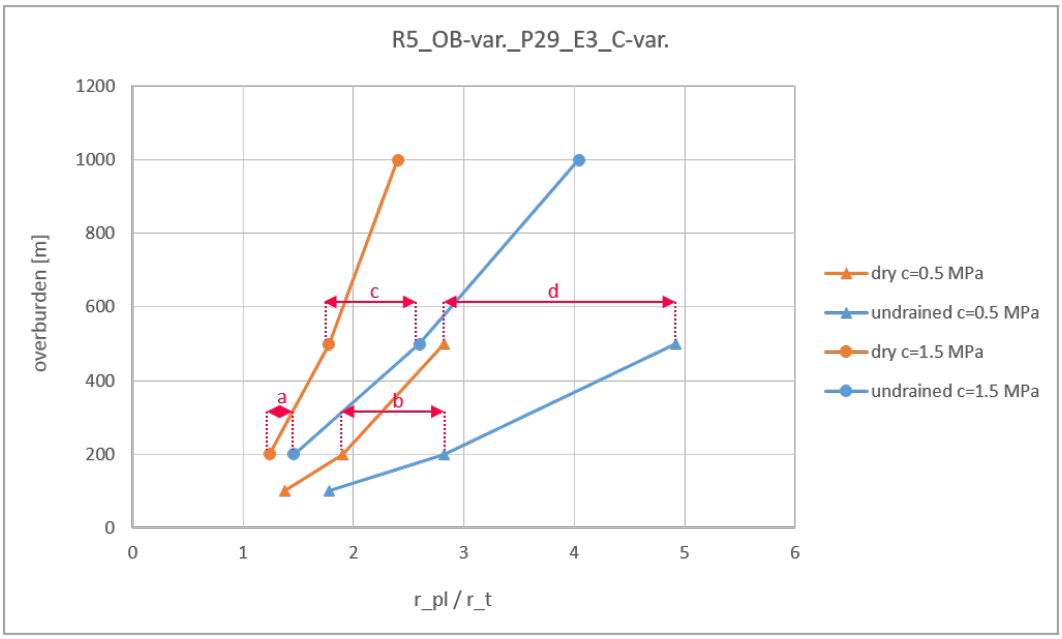

Figure 6.2: Influence of the cohesion on the plastic radii for dry and undrained conditions.

It is obtained that the stiffness of the undrained ground affects the normalized plastic radius (figures 5.12 and 5.13). A higher stiffness increases the undrained normalized plastic radius. For the dry case, the Young's modulus has no impact on the plastic radius (equation 4.4). Subsequently the question of why the undrained plastic radius is higher in stiffer ground, arises. For this reason the pore pressure distributions for the parameter sets of "R5_OB1000_P29_E-var._C3" with varying Young's moduli of $E = 3000\,MPa$ and $E = 10000\,MPa$ are investigated. The results in pore pressure distribution are shown in figure 6.3. It can be observed that the pore pressure is higher in the vicinity of the tunnel in the model with $E = 10000\,MPa$. When considering the reduction to effective stresses due to the pore pressure (equation 2.8), the effective stresses become smaller. Therefore the resistance against shear failure is smaller for the model with $E = 10000\,MPa$. This leads to a higher plastic radius. As a next step, the reason for the higher pore pressure distribution in the model with $E = 10000\,MPa$ is investigated. According to the user manual the theory of *Skempton (1954)* is used in $FLAC^{3D}$ (Itasca, 2016) to calculate the effective stresses. Coefficient B is defined as the relationship in compressibility between rock mass considering the porosity, and water. First the Young's moduli are converted to Bulk moduli (equation 2.7). Then the coefficients B are calculated as follows (equation 2.6):

- $B_{E=3000MPa} = 0.83$
- $B_{E=10000MPa} = 0.60$

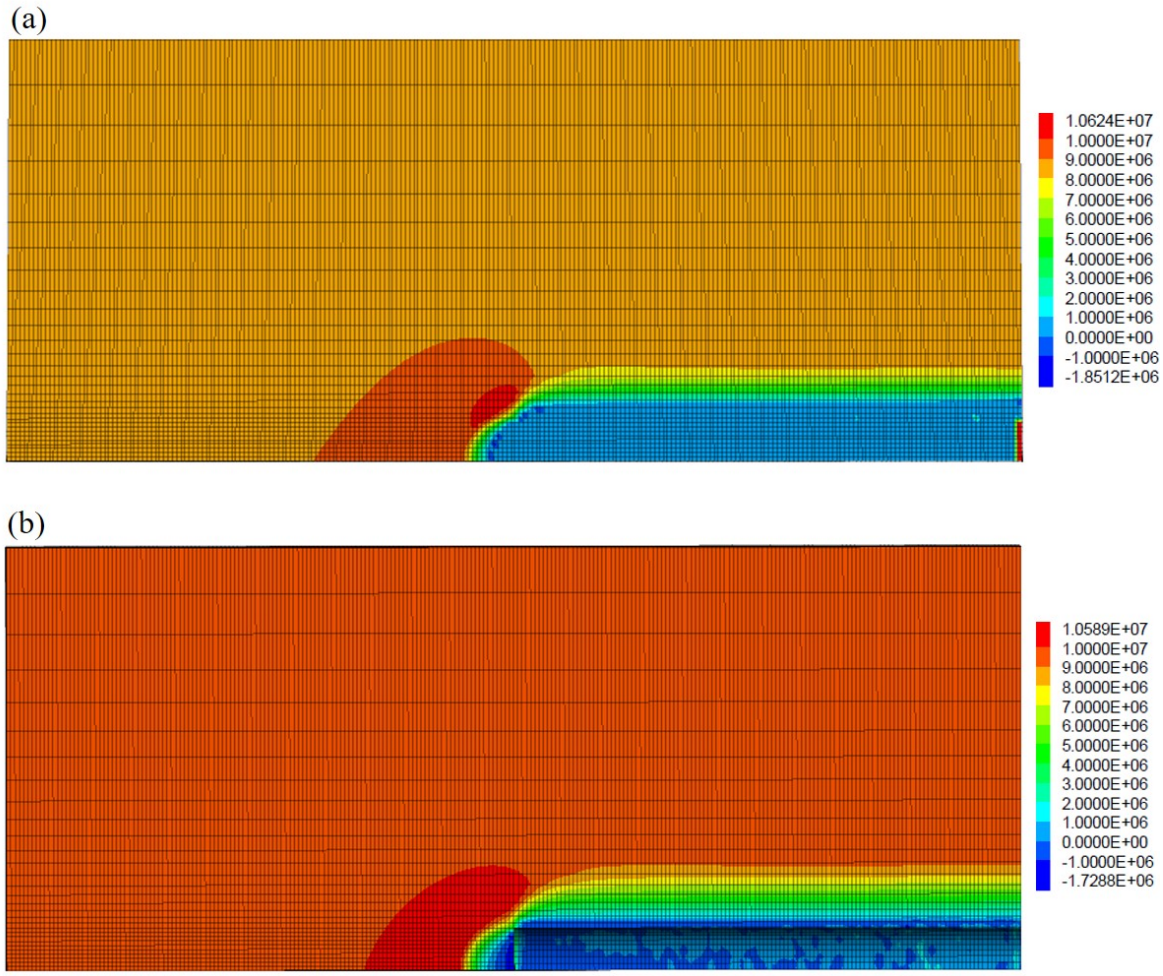

Figure 6.3: Pore pressure distribution for the parameter sets "R5_OB1000_P29_E-var._C3" with various Young's moduli - (a) E=3000 MPa; (b) E=10000 MPa

The calculated pore pressure coefficients B are smaller than $B = 1$ (for saturated soils). The effect of the grain compressibility is significant for rocks, because the compressibility of the rock mass is not negligible compared to the compressibility of water (Bulk modulus ~2 GPa) (Yang, J., 2005). Additionally, Coussy (2004) shows the relationship between the Skempton coefficient (with incompressible matrix) and the Biot's coefficient with considered matrix compressibility. Due to the higher coefficient of $B_{E=3000MPa}$, the drop in pore pressure is higher. The smaller Young's modulus leads to higher negative volumetric strains. Therefore the reduction of the pore water pressure is higher. Consequently the reduction of pore pressure in "weak" rock mass is higher. Finally this leads to a higher pore pressure distribution in the model with $E = 10000\,MPa$.

6.4 Normalized radial displacements vs. normalized plastic radii

In terms of the normalized displacements vs. the normalized plastic radii (figure 5.14) the numerical results for dry conditions do not follow the trend according to Vlachopoulos & Diederichs (2009). The reason is found by applying different mesh properties. The form of the single elements of the mesh highly influences the normalized displacements. By doing additional calculations with "treated mesh" properties, a approximately systematical factor can be found (figure 5.15). The normalized radial displacements increase by this factor, while the normalized plastic radii remain constant. This is obtained from parameter sets of "R5_OB500_P29_E3_C3" and "R5_OB1000_P29_E3_C3" for dry and undrained ground conditions (see the parallel trends in figure 5.19). In terms of undrained conditions no obvious correlation between the normalized displacements (u_0/u_{max}) and the normalized plastic radii (r_{pl}/r_t) for undrained ground conditions is found. This means that all comparable results for undrained conditions do not show any significant changes in normalized displacements for increased normalized plastic radii (figure 5.16, 5.17, 5.18 and 5.19).

Furthermore it is obtained that the impact of different tunnel radii on both, the normalized radial displacements and the normalized plastic radii is negligible for undrained conditions (figures 5.11, 5.17 and 5.19).

7 Conclusion and outlook

The current thesis leads to following conclusions:

- Undrained ground behaviour leads to larger plastic zones compared to dry ground conditions. The plastic radius for undrained conditions is linearly related to the shear strength.
- The longitudinal displacement profiles (LDP) of undrained ground conditions contain approximately 40 % higher normalized pre-displacements (u_0/u_{max}) compared to dry ground conditions, due to larger plastic radii.
- Higher spreading of normalized radial displacements is noticed behind the face. Larger plastic radius increases the influence length of the excavation.
- No correlations have been found between the normalized radial displacements and the normalized plastic radius for undrained ground conditions.
- The tunnel radius does have negligible influence on both, the normalized plastic radius and the normalized displacements for undrained ground behaviour.
- The stiffness (Young's modulus) has an impact on the undrained plastic radius. Higher stiffness leads to larger undrained plastic radii.
- The mesh discretization influences the normalized radial displacements. A cubical form of the single elements of the mesh is recommended.

The current thesis confirms the influences of the rockmass-stiffness on the plastic radius. A further step is to investigate the relationship of the Young's modulus on the undrained plastic radius and consequently on the displacement development. It is recommended to do a mesh study before the main simulations are started. When doing undrained numerical analysis it is recommended to carefully evaluate convergence criteria, as they may differ for dry and undrained conditions.

8 Summary

Water, especially the pore water pressure affects the rock mass behaviour. The aim of this thesis is to show how pore water influences the displacement development due to tunnel excavation. The approach of the Convergence Confinement Method (CCM) to assume the displacement development, does not consider water. Consequently analytical and numerical analyses of dry and undrained ground conditions were done to show the differences in radial displacement development.

Analytical displacements were calculated with formulas according to Sulem et al. (1987) and Anagnostou (2009). Thus, the Longitudinal Displacement Profile (LDP) was plotted according to the procedure proposed by Vlachopoulos & Diederichs (2009). The numerical analysis was done with models for dry and for undrained ground conditions. The model was assumed as an axisymmetrical, deep, circular tunnel with homogeneous isotropic ground conditions, applying the Mohr-Coulomb failure criterion. Different sets of input parameters with varying tunnel radii, stress levels, stiffnesses and shear strengths were used for the analysis of dry and undrained conditions. The numerical analysis is based on effective input parameters. The defined fluid modulus, the porosity of the rock mass and the density of water consider the impact of water on the undrained ground behaviour. Concerning the undrained analysis, influence of time dependent behaviour is neglected in this thesis. Thus the short term behaviour is analyzed, which is more favorable than the long term behaviour (Anagnostou, 2006). Finally the dry and undrained results are compared in terms of LDP, plastic radius and mesh impacts.

Radial displacements remain smaller in undrained conditions. This is checked by analytical approaches according to Anagnostou (2009). The radial displacements at the face are approximately 40 % higher for undrained conditions, compared to dry conditions. No correlation between the normalized radial displacements and the normalized plastic radii is observed. In undrained conditions, the excavation influenced length is larger than in dry conditions. The

reason of this lies in the higher undrained plastic radii compared to the plastic radii for dry ground conditions. The cohesion affects the normalized plastic radii linearly in both, dry and undrained conditions. Furthermore the analysis shows impacts of the Young's modulus on the plastic radius for undrained conditions. Higher Young's moduli lead to larger plastic radii for undrained conditions. The tunnel radius has negligible impact on the normalized plastic radius (r_{pl}/r_t). Cubical mesh elements are recommended to avoid inaccuracies in displacements.

Additional numerical analysis should be done to evaluate the influence of stiffness on the ground behaviour in detail. Furthermore the convergence criterion has to be considered carefully for undrained numerical analysis.

Bibliography

Alam, M. M., Borre, M. K., Fabricius, I. L., Hedegaard, K., Røgen, B., Hossain, Z., & Krogsbøll, A. S. (2010). Biot's coefficient as an indicator of strength and porosity reduction: Calcareous sediments from kerguelen plateau. *Journal of Petroleum Science and Engineering*, *70*(3-4), 282–297.

Amann, F., Wild, K., & Wymann, L. (2014). Dependency of deformability, strength and failure characteristics of clay shales on total suction. *Rock Engineering and Rock Mechanics: Structures in and on Rock Masses*, 1423–1426.

Anagnostou, G. (2006). *Tunnel stability and deformations in water-bearing ground.* Zuerich, Switzerland: Eurock 06, ISRM Symposium on Multiphysics coupling and long term behaviour in rock mechanics, Belgium.

Anagnostou, G. (2009). *The effect of advanced-drainage on the short-term behaviour of squeezing rocks in tunneling.* Zuerich, Switzerland: International Symbosium on Computational Geomechanics, France.

Biot, M. A. (1941). General Theory of Three–Dimensional Consolidation. *Journal of Applied Physics*, *12*(2), 155–164.

Coussy, O. (2004). *Poromechanics. Mechanics of porous continua.* (2nd ed. ed.). Chichester: Wiley.

Feder, G. & Arwanitakis, M. (1976). Zur Gebirgsmechanik ausbruchsnaher Bereiche tiefliegender Hohlraumbauten. *BHM*, *4*(Jg. 121), 103–117.

Gschwandtner, G. G. (2010). *Analytische Berechnungsverfahren zum Kennlinienverfahren.* Master's Thesis, Montanuniversität Leoben.

Itasca, C. (2016). *FLAC3D: Fast Lagrangian Analysis of Continua in 3 Dimensions - Users Guide* (Version 6.0 ed.). Minnesota: Itasca Consulting Group Inc.

Kainrath, S., Gschwandtner, G., & Galler, R. (2009). The convergence confinement method as an aid in the design of deep tunnels. *Geomechanik und Tunnelbau*, *2*(5), 553–560.

OEGG (2010). *Guidline of the Geotechnical Design of Underground Structures with Conventional Excavation* (Translated from version 2.1 ed.). Salzburg: Austrian Society for Geomechanics.

Oreste (2009). The Convergence-Confinement Method: Roles and Limits in Modern Geomechanical Tunnel Design. *American Journal of Applied Sciences*, *6*(4), 757–771.

Panet, M. & Guenot, A. (1982). Analysis of convergence behind the face of a tunnel. *Proceedings of the 3rd international symposium, Tunneling 82*, 197–204.

Radoncic, N. (2011). *Tunnel design and prediction of system behaviour in weak ground.* Doctoral Thesis, Graz University of Technology, Graz.

Radoncic, N., Pilgersdorfer T., & Schubert W. (2009). *PREDICTION OF DISPLACEMENTS IN TUNNELS.* Graz, Austria: Institute for Rock Mechanics and Tunnelling, Graz University of Technology.

Schwaiger, H. (2016). *Lecture notes in Computational Geotechnics: Part 1 - Introduction.* Graz: Institute for Soil Mechanics and Foundation Engineering, Graz University of Technology.

Skempton, A. W. (1954). The Pore-Pressure Coefficients A and B. *Géotechnique*, *4*(4), 143–147.

Sulem, J., Panet, M., & Guenot, A. (1987). An analytical solution for time-dependent displacements in a circular tunnel. *International Journal of Rock Mechanics and Mining Sciences & Geomechanics Abstracts*, *24*(3), 155–164.

Terzaghi, K. (1936). *The shearing resistance of saturated soils and the angle between the planes of shear*, volume 1. Cambridge.

Vlachopoulos, N. & Diederichs, M. S. (2009). Improved Longitudinal Displacement Profiles for Convergence Confinement Analysis of Deep Tunnels. *Rock Mechanics and Rock Engineering*, *42*(2), 131–146.

Vogelhuber, M. (2007). *Der Einfluss des Porenwasserdrucks auf das mechanische Verhalten kakiritisierter Gesteine.* Dissertation, ETH Zuerich, Zuerich.

Yang, J. (2005). Pore pressure coefficient for soil and rock and its relation to compressional wave velocity. *Geotechnique, 2005, v.55, n.3*, 251–256.

Appendix A - Results of dry analysis using the ”original mesh” properties

number	1	2	3	4	5	6	7	8	9	10	11
model	**R3_OB50_P23_E1_C0.1**	**R3_OB50_P29_E3_C1.5**	**R3_OB100_P29_E3_C1.5**	**R3_OB200_P29_E3_C1.5**	**R3_OB500_P29_E3_C3**	**R3_OB500_P35_E10_C3**	**R3_OB1000_P29_E3_C1.5**	**R3_OB1000_P35_E10_C3**	**R5_OB100_P29_E3_C0.5**	**R5_OB200_P29_E3_C0.5**	**R5_OB200_P29_E3_C1.5**
pl. Radius [m]	8.5	3.2	3.2	3.7	3.9	3.7	7	4.6	6.9	9.5	6.2
pl. Rad._analytical [m]	8.6	0	0	3.7	4	3.6	7.3	4.5	7.1	9.5	6.1
shear strength c' [Mpa]	0.1	1.5	1.5	1.5	3	3	1.5	3	0.5	0.5	1.5
friction angle	23	29	29	29	29	35	29	35	29	29	29
Young's Modulus [Mpa]	1000	3000	3000	3000	3000	10000	3000	10000	3000	3000	3000
UCS [Mpa]	0.302167	5.092989	5.092989	5.092989	10.18598	11.52589	5.092989	11.52589	1.697663	1.697663	5.092989
Overburden [m]	50	50	100	200	500	500	1000	1000	100	200	200
Sigma 0 effective [Mpa]	1.25	1.25	2.5	5	12.5	12.5	25	25	2.5	5	5
UCS / Sigma 0,eff	0.241734	4.074391	2.037196	1.018598	0.814878	0.922071	0.20372	0.461036	0.679065	0.339533	1.018598
tunnelradius [m]	3	3	3	3	3	3	3	3	5	5	5
rpl/rt	2.833333	1.066667	1.066667	1.233333	1.3	1.233333	2.333333	1.533333	1.38	1.9	1.24
u0/umax	0.189295	0.244648	0.245269	0.216077	0.189179	0.209098	0.161201	0.14316	0.15919	0.191496	0.172194
Station	z_disp	z_disp	z_disp	z_disp	z_disp	z_disp	z_disp	z_disp	z_disp	z_disp	z_disp
1	-5.53E-08	-2.45E-08	-2.47E-08	-2.44E-08	-2.42E-08	-7.33E-09	-1.77E-08	-6.69E-09	-1.25E-06	-2.41E-06	-2.28E-06
2	5.16E-09	-1.73E-08	-1.58E-08	-1.39E-08	3.22E-09	-1.15E-09	2.62E-07	1.48E-08	-1.51E-06	-3.28E-06	-2.70E-06
3	4.69E-08	-1.26E-08	-3.93E-09	1.66E-08	6.73E-08	1.89E-08	5.27E-07	6.32E-08	-1.61E-06	-3.72E-06	-2.87E-06
4	2.01E-08	-5.39E-09	6.58E-09	3.93E-08	1.30E-07	3.46E-08	5.13E-07	9.03E-08	-1.68E-06	-3.87E-06	-2.98E-06
5	-4.13E-08	-2.45E-09	1.55E-08	5.38E-08	1.73E-07	5.12E-08	4.00E-08	7.80E-08	-1.73E-06	-3.98E-06	-3.04E-06
6	-8.83E-08	-3.67E-09	1.36E-08	6.74E-08	1.97E-07	5.74E-08	-2.22E-07	1.03E-07	-1.76E-06	-4.01E-06	-3.10E-06
7	-8.27E-08	-1.99E-09	1.66E-08	7.44E-08	1.62E-07	6.93E-08	-1.02E-07	1.30E-07	-1.81E-06	-4.04E-06	-3.16E-06
8	-7.49E-08	-2.23E-09	2.00E-08	7.73E-08	1.41E-07	4.66E-08	-2.14E-07	1.07E-07	-1.87E-06	-4.03E-06	-3.24E-06
9	-5.16E-11	2.77E-09	2.64E-08	7.73E-08	2.27E-07	6.20E-08	1.11E-07	1.45E-07	-1.92E-06	-4.04E-06	-3.36E-06
10	5.92E-08	6.15E-09	2.01E-08	7.41E-08	1.62E-07	6.18E-08	3.73E-07	1.48E-07	-2.00E-06	-4.09E-06	-3.49E-06
11	1.51E-07	8.56E-09	3.80E-08	9.21E-08	2.37E-07	6.38E-08	7.75E-07	1.47E-07	-2.09E-06	-4.16E-06	-3.64E-06
12	2.47E-07	1.08E-08	4.16E-08	1.14E-07	2.01E-07	9.43E-08	1.18E-06	2.01E-07	-2.20E-06	-4.26E-06	-3.83E-06
13	3.14E-07	1.98E-08	3.90E-08	1.23E-07	2.64E-07	1.03E-07	1.58E-06	2.01E-07	-2.33E-06	-4.42E-06	-4.05E-06
14	4.06E-07	1.53E-08	5.35E-08	1.22E-07	2.87E-07	1.14E-07	1.88E-06	2.62E-07	-2.49E-06	-4.63E-06	-4.30E-06
15	4.92E-07	2.00E-08	5.45E-08	1.33E-07	3.48E-07	1.07E-07	2.21E-06	2.87E-07	-2.66E-06	-4.91E-06	-4.64E-06
16	5.77E-07	2.12E-08	6.18E-08	1.34E-07	4.03E-07	1.15E-07	2.39E-06	2.82E-07	-2.87E-06	-5.26E-06	-4.98E-06
17	6.23E-07	2.53E-08	7.18E-08	1.65E-07	3.89E-07	1.25E-07	2.71E-06	2.80E-07	-3.15E-06	-5.70E-06	-5.42E-06
18	6.79E-07	2.51E-08	7.02E-08	1.56E-07	3.43E-07	1.25E-07	2.80E-06	2.90E-07	-3.41E-06	-6.21E-06	-5.93E-06
19	7.28E-07	2.11E-08	6.53E-08	1.54E-07	3.45E-07	1.11E-07	2.86E-06	2.71E-07	-3.75E-06	-6.85E-06	-6.50E-06
20	7.69E-07	1.99E-08	5.90E-08	1.42E-07	2.92E-07	1.08E-07	2.94E-06	2.51E-07	-4.12E-06	-7.58E-06	-7.17E-06
21	7.90E-07	1.32E-08	5.08E-08	1.11E-07	2.26E-07	8.36E-08	2.77E-06	1.83E-07	-4.54E-06	-8.46E-06	-7.90E-06
22	7.97E-07	5.33E-09	3.30E-08	7.45E-08	1.37E-07	4.57E-08	2.62E-06	1.34E-07	-5.02E-06	-9.43E-06	-8.76E-06
23	7.61E-07	-2.14E-09	8.99E-09	5.06E-08	3.30E-08	2.89E-08	2.15E-06	2.81E-08	-5.57E-06	-1.06E-05	-9.74E-06
24	7.23E-07	-1.17E-08	-5.45E-09	-2.36E-08	-1.74E-07	-1.75E-08	1.56E-06	-7.14E-08	-6.21E-06	-1.20E-05	-1.08E-05
25	6.28E-07	-2.59E-08	-3.73E-08	-8.85E-08	-3.42E-07	-6.68E-08	8.45E-07	-2.03E-07	-6.92E-06	-1.35E-05	-1.21E-05
26	5.04E-07	-4.31E-08	-7.46E-08	-1.86E-07	-6.14E-07	-1.30E-07	6.00E-08	-3.77E-07	-7.71E-06	-1.53E-05	-1.35E-05
27	3.41E-07	-6.61E-08	-1.24E-07	-2.93E-07	-8.79E-07	-2.22E-07	-1.01E-06	-6.20E-07	-8.64E-06	-1.74E-05	-1.51E-05
28	1.52E-07	-9.61E-08	-1.77E-07	-4.22E-07	-1.27E-06	-3.27E-07	-2.46E-06	-8.25E-07	-9.68E-06	-1.97E-05	-1.69E-05
29	-1.20E-07	-1.34E-07	-2.51E-07	-5.78E-07	-1.68E-06	-4.58E-07	-4.12E-06	-1.15E-06	-1.09E-05	-2.25E-05	-1.91E-05
30	-4.42E-07	-1.72E-07	-3.21E-07	-7.75E-07	-2.20E-06	-5.83E-07	-6.38E-06	-1.53E-06	-1.22E-05	-2.56E-05	-2.14E-05
31	-8.18E-07	-2.18E-07	-4.17E-07	-9.98E-07	-2.80E-06	-7.55E-07	-8.65E-06	-1.97E-06	-1.37E-05	-2.92E-05	-2.41E-05
32	-1.26E-06	-2.77E-07	-5.35E-07	-1.27E-06	-3.51E-06	-9.41E-07	-1.16E-05	-2.48E-06	-1.55E-05	-3.33E-05	-2.72E-05
33	-1.86E-06	-3.46E-07	-6.85E-07	-1.58E-06	-4.27E-06	-1.16E-06	-1.54E-05	-3.11E-06	-1.75E-05	-3.81E-05	-3.08E-05
34	-2.57E-06	-4.29E-07	-8.45E-07	-1.96E-06	-5.29E-06	-1.44E-06	-1.97E-05	-3.84E-06	-1.98E-05	-4.36E-05	-3.49E-05
35	-3.34E-06	-5.29E-07	-1.06E-06	-2.33E-06	-6.43E-06	-1.74E-06	-2.46E-05	-4.70E-06	-2.25E-05	-4.99E-05	-3.96E-05
36	-4.39E-06	-6.35E-07	-1.28E-06	-2.86E-06	-7.81E-06	-2.13E-06	-3.09E-05	-5.70E-06	-2.56E-05	-5.73E-05	-4.50E-05
37	-5.53E-06	-7.93E-07	-1.57E-06	-3.44E-06	-9.35E-06	-2.55E-06	-3.76E-05	-6.96E-06	-2.91E-05	-6.58E-05	-5.13E-05
38	-6.93E-06	-9.41E-07	-1.88E-06	-4.15E-06	-1.14E-05	-3.08E-06	-4.67E-05	-8.34E-06	-3.32E-05	-7.58E-05	-5.86E-05
39	-8.66E-06	-1.15E-06	-2.25E-06	-5.05E-06	-1.37E-05	-3.75E-06	-5.68E-05	-1.01E-05	-3.80E-05	-8.75E-05	-6.72E-05
40	-1.08E-05	-1.37E-06	-2.71E-06	-5.91E-06	-1.65E-05	-4.51E-06	-6.96E-05	-1.22E-05	-4.36E-05	-1.01E-04	-7.72E-05
41	-1.33E-05	-1.64E-06	-3.25E-06	-7.23E-06	-2.02E-05	-5.39E-06	-8.45E-05	-1.46E-05	-5.03E-05	-1.17E-04	-8.89E-05
42	-1.63E-05	-1.98E-06	-3.90E-06	-8.84E-06	-2.40E-05	-6.50E-06	-1.03E-04	-1.76E-05	-5.81E-05	-1.37E-04	-1.03E-04
43	-2.01E-05	-2.36E-06	-4.74E-06	-1.07E-05	-2.92E-05	-7.79E-06	-1.26E-04	-2.12E-05	-6.74E-05	-1.60E-04	-1.20E-04
44	-2.48E-05	-2.87E-06	-5.74E-06	-1.27E-05	-3.56E-05	-9.44E-06	-1.55E-04	-2.56E-05	-7.86E-05	-1.87E-04	-1.39E-04
45	-3.05E-05	-3.52E-06	-7.05E-06	-1.57E-05	-4.30E-05	-1.16E-05	-1.91E-04	-3.11E-05	-9.18E-05	-2.20E-04	-1.63E-04
46	-3.82E-05	-4.30E-06	-8.60E-06	-1.92E-05	-5.32E-05	-1.43E-05	-2.35E-04	-3.80E-05	-1.08E-04	-2.61E-04	-1.92E-04
47	-4.79E-05	-5.36E-06	-1.07E-05	-2.34E-05	-6.55E-05	-1.76E-05	-2.89E-04	-4.65E-05	-1.27E-04	-3.10E-04	-2.27E-04
48	-6.05E-05	-6.68E-06	-1.34E-05	-2.90E-05	-8.05E-05	-2.20E-05	-3.65E-04	-5.82E-05	-1.51E-04	-3.71E-04	-2.70E-04
49	-7.77E-05	-8.51E-06	-1.68E-05	-3.70E-05	-1.01E-04	-2.77E-05	-4.66E-04	-7.43E-05	-1.81E-04	-4.47E-04	-3.23E-04
50	-1.02E-04	-1.09E-05	-2.18E-05	-4.74E-05	-1.31E-04	-3.57E-05	-6.01E-04	-9.57E-05	-2.17E-04	-5.43E-04	-3.88E-04
51	-1.34E-04	-1.43E-05	-2.89E-05	-6.12E-05	-1.71E-04	-4.84E-05	-7.88E-04	-1.25E-04	-2.62E-04	-6.64E-04	-4.69E-04
52	-1.81E-04	-2.01E-05	-3.96E-05	-8.48E-05	-2.35E-04	-6.31E-05	-1.05E-03	-1.68E-04	-3.18E-04	-8.19E-04	-5.69E-04
53	-2.50E-04	-2.73E-05	-5.24E-05	-1.16E-04	-3.22E-04	-8.82E-05	-1.42E-03	-2.30E-04	-3.87E-04	-1.02E-03	-6.94E-04
54	-3.47E-04	-3.77E-05	-7.94E-05	-1.65E-04	-4.46E-04	-1.27E-04	-1.99E-03	-3.18E-04	-4.73E-04	-1.28E-03	-8.47E-04
55	-5.00E-04	-5.63E-05	-1.14E-04	-2.36E-04	-6.38E-04	-1.79E-04	-2.79E-03	-4.54E-04	-5.79E-04	-1.63E-03	-1.04E-03
56	-7.38E-04	-8.18E-05	-1.65E-04	-3.50E-04	-9.51E-04	-2.65E-04	-4.04E-03	-6.62E-04	-7.06E-04	-2.08E-03	-1.26E-03
57	-1.16E-03	-1.23E-04	-2.49E-04	-5.19E-04	-1.38E-03	-3.88E-04	-5.97E-03	-9.69E-04	-8.55E-04	-2.68E-03	-1.52E-03
58	-1.79E-03	-1.86E-04	-3.70E-04	-7.80E-04	-2.05E-03	-5.86E-04	-9.36E-03	-1.41E-03	-1.03E-03	-3.47E-03	-1.81E-03
59	-2.91E-03	-2.62E-04	-5.21E-04	-1.08E-03	-2.86E-03	-8.23E-04	-1.46E-02	-2.03E-03	-1.24E-03	-4.52E-03	-2.05E-03
60	-4.48E-03	-4.01E-04	-8.03E-04	-1.66E-03	-4.24E-03	-1.24E-03	-2.15E-02	-2.63E-03	-1.47E-03	-5.32E-03	-2.51E-03
61	-1.00E-02	-1.07E-03	-2.14E-03	-4.86E-03	-1.42E-02	-3.78E-03	-6.23E-02	-1.17E-02	-5.26E-03	-1.36E-02	-7.96E-03
62	-1.27E-02	-1.29E-03	-2.57E-03	-5.85E-03	-1.71E-02	-4.53E-03	-7.83E-02	-1.39E-02	-6.57E-03	-1.67E-02	-1.01E-02
63	-1.47E-02	-1.40E-03	-2.79E-03	-6.37E-03	-1.86E-02	-4.94E-03	-8.94E-02	-1.51E-02	-7.26E-03	-1.87E-02	-1.13E-02
64	-1.62E-02	-1.47E-03	-2.93E-03	-6.72E-03	-1.96E-02	-5.20E-03	-9.77E-02	-1.59E-02	-7.69E-03	-2.02E-02	-1.21E-02
65	-1.74E-02	-1.51E-03	-3.02E-03	-6.95E-03	-2.03E-02	-5.36E-03	-1.04E-01	-1.64E-02	-7.99E-03	-2.14E-02	-1.26E-02
66	-1.83E-02	-1.54E-03	-3.08E-03	-7.12E-03	-2.07E-02	-5.49E-03	-1.09E-01	-1.68E-02	-8.22E-03	-2.24E-02	-1.30E-02
67	-1.91E-02	-1.57E-03	-3.13E-03	-7.25E-03	-2.11E-02	-5.58E-03	-1.13E-01	-1.71E-02	-8.39E-03	-2.32E-02	-1.33E-02
68	-1.98E-02	-1.58E-03	-3.15E-03	-7.34E-03	-2.14E-02	-5.65E-03	-1.16E-01	-1.74E-02	-8.53E-03	-2.38E-02	-1.35E-02
69	-2.03E-02	-1.59E-03	-3.18E-03	-7.41E-03	-2.16E-02	-5.70E-03	-1.19E-01	-1.75E-02	-8.64E-03	-2.44E-02	-1.37E-02
70	-2.08E-02	-1.60E-03	-3.20E-03	-7.46E-03	-2.17E-02	-5.74E-03	-1.21E-01	-1.77E-02	-8.73E-03	-2.48E-02	-1.38E-02
71	-2.12E-02	-1.61E-03	-3.21E-03	-7.51E-03	-2.19E-02	-5.77E-03	-1.23E-01	-1.78E-02	-8.80E-03	-2.52E-02	-1.40E-02
72	-2.15E-02	-1.61E-03	-3.22E-03	-7.54E-03	-2.19E-02	-5.79E-03	-1.24E-01	-1.79E-02	-8.86E-03	-2.56E-02	-1.41E-02
73	-2.18E-02	-1.62E-03	-3.23E-03	-7.57E-03	-2.20E-02	-5.81E-03	-1.26E-01	-1.80E-02	-8.91E-03	-2.59E-02	-1.41E-02
74	-2.20E-02	-1.62E-03	-3.24E-03	-7.59E-03	-2.21E-02	-5.83E-03	-1.27E-01	-1.81E-02	-8.95E-03	-2.61E-02	-1.42E-02
75	-2.22E-02	-1.63E-03	-3.24E-03	-7.61E-03	-2.21E-02	-5.84E-03	-1.28E-01	-1.81E-02	-8.99E-03	-2.63E-02	-1.43E-02
76	-2.24E-02	-1.63E-03	-3.25E-03	-7.63E-03	-2.22E-02	-5.85E-03	-1.28E-01	-1.82E-02	-9.02E-03	-2.65E-02	-1.43E-02
77	-2.26E-02	-1.63E-03	-3.25E-03	-7.64E-03	-2.22E-02	-5.86E-03	-1.29E-01	-1.82E-02	-9.05E-03	-2.67E-02	-1.44E-02
78	-2.27E-02	-1.63E-03	-3.26E-03	-7.65E-03	-2.23E-02	-5.87E-03	-1.30E-01	-1.82E-02	-9.07E-03	-2.68E-02	-1.44E-02
79	-2.28E-02	-1.63E-03	-3.26E-03	-7.66E-03	-2.23E-02	-5.88E-03	-1.30E-01	-1.82E-02	-9.09E-03	-2.69E-02	-1.44E-02
80	-2.29E-02	-1.63E-03	-3.26E-03	-7.67E-03	-2.23E-02	-5.88E-03	-1.31E-01	-1.83E-02	-9.11E-03	-2.70E-02	-1.44E-02
81	-2.30E-02	-1.64E-03	-3.26E-03	-7.67E-03	-2.23E-02	-5.89E-03	-1.31E-01	-1.83E-02	-9.12E-03	-2.71E-02	-1.45E-02
82	-2.31E-02	-1.64E-03	-3.27E-03	-7.68E-03	-2.23E-02	-5.89E-03	-1.31E-01	-1.83E-02	-9.13E-03	-2.72E-02	-1.45E-02
83	-2.32E-02	-1.64E-03	-3.27E-03	-7.68E-03	-2.24E-02	-5.89E-03	-1.32E-01	-1.83E-02	-9.14E-03	-2.73E-02	-1.45E-02
84	-2.32E-02	-1.64E-03	-3.27E-03	-7.68E-03	-2.24E-02	-5.90E-03	-1.32E-01	-1.83E-02	-9.15E-03	-2.73E-02	-1.45E-02
85	-2.33E-02	-1.64E-03	-3.27E-03	-7.69E-03	-2.24E-02	-5.90E-03	-1.32E-01	-1.83E-02	-9.16E-03	-2.74E-02	-1.45E-02
86	-2.33E-02	-1.64E-03	-3.27E-03	-7.69E-03	-2.24E-02	-5.90E-03	-1.32E-01	-1.83E-02	-9.17E-03	-2.74E-02	-1.45E-02
87	-2.34E-02	-1.64E-03	-3.27E-03	-7.69E-03	-2.24E-02	-5.90E-03	-1.32E-01	-1.84E-02	-9.18E-03	-2.75E-02	-1.45E-02
88	-2.34E-02	-1.64E-03	-3.27E-03	-7.70E-03	-2.24E-02	-5.90E-03	-1.33E-01	-1.84E-02	-9.18E-03	-2.75E-02	-1.46E-02
89	-2.34E-02	-1.64E-03	-3.27E-03	-7.70E-03	-2.24E-02	-5.91E-03	-1.33E-01	-1.84E-02	-9.19E-03	-2.76E-02	-1.46E-02
90	-2.35E-02	-1.64E-03	-3.27E-03	-7.70E-03	-2.24E-02	-5.91E-03	-1.33E-01	-1.84E-02	-9.19E-03	-2.76E-02	-1.46E-02
91	-2.35E-02	-1.64E-03	-3.27E-03	-7.70E-03	-2.24E-02	-5.91E-03	-1.33E-01	-1.84E-02	-9.19E-03	-2.76E-02	-1.46E-02
92	-2.35E-02	-1.64E-03	-3.27E-03	-7.70E-03	-2.24E-02	-5.91E-03	-1.33E-01	-1.84E-02	-9.20E-03	-2.76E-02	-1.46E-02
93	-2.35E-02	-1.64E-03	-3.27E-03	-7.70E-03	-2.24E-02	-5.91E-03	-1.33E-01	-1.84E-02	-9.20E-03	-2.77E-02	-1.46E-02
94	-2.36E-02	-1.64E-03	-3.27E-03	-7.70E-03	-2.24E-02	-5.91E-03	-1.33E-01	-1.84E-02	-9.20E-03	-2.77E-02	-1.46E-02
95	-2.36E-02	-1.64E-03	-3.27E-03	-7.70E-03	-2.24E-02	-5.91E-03	-1.33E-01	-1.84E-02	-9.20E-03	-2.77E-02	-1.46E-02
96	-2.36E-02	-1.64E-03	-3.27E-03	-7.70E-03	-2.24E-02	-5.91E-03	-1.33E-01	-1.84E-02	-9.21E-03	-2.77E-02	-1.46E-02
97	-2.36E-02	-1.64E-03	-3.27E-03	-7.70E-03	-2.24E-02	-5.91E-03	-1.33E-01	-1.84E-02	-9.21E-03	-2.77E-02	-1.46E-02
98	-2.36E-02	-1.64E-03	-3.27E-03	-7.70E-03	-2.24E-02	-5.91E-03	-1.33E-01	-1.84E-02	-9.21E-03	-2.77E-02	-1.46E-02
99	-2.36E-02	-1.64E-03	-3.27E-03	-7.71E-03	-2.24E-02	-5.91E-03	-1.33E-01	-1.84E-02	-9.21E-03	-2.77E-02	-1.46E-02
100	-2.36E-02	-1.64E-03	-3.27E-03	-7.71E-03	-2.24E-02	-5.91E-03	-1.33E-01	-1.84E-02	-9.21E-03	-2.77E-02	-1.46E-02
101	-2.36E-02	-1.64E-03	-3.27E-03	-7.71E-03	-2.24E-02	-5.91E-03	-1.33E-01	-1.84E-02	-9.21E-03	-2.77E-02	-1.46E-02
102	-2.36E-02	-1.64E-03	-3.27E-03	-7.71E-03	-2.24E-02	-5.91E-03	-1.33E-01	-1.84E-02	-9.21E-03	-2.78E-02	-1.46E-02
103	-2.36E-02	-1.64E-03	-3.27E-03	-7.71E-03	-2.24E-02	-5.91E-03	-1.33E-01	-1.84E-02	-9.21E-03	-2.78E-02	-1.46E-02
104	-2.36E-02	-1.64E-03	-3.27E-03	-7.71E-03	-2.24E-02	-5.91E-03	-1.34E-01	-1.84E-02	-9.21E-03	-2.78E-02	-1.46E-02
105	-2.36E-02	-1.64E-03	-3.27E-03	-7.71E-03	-2.24E-02	-5.91E-03	-1.34E-01	-1.84E-02	-9.21E-03	-2.78E-02	-1.46E-02
106	-2.36E-02	-1.64E-03	-3.27E-03	-7.71E-03	-2.24E-02	-5.91E-03	-1.34E-01	-1.84E-02	-9.21E-03	-2.78E-02	-1.46E-02
107	-2.36E-02	-1.64E-03	-3.27E-03	-7.71E-03	-2.24E-02	-5.91E-03	-1.34E-01	-1.84E-02	-9.21E-03	-2.78E-02	-1.46E-02
108	-2.36E-02	-1.64E-03	-3.27E-03	-7.71E-03	-2.24E-02	-5.91E-03	-1.34E-01	-1.84E-02	-9.21E-03	-2.78E-02	-1.46E-02
109	-2.36E-02	-1.64E-03	-3.27E-03	-7.71E-03	-2.24E-02	-5.91E-03	-1.34E-01	-1.84E-02	-9.21E-03	-2.78E-02	-1.46E-02
110	-2.36E-02	-1.64E-03	-3.27E-03	-7.71E-03	-2.24E-02	-5.91E-03	-1.34E-01	-1.84E-02	-9.21E-03	-2.78E-02	-1.46E-02
111	-2.36E-02	-1.64E-03	-3.27E-03	-7.71E-03	-2.24E-02	-5.91E-03	-1.34E-01	-1.84E-02	-9.21E-03	-2.78E-02	-1.46E-02
112	-2.36E-02	-1.64E-03	-3.27E-03	-7.71E-03	-2.24E-02	-5.91E-03	-1.34E-01	-1.84E-02	-9.21E-03	-2.78E-02	-1.46E-02
113	-2.36E-02	-1.64E-03	-3.27E-03	-7.71E-03	-2.24E-02	-5.91E-03	-1.34E-01	-1.84E-02	-9.21E-03	-2.78E-02	-1.46E-02
114	-2.36E-02	-1.64E-03	-3.27E-03	-7.71E-03	-2.24E-02	-5.91E-03	-1.34E-01	-1.84E-02	-9.21E-03	-2.78E-02	-1.46E-02
115	-2.37E-02	-1.64E-03	-3.27E-03	-7.71E-03	-2.24E-02	-5.91E-03	-1.34E-01	-1.84E-02	-9.21E-03	-2.78E-02	-1.46E-02
116	-2.37E-02	-1.64E-03	-3.27E-03	-7.71E-03	-2.24E-02	-5.91E-03	-1.34E-01	-1.84E-02	-9.21E-03	-2.78E-02	-1.46E-02
117	-2.37E-02	-1.64E-03	-3.27E-03	-7.71E-03	-2.24E-02	-5.91E-03	-1.34E-01	-1.84E-02	-9.21E-03	-2.78E-02	-1.46E-02
118	-2.37E-02	-1.64E-03	-3.27E-03	-7.71E-03	-2.24E-02	-5.91E-03	-1.34E-01	-1.84E-02	-9.21E-03	-2.78E-02	-1.46E-02
119	-2.36E-02	-1.64E-03	-3.27E-03	-7.71E-03	-2.24E-02	-5.91E-03	-1.34E-01	-1.84E-02	-9.21E-03	-2.78E-02	-1.46E-02
120	-2.36E-02	-1.64E-03	-3.27E-03	-7.71E-03	-2.24E-02	-5.91E-03	-1.34E-01	-1.84E-02	-9.21E-03	-2.78E-02	-1.46E-02

														additional models	
number	12	13	14	15	16	17	18	19	20	21	22	23	24	25	26
model	**R5_OB500_P29_E3_C0.5**	**R5_OB500_P29_E3_C1.5**	**R5_OB500_P29_E3_C3**	**R5_OB500_P35_E10_C3**	**R5_OB1000_P29_E3_C1.5**	**R5_OB1000_P29_E3_C3**	**R5_OB1000_P35_E10_C3**	**R7_OB50_P29_E3_C0.5**	**R7_OB100_P29_E3_C0.5**	**R7_OB200_P29_E3_C1.5**	**R7_OB500_P29_E3_C3**	**R7_OB1000_P29_E3_C3**	**R7_OB1000_P35_E10_C3**	**R5_OB500_P29_E10_C3**	**R5_OB1000_P29_E10_C3**
pl. Radius [m]	14.1	8.9	6.5	6.2	12	8.9	7.3	7.9	9.6	8.8	9.2	12	10.1	6.5	8.9
pl. Rad._analytical [m]	14.7	8.8	6.6	6.1	12.1	8.8	7.4	7.8	10	8.6	9.3	12.3	10.4		
shear strength c' [Mpa]	0.5	1.5	3	3	1.5	3	3	0.5	0.5	1.5	3	3	3	3	3
friction angle	29	29	29	35	29	29	35	29	29	29	29	29	35	29	29
Young's Modulus [Mpa]	3000	3000	3000	10000	3000	3000	10000	3000	3000	3000	3000	3000	10000	10000	10000
UCS [Mpa]	1.697663	5.092989	10.18598	11.52589	5.092989	10.18598	11.52589	1.697663	1.697663	5.092989	10.18598	10.18598	11.52589	10.18598	10.18598
Overburden [m]	500	500	500	500	1000	1000	1000	50	100	200	500	1000	1000	500	1000
Sigma 0 effective [Mpa]	12.5	12.5	12.5	12.5	25	25	25	1.25	2.5	5	12.5	25	25	12.5	25
UCS / Sigma 0,eff	0.135813	0.407439	0.814878	0.922071	0.20372	0.407439	0.461036	1.35813	0.679065	1.018598	0.814878	0.407439	0.461036	0.814878	0.407439
tunnelradius [m]	5	5	5	5	5	5	5	7	7	7	7	7	7	5	5
rpl/rt	2.82	1.78	1.3	1.24	2.4	1.78	1.46	1.128571	1.371429	1.257143	1.314286	1.714286	1.442857	1.3	1.78
u0/umax	0.226571	0.181831	0.157453	0.16089	0.22268	0.180036	0.156255	0.162727	0.150206	0.146723	0.142232	0.190968	0.162121	0.157586	0.181599
Station	z_disp	z_disp	z_disp	z_disp	z_disp	z_disp	z_disp	z_disp	z_disp	z_disp	z_disp	z_disp	z_disp	z_disp	z_disp
1	-7.16E-06	-6.17E-06	-5.92E-06	-1.70E-06	-1.24E-05	-1.23E-05	-3.61E-06	-1.04E-06	-2.53E-06	-4.44E-06	-1.22E-05	-2.32E-05	-6.48E-06	-1.78E-06	-3.66E-06
2	-1.04E-05	-7.93E-06	-7.08E-06	-2.02E-06	-1.79E-05	-1.59E-05	-4.50E-06	-1.81E-06	-4.07E-06	-7.57E-06	-1.95E-05	-4.38E-05	-1.15E-05	-2.11E-06	-4.79E-06
3	-1.25E-05	-8.86E-06	-7.51E-06	-2.13E-06	-2.08E-05	-1.77E-05	-4.90E-06	-2.14E-06	-4.89E-06	-8.85E-06	-2.33E-05	-5.28E-05	-1.47E-05	-2.27E-06	-5.30E-06
4	-1.40E-05	-9.19E-06	-7.87E-06	-2.22E-06	-2.22E-05	-1.83E-05	-5.12E-06	-2.36E-06	-5.41E-06	-9.79E-06	-2.59E-05	-6.03E-05	-1.68E-05	-2.36E-06	-5.51E-06
5	-1.46E-05	-9.44E-06	-8.09E-06	-2.28E-06	-2.26E-05	-1.88E-05	-5.35E-06	-2.52E-06	-5.92E-06	-1.07E-05	-2.82E-05	-6.53E-05	-1.84E-05	-2.42E-06	-5.66E-06
6	-1.49E-05	-9.69E-06	-8.31E-06	-2.32E-06	-2.24E-05	-1.93E-05	-5.45E-06	-2.64E-06	-6.24E-06	-1.12E-05	-2.96E-05	-6.92E-05	-1.96E-05	-2.49E-06	-5.77E-06
7	-1.47E-05	-9.79E-06	-8.51E-06	-2.37E-06	-2.16E-05	-1.96E-05	-5.63E-06	-2.74E-06	-6.55E-06	-1.17E-05	-3.06E-05	-7.19E-05	-2.05E-05	-2.57E-06	-5.88E-06
8	-1.44E-05	-1.00E-05	-8.75E-06	-2.44E-06	-2.08E-05	-1.98E-05	-5.80E-06	-2.83E-06	-6.81E-06	-1.21E-05	-3.18E-05	-7.41E-05	-2.13E-05	-2.63E-06	-5.99E-06
9	-1.38E-05	-1.01E-05	-9.08E-06	-2.52E-06	-1.98E-05	-2.02E-05	-6.00E-06	-2.92E-06	-7.12E-06	-1.26E-05	-3.30E-05	-7.66E-05	-2.22E-05	-2.73E-06	-6.06E-06
10	-1.32E-05	-1.03E-05	-9.41E-06	-2.62E-06	-1.90E-05	-2.06E-05	-6.26E-06	-3.02E-06	-7.43E-06	-1.31E-05	-3.47E-05	-7.95E-05	-2.31E-05	-2.84E-06	-6.21E-06
11	-1.27E-05	-1.07E-05	-9.79E-06	-2.73E-06	-1.84E-05	-2.12E-05	-6.54E-06	-3.16E-06	-7.77E-06	-1.36E-05	-3.64E-05	-8.23E-05	-2.42E-05	-2.97E-06	-6.36E-06
12	-1.24E-05	-1.10E-05	-1.04E-05	-2.88E-06	-1.82E-05	-2.20E-05	-6.83E-06	-3.32E-06	-8.14E-06	-1.42E-05	-3.83E-05	-8.58E-05	-2.53E-05	-3.12E-06	-6.59E-06
13	-1.21E-05	-1.15E-05	-1.10E-05	-3.05E-06	-1.79E-05	-2.30E-05	-7.25E-06	-3.49E-06	-8.63E-06	-1.51E-05	-4.05E-05	-9.03E-05	-2.66E-05	-3.31E-06	-6.92E-06
14	-1.19E-05	-1.21E-05	-1.17E-05	-3.25E-06	-1.79E-05	-2.43E-05	-7.74E-06	-3.69E-06	-9.11E-06	-1.59E-05	-4.29E-05	-9.53E-05	-2.82E-05	-3.54E-06	-7.30E-06
15	-1.21E-05	-1.29E-05	-1.26E-05	-3.50E-06	-1.85E-05	-2.59E-05	-8.29E-06	-3.92E-06	-9.71E-06	-1.69E-05	-4.57E-05	-1.01E-04	-3.01E-05	-3.79E-06	-7.75E-06
16	-1.25E-05	-1.39E-05	-1.36E-05	-3.77E-06	-1.94E-05	-2.77E-05	-8.93E-06	-4.21E-06	-1.04E-05	-1.83E-05	-4.91E-05	-1.08E-04	-3.22E-05	-4.08E-06	-8.33E-06
17	-1.32E-05	-1.51E-05	-1.48E-05	-4.11E-06	-2.09E-05	-3.00E-05	-9.76E-06	-4.51E-06	-1.12E-05	-1.97E-05	-5.28E-05	-1.16E-04	-3.48E-05	-4.43E-06	-9.04E-06
18	-1.43E-05	-1.64E-05	-1.61E-05	-4.50E-06	-2.28E-05	-3.30E-05	-1.07E-05	-4.88E-06	-1.21E-05	-2.14E-05	-5.70E-05	-1.26E-04	-3.75E-05	-4.85E-06	-9.89E-06
19	-1.58E-05	-1.80E-05	-1.77E-05	-4.90E-06	-2.53E-05	-3.61E-05	-1.17E-05	-5.34E-06	-1.32E-05	-2.33E-05	-6.18E-05	-1.36E-04	-4.10E-05	-5.30E-06	-1.08E-05
20	-1.77E-05	-1.99E-05	-1.94E-05	-5.42E-06	-2.86E-05	-3.99E-05	-1.29E-05	-5.77E-06	-1.43E-05	-2.56E-05	-6.73E-05	-1.49E-04	-4.49E-05	-5.85E-06	-1.20E-05
21	-2.01E-05	-2.22E-05	-2.14E-05	-5.99E-06	-3.27E-05	-4.43E-05	-1.41E-05	-6.41E-06	-1.56E-05	-2.77E-05	-7.34E-05	-1.62E-04	-4.91E-05	-6.41E-06	-1.33E-05
22	-2.29E-05	-2.48E-05	-2.38E-05	-6.66E-06	-3.75E-05	-4.95E-05	-1.57E-05	-7.01E-06	-1.71E-05	-3.04E-05	-8.03E-05	-1.78E-04	-5.37E-05	-7.12E-06	-1.48E-05
23	-2.65E-05	-2.76E-05	-2.64E-05	-7.41E-06	-4.34E-05	-5.54E-05	-1.74E-05	-7.75E-06	-1.89E-05	-3.35E-05	-8.86E-05	-1.97E-04	-5.96E-05	-7.90E-06	-1.66E-05
24	-3.08E-05	-3.11E-05	-2.94E-05	-8.23E-06	-5.02E-05	-6.20E-05	-1.94E-05	-8.43E-06	-2.08E-05	-3.67E-05	-9.76E-05	-2.18E-04	-6.55E-05	-8.79E-06	-1.86E-05
25	-3.59E-05	-3.49E-05	-3.28E-05	-9.18E-06	-5.85E-05	-6.96E-05	-2.16E-05	-9.33E-06	-2.30E-05	-4.04E-05	-1.08E-04	-2.42E-04	-7.24E-05	-9.81E-06	-2.09E-05
26	-4.19E-05	-3.94E-05	-3.66E-05	-1.02E-05	-6.81E-05	-7.85E-05	-2.42E-05	-1.04E-05	-2.55E-05	-4.46E-05	-1.20E-04	-2.69E-04	-8.01E-05	-1.09E-05	-2.36E-05
27	-4.90E-05	-4.43E-05	-4.09E-05	-1.15E-05	-7.95E-05	-8.86E-05	-2.70E-05	-1.16E-05	-2.82E-05	-4.98E-05	-1.33E-04	-3.00E-04	-8.87E-05	-1.23E-05	-2.66E-05
28	-5.74E-05	-5.01E-05	-4.58E-05	-1.29E-05	-9.27E-05	-1.00E-04	-3.04E-05	-1.28E-05	-3.15E-05	-5.52E-05	-1.48E-04	-3.36E-04	-9.91E-05	-1.38E-05	-3.01E-05
29	-6.70E-05	-5.68E-05	-5.13E-05	-1.44E-05	-1.08E-04	-1.13E-04	-3.40E-05	-1.42E-05	-3.49E-05	-6.14E-05	-1.65E-04	-3.76E-04	-1.10E-04	-1.54E-05	-3.40E-05
30	-7.83E-05	-6.42E-05	-5.77E-05	-1.62E-05	-1.26E-04	-1.28E-04	-3.84E-05	-1.59E-05	-3.90E-05	-6.83E-05	-1.83E-04	-4.21E-04	-1.22E-04	-1.73E-05	-3.86E-05
31	-9.14E-05	-7.28E-05	-6.50E-05	-1.83E-05	-1.46E-04	-1.46E-04	-4.32E-05	-1.77E-05	-4.33E-05	-7.62E-05	-2.05E-04	-4.72E-04	-1.36E-04	-1.95E-05	-4.37E-05
32	-1.07E-04	-8.27E-05	-7.34E-05	-2.06E-05	-1.70E-04	-1.66E-04	-4.88E-05	-1.99E-05	-4.85E-05	-8.54E-05	-2.30E-04	-5.30E-04	-1.53E-04	-2.20E-05	-4.97E-05
33	-1.24E-04	-9.41E-05	-8.29E-05	-2.33E-05	-1.98E-04	-1.88E-04	-5.51E-05	-2.22E-05	-5.42E-05	-9.57E-05	-2.57E-04	-5.96E-04	-1.72E-04	-2.49E-05	-5.65E-05
34	-1.45E-04	-1.07E-04	-9.39E-05	-2.64E-05	-2.30E-04	-2.14E-04	-6.25E-05	-2.49E-05	-6.07E-05	-1.07E-04	-2.88E-04	-6.69E-04	-1.92E-04	-2.82E-05	-6.44E-05
35	-1.69E-04	-1.22E-04	-1.06E-04	-2.99E-05	-2.68E-04	-2.45E-04	-7.08E-05	-2.81E-05	-6.83E-05	-1.21E-04	-3.23E-04	-7.56E-04	-2.16E-04	-3.20E-05	-7.35E-05
36	-1.97E-04	-1.40E-04	-1.21E-04	-3.40E-05	-3.12E-04	-2.80E-04	-8.05E-05	-3.18E-05	-7.67E-05	-1.37E-04	-3.64E-04	-8.54E-04	-2.43E-04	-3.63E-05	-8.40E-05
37	-2.29E-04	-1.60E-04	-1.38E-04	-3.88E-05	-3.63E-04	-3.21E-04	-9.18E-05	-3.59E-05	-8.67E-05	-1.54E-04	-4.11E-04	-9.67E-04	-2.74E-04	-4.14E-05	-9.64E-05
38	-2.68E-04	-1.84E-04	-1.58E-04	-4.44E-05	-4.23E-04	-3.68E-04	-1.05E-04	-4.08E-05	-9.81E-05	-1.74E-04	-4.65E-04	-1.09E-03	-3.09E-04	-4.73E-05	-1.10E-04
39	-3.13E-04	-2.12E-04	-1.81E-04	-5.08E-05	-4.94E-04	-4.24E-04	-1.20E-04	-4.60E-05	-1.11E-04	-1.97E-04	-5.27E-04	-1.24E-03	-3.50E-04	-5.42E-05	-1.27E-04
40	-3.67E-04	-2.44E-04	-2.07E-04	-5.84E-05	-5.77E-04	-4.88E-04	-1.38E-04	-5.23E-05	-1.26E-04	-2.23E-04	-5.98E-04	-1.42E-03	-3.97E-04	-6.22E-05	-1.47E-04
41	-4.31E-04	-2.82E-04	-2.39E-04	-6.73E-05	-6.76E-04	-5.64E-04	-1.59E-04	-5.96E-05	-1.43E-04	-2.54E-04	-6.80E-04	-1.62E-03	-4.51E-04	-7.16E-05	-1.70E-04
42	-5.08E-04	-3.27E-04	-2.76E-04	-7.78E-05	-7.95E-04	-6.55E-04	-1.84E-04	-6.81E-05	-1.63E-04	-2.91E-04	-7.75E-04	-1.85E-03	-5.14E-04	-8.28E-05	-1.97E-04
43	-6.00E-04	-3.81E-04	-3.20E-04	-9.03E-05	-9.37E-04	-7.63E-04	-2.13E-04	-7.79E-05	-1.86E-04	-3.32E-04	-8.85E-04	-2.12E-03	-5.87E-04	-9.62E-05	-2.29E-04
44	-7.12E-04	-4.46E-04	-3.73E-04	-1.05E-04	-1.11E-03	-8.92E-04	-2.48E-04	-8.94E-05	-2.13E-04	-3.81E-04	-1.01E-03	-2.43E-03	-6.72E-04	-1.12E-04	-2.67E-04
45	-8.48E-04	-5.23E-04	-4.37E-04	-1.23E-04	-1.32E-03	-1.05E-03	-2.90E-04	-1.03E-04	-2.45E-04	-4.38E-04	-1.16E-03	-2.81E-03	-7.70E-04	-1.31E-04	-3.14E-04
46	-1.02E-03	-6.18E-04	-5.14E-04	-1.45E-04	-1.58E-03	-1.24E-03	-3.41E-04	-1.19E-04	-2.81E-04	-5.03E-04	-1.34E-03	-3.25E-03	-8.88E-04	-1.54E-04	-3.71E-04
47	-1.23E-03	-7.33E-04	-6.07E-04	-1.71E-04	-1.90E-03	-1.47E-03	-4.03E-04	-1.37E-04	-3.24E-04	-5.82E-04	-1.54E-03	-3.77E-03	-1.03E-03	-1.82E-04	-4.40E-04
48	-1.49E-03	-8.74E-04	-7.21E-04	-2.04E-04	-2.30E-03	-1.75E-03	-4.78E-04	-1.59E-04	-3.75E-04	-6.72E-04	-1.78E-03	-4.40E-03	-1.19E-03	-2.17E-04	-5.25E-04
49	-1.84E-03	-1.05E-03	-8.61E-04	-2.43E-04	-2.81E-03	-2.10E-03	-5.71E-04	-1.84E-04	-4.33E-04	-7.77E-04	-2.07E-03	-5.14E-03	-1.38E-03	-2.58E-04	-6.30E-04
50	-2.28E-03	-1.27E-03	-1.03E-03	-2.92E-04	-3.46E-03	-2.54E-03	-6.87E-04	-2.13E-04	-5.03E-04	-9.01E-04	-2.39E-03	-6.02E-03	-1.60E-03	-3.10E-04	-7.61E-04
51	-2.86E-03	-1.54E-03	-1.25E-03	-3.53E-04	-4.31E-03	-3.09E-03	-8.30E-04	-2.48E-04	-5.83E-04	-1.05E-03	-2.77E-03	-7.10E-03	-1.87E-03	-3.75E-04	-9.26E-04
52	-3.64E-03	-1.89E-03	-1.51E-03	-4.29E-04	-5.42E-03	-3.78E-03	-1.01E-03	-2.88E-04	-6.76E-04	-1.21E-03	-3.21E-03	-8.39E-03	-2.19E-03	-4.54E-04	-1.14E-03
53	-4.70E-03	-2.34E-03	-1.84E-03	-5.23E-04	-6.92E-03	-4.68E-03	-1.23E-03	-3.34E-04	-7.84E-04	-1.40E-03	-3.71E-03	-9.95E-03	-2.56E-03	-5.53E-04	-1.40E-03
54	-6.15E-03	-2.91E-03	-2.25E-03	-6.38E-04	-8.93E-03	-5.81E-03	-1.52E-03	-3.87E-04	-9.07E-04	-1.62E-03	-4.28E-03	-1.18E-02	-2.99E-03	-6.75E-04	-1.74E-03
55	-8.22E-03	-3.64E-03	-2.74E-03	-7.81E-04	-1.17E-02	-7.27E-03	-1.87E-03	-4.46E-04	-1.04E-03	-1.87E-03	-4.91E-03	-1.41E-02	-3.51E-03	-8.23E-04	-2.18E-03
56	-1.09E-02	-4.59E-03	-3.33E-03	-9.51E-04	-1.55E-02	-9.17E-03	-2.32E-03	-5.11E-04	-1.20E-03	-2.13E-03	-5.60E-03	-1.68E-02	-4.11E-03	-9.99E-04	-2.75E-03
57	-1.50E-02	-5.82E-03	-4.01E-03	-1.15E-03	-2.06E-02	-1.16E-02	-2.86E-03	-5.78E-04	-1.37E-03	-2.41E-03	-6.31E-03	-2.01E-02	-4.81E-03	-1.20E-03	-3.49E-03
58	-2.06E-02	-7.45E-03	-4.74E-03	-1.37E-03	-2.77E-02	-1.49E-02	-3.55E-03	-6.46E-04	-1.56E-03	-2.67E-03	-7.05E-03	-2.40E-02	-5.65E-03	-1.42E-03	-4.48E-03
59	-2.69E-02	-9.64E-03	-5.52E-03	-1.57E-03	-3.67E-02	-1.93E-02	-4.43E-03	-6.93E-04	-1.81E-03	-2.90E-03	-7.91E-03	-2.88E-02	-6.69E-03	-1.65E-03	-5.79E-03
60	-3.31E-02	-1.12E-02	-6.61E-03	-1.81E-03	-4.57E-02	-2.23E-02	-4.92E-03	-7.93E-04	-1.99E-03	-3.21E-03	-8.74E-03	-3.20E-02	-7.05E-03	-1.98E-03	-6.70E-03
61	-5.29E-02	-3.20E-02	-2.34E-02	-6.29E-03	-8.39E-02	-6.51E-02	-1.83E-02	-2.30E-03	-6.75E-03	-1.10E-02	-3.12E-02	-7.95E-02	-2.27E-02	-7.07E-03	-1.93E-02
62	-6.51E-02	-3.90E-02	-2.98E-02	-7.91E-03	-1.04E-01	-7.94E-02	-2.23E-02	-3.01E-03	-8.67E-03	-1.43E-02	-4.03E-02	-9.98E-02	-2.86E-02	-8.96E-03	-2.35E-02
63	-7.54E-02	-4.32E-02	-3.32E-02	-8.89E-03	-1.19E-01	-8.77E-02	-2.44E-02	-3.46E-03	-9.89E-03	-1.62E-02	-4.59E-02	-1.12E-01	-3.20E-02	-9.95E-03	-2.60E-02
64	-8.42E-02	-4.64E-02	-3.52E-02	-9.47E-03	-1.32E-01	-9.40E-02	-2.57E-02	-3.78E-03	-1.06E-02	-1.74E-02	-4.93E-02	-1.20E-01	-3.41E-02	-1.06E-02	-2.79E-02
65	-9.18E-02	-4.88E-02	-3.66E-02	-9.86E-03	-1.42E-01	-9.89E-02	-2.67E-02	-4.01E-03	-1.11E-02	-1.83E-02	-5.16E-02	-1.27E-01	-3.56E-02	-1.10E-02	-2.94E-02
66	-9.84E-02	-5.08E-02	-3.77E-02	-1.01E-02	-1.51E-01	-1.03E-01	-2.74E-02	-4.18E-03	-1.15E-02	-1.89E-02	-5.33E-02	-1.32E-01	-3.67E-02	-1.13E-02	-3.06E-02
67	-1.04E-01	-5.24E-02	-3.85E-02	-1.04E-02	-1.58E-01	-1.06E-01	-2.80E-02	-4.31E-03	-1.17E-02	-1.94E-02	-5.45E-02	-1.37E-01	-3.76E-02	-1.15E-02	-3.15E-02
68	-1.09E-01	-5.37E-02	-3.91E-02	-1.05E-02	-1.65E-01	-1.09E-01	-2.86E-02	-4.41E-03	-1.20E-02	-1.98E-02	-5.56E-02	-1.41E-01	-3.83E-02	-1.17E-02	-3.23E-02
69	-1.13E-01	-5.48E-02	-3.96E-02	-1.06E-02	-1.70E-01	-1.11E-01	-2.90E-02	-4.48E-03	-1.22E-02	-2.01E-02	-5.64E-02	-1.44E-01	-3.90E-02	-1.19E-02	-3.30E-02
70	-1.17E-01	-5.57E-02	-4.00E-02	-1.08E-02	-1.75E-01	-1.13E-01	-2.93E-02	-4.54E-03	-1.23E-02	-2.03E-02	-5.71E-02	-1.47E-01	-3.95E-02	-1.20E-02	-3.35E-02
71	-1.21E-01	-5.65E-02	-4.03E-02	-1.08E-02	-1.78E-01	-1.14E-01	-2.97E-02	-4.59E-03	-1.24E-02	-2.05E-02	-5.77E-02	-1.49E-01	-4.00E-02	-1.21E-02	-3.40E-02
72	-1.23E-01	-5.72E-02	-4.06E-02	-1.09E-02	-1.82E-01	-1.16E-01	-2.99E-02	-4.63E-03	-1.25E-02	-2.07E-02	-5.82E-02	-1.51E-01	-4.04E-02	-1.22E-02	-3.44E-02
73	-1.26E-01	-5.77E-02	-4.08E-02	-1.10E-02	-1.85E-01	-1.17E-01	-3.01E-02	-4.66E-03	-1.26E-02	-2.09E-02	-5.87E-02	-1.53E-01	-4.08E-02	-1.22E-02	-3.47E-02
74	-1.28E-01	-5.82E-02	-4.10E-02	-1.10E-02	-1.87E-01	-1.18E-01	-3.03E-02	-4.69E-03	-1.27E-02	-2.10E-02	-5.90E-02	-1.55E-01	-4.11E-02	-1.23E-02	-3.50E-02
75	-1.30E-01	-5.86E-02	-4.11E-02	-1.11E-02	-1.90E-01	-1.19E-01	-3.05E-02	-4.71E-03	-1.28E-02	-2.11E-02	-5.93E-02	-1.56E-01	-4.14E-02	-1.23E-02	-3.53E-02
76	-1.32E-01	-5.90E-02	-4.12E-02	-1.11E-02	-1.92E-01	-1.19E-01	-3.06E-02	-4.74E-03	-1.29E-02	-2.12E-02	-5.96E-02	-1.58E-01	-4.16E-02	-1.24E-02	-3.55E-02
77	-1.34E-01	-5.93E-02	-4.13E-02	-1.11E-02	-1.93E-01	-1.20E-01	-3.07E-02	-4.75E-03	-1.29E-02	-2.13E-02	-5.99E-02	-1.59E-01	-4.19E-02	-1.24E-02	-3.57E-02
78	-1.35E-01	-5.95E-02	-4.14E-02	-1.11E-02	-1.95E-01	-1.20E-01	-3.08E-02	-4.77E-03	-1.30E-02	-2.14E-02	-6.01E-02	-1.60E-01	-4.21E-02	-1.24E-02	-3.58E-02
79	-1.36E-01	-5.98E-02	-4.15E-02	-1.12E-02	-1.96E-01	-1.21E-01	-3.09E-02	-4.78E-03	-1.30E-02	-2.15E-02	-6.02E-02	-1.61E-01	-4.22E-02	-1.25E-02	-3.60E-02
80	-1.37E-01	-6.00E-02	-4.16E-02	-1.12E-02	-1.97E-01	-1.21E-01	-3.10E-02	-4.79E-03	-1.30E-02	-2.15E-02	-6.04E-02	-1.61E-01	-4.24E-02	-1.25E-02	-3.61E-02
81	-1.38E-01	-6.02E-02	-4.16E-02	-1.12E-02	-1.98E-01	-1.22E-01	-3.10E-02	-4.80E-03	-1.31E-02	-2.16E-02	-6.05E-02	-1.62E-01	-4.25E-02	-1.25E-02	-3.62E-02
82	-1.39E-01	-6.03E-02	-4.17E-02	-1.12E-02	-1.99E-01	-1.22E-01	-3.11E-02	-4.81E-03	-1.31E-02	-2.16E-02	-6.07E-02	-1.63E-01	-4.26E-02	-1.25E-02	-3.63E-02
83	-1.40E-01	-6.05E-02	-4.17E-02	-1.12E-02	-2.00E-01	-1.22E-01	-3.12E-02	-4.82E-03	-1.31E-02	-2.16E-02	-6.08E-02	-1.63E-01	-4.27E-02	-1.25E-02	-3.64E-02
84	-1.41E-01	-6.06E-02	-4.18E-02	-1.12E-02	-2.01E-01	-1.22E-01	-3.12E-02	-4.83E-03	-1.31E-02	-2.17E-02	-6.09E-02	-1.64E-01	-4.28E-02	-1.25E-02	-3.64E-02
85	-1.41E-01	-6.07E-02	-4.18E-02	-1.12E-02	-2.01E-01	-1.23E-01	-3.12E-02	-4.83E-03	-1.32E-02	-2.17E-02	-6.09E-02	-1.64E-01	-4.29E-02	-1.25E-02	-3.65E-02
86	-1.42E-01	-6.08E-02	-4.18E-02	-1.12E-02	-2.02E-01	-1.23E-01	-3.13E-02	-4.84E-03	-1.32E-02	-2.17E-02	-6.10E-02	-1.65E-01	-4.30E-02	-1.25E-02	-3.66E-02
87	-1.42E-01	-6.09E-02	-4.19E-02	-1.12E-02	-2.02E-01	-1.23E-01	-3.13E-02	-4.84E-03	-1.32E-02	-2.18E-02	-6.11E-02	-1.65E-01	-4.31E-02	-1.26E-02	-3.66E-02
88	-1.43E-01	-6.09E-02	-4.19E-02	-1.13E-02	-2.03E-01	-1.23E-01	-3.13E-02	-4.85E-03	-1.32E-02	-2.18E-02	-6.11E-02	-1.65E-01	-4.31E-02	-1.26E-02	-3.66E-02
89	-1.43E-01	-6.10E-02	-4.19E-02	-1.13E-02	-2.03E-01	-1.23E-01	-3.13E-02	-4.85E-03	-1.32E-02	-2.18E-02	-6.12E-02	-1.66E-01	-4.32E-02	-1.26E-02	-3.67E-02
90	-1.43E-01	-6.10E-02	-4.19E-02	-1.13E-02	-2.03E-01	-1.23E-01	-3.14E-02	-4.86E-03	-1.32E-02	-2.18E-02	-6.12E-02	-1.66E-01	-4.32E-02	-1.26E-02	-3.67E-02
91	-1.44E-01	-6.11E-02	-4.19E-02	-1.13E-02	-2.04E-01	-1.23E-01	-3.14E-02	-4.86E-03	-1.32E-02	-2.18E-02	-6.13E-02	-1.66E-01	-4.33E-02	-1.26E-02	-3.67E-02
92	-1.44E-01	-6.11E-02	-4.19E-02	-1.13E-02	-2.04E-01	-1.24E-01	-3.14E-02	-4.86E-03	-1.32E-02	-2.18E-02	-6.13E-02	-1.66E-01	-4.33E-02	-1.26E-02	-3.68E-02
93	-1.44E-01	-6.12E-02	-4.19E-02	-1.13E-02	-2.04E-01	-1.24E-01	-3.14E-02	-4.86E-03	-1.32E-02	-2.18E-02	-6.13E-02	-1.67E-01	-4.33E-02	-1.26E-02	-3.68E-02
94	-1.45E-01	-6.12E-02	-4.20E-02	-1.13E-02	-2.04E-01	-1.24E-01	-3.14E-02	-4.87E-03	-1.33E-02	-2.18E-02	-6.14E-02	-1.67E-01	-4.34E-02	-1.26E-02	-3.68E-02
95	-1.45E-01	-6.12E-02	-4.20E-02	-1.13E-02	-2.04E-01	-1.24E-01	-3.14E-02	-4.87E-03	-1.33E-02	-2.19E-02	-6.14E-02	-1.67E-01	-4.34E-02	-1.26E-02	-3.68E-02
96	-1.45E-01	-6.13E-02	-4.20E-02	-1.13E-02	-2.05E-01	-1.24E-01	-3.14E-02	-4.87E-03	-1.33E-02	-2.19E-02	-6.14E-02	-1.67E-01	-4.34E-02	-1.26E-02	-3.68E-02
97	-1.45E-01	-6.13E-02	-4.20E-02	-1.13E-02	-2.05E-01	-1.24E-01	-3.14E-02	-4.87E-03	-1.33E-02	-2.19E-02	-6.14E-02	-1.67E-01	-4.34E-02	-1.26E-02	-3.69E-02
98	-1.45E-01	-6.13E-02	-4.20E-02	-1.13E-02	-2.05E-01	-1.24E-01	-3.15E-02	-4.87E-03	-1.33E-02	-2.19E-02	-6.14E-02	-1.67E-01	-4.35E-02	-1.26E-02	-3.69E-02
99	-1.45E-01	-6.13E-02	-4.20E-02	-1.13E-02	-2.05E-01	-1.24E-01	-3.15E-02	-4.87E-03	-1.33E-02	-2.19E-02	-6.14E-02	-1.67E-01	-4.35E-02	-1.26E-02	-3.69E-02
100	-1.45E-01	-6.13E-02	-4.20E-02	-1.13E-02	-2.05E-01	-1.24E-01	-3.15E-02	-4.87E-03	-1.33E-02	-2.19E-02	-6.15E-02	-1.67E-01	-4.35E-02	-1.26E-02	-3.69E-02
101	-1.45E-01	-6.13E-02	-4.20E-02	-1.13E-02	-2.05E-01	-1.24E-01	-3.15E-02	-4.87E-03	-1.33E-02	-2.19E-02	-6.15E-02	-1.68E-01	-4.35E-02	-1.26E-02	-3.69E-02
102	-1.46E-01	-6.13E-02	-4.20E-02	-1.13E-02	-2.05E-01	-1.24E-01	-3.15E-02	-4.87E-03	-1.33E-02	-2.19E-02	-6.15E-02	-1.68E-01	-4.35E-02	-1.26E-02	-3.69E-02
103	-1.46E-01	-6.14E-02	-4.20E-02	-1.13E-02	-2.05E-01	-1.24E-01	-3.15E-02	-4.87E-03	-1.33E-02	-2.19E-02	-6.15E-02	-1.68E-01	-4.35E-02	-1.26E-02	-3.69E-02
104	-1.46E-01	-6.14E-02	-4.20E-02	-1.13E-02	-2.05E-01	-1.24E-01	-3.15E-02	-4.87E-03	-1.33E-02	-2.19E-02	-6.15E-02	-1.68E-01	-4.35E-02	-1.26E-02	-3.69E-02
105	-1.46E-01	-6.14E-02	-4.20E-02	-1.13E-02	-2.05E-01	-1.24E-01	-3.15E-02	-4.87E-03	-1.33E-02	-2.19E-02	-6.15E-02	-1.68E-01	-4.35E-02	-1.26E-02	-3.69E-02
106	-1.46E-01	-6.14E-02	-4.20E-02	-1.13E-02	-2.05E-01	-1.24E-01	-3.15E-02	-4.87E-03	-1.33E-02	-2.19E-02	-6.15E-02	-1.68E-01	-4.35E-02	-1.26E-02	-3.69E-02
107	-1.46E-01	-6.14E-02	-4.20E-02	-1.13E-02	-2.05E-01	-1.24E-01	-3.15E-02	-4.87E-03	-1.33E-02	-2.19E-02	-6.15E-02	-1.68E-01	-4.35E-02	-1.26E-02	-3.69E-02
108	-1.46E-01	-6.14E-02	-4.20E-02	-1.13E-02	-2.05E-01	-1.24E-01	-3.15E-02	-4.87E-03	-1.33E-02	-2.19E-02	-6.15E-02	-1.68E-01	-4.35E-02	-1.26E-02	-3.69E-02
109	-1.46E-01	-6.14E-02	-4.20E-02	-1.13E-02	-2.05E-01	-1.24E-01	-3.15E-02	-4.87E-03	-1.33E-02	-2.19E-02	-6.15E-02	-1.68E-01	-4.35E-02	-1.26E-02	-3.69E-02
110	-1.46E-01	-6.14E-02	-4.20E-02	-1.13E-02	-2.05E-01	-1.24E-01	-3.15E-02	-4.87E-03	-1.33E-02	-2.19E-02	-6.15E-02	-1.68E-01	-4.35E-02	-1.26E-02	-3.69E-02
111	-1.46E-01	-6.14E-02	-4.20E-02	-1.13E-02	-2.05E-01	-1.24E-01	-3.15E-02	-4.87E-03	-1.33E-02	-2.19E-02	-6.15E-02	-1.68E-01	-4.35E-02	-1.26E-02	-3.69E-02
112	-1.46E-01	-6.14E-02	-4.20E-02	-1.13E-02	-2.05E-01	-1.24E-01	-3.15E-02	-4.87E-03	-1.33E-02	-2.19E-02	-6.15E-02	-1.68E-01	-4.35E-02	-1.26E-02	-3.69E-02
113	-1.46E-01	-6.14E-02	-4.20E-02	-1.13E-02	-2.05E-01	-1.24E-01	-3.15E-02	-4.87E-03	-1.33E-02	-2.19E-02	-6.15E-02	-1.68E-01	-4.35E-02	-1.26E-02	-3.69E-02
114	-1.46E-01	-6.14E-02	-4.20E-02	-1.13E-02	-2.05E-01	-1.24E-01	-3.15E-02	-4.87E-03	-1.33E-02	-2.19E-02	-6.15E-02	-1.68E-01	-4.35E-02	-1.26E-02	-3.69E-02
115	-1.46E-01	-6.14E-02	-4.20E-02	-1.13E-02	-2.05E-01	-1.24E-01	-3.15E-02	-4.87E-03	-1.33E-02	-2.19E-02	-6.15E-02	-1.68E-01	-4.35E-02	-1.26E-02	-3.69E-02
116	-1.46E-01	-6.14E-02	-4.20E-02	-1.13E-02	-2.05E-01	-1.24E-01	-3.15E-02	-4.87E-03	-1.33E-02	-2.19E-02	-6.15E-02	-1.68E-01	-4.35E-02	-1.26E-02	-3.69E-02
117	-1.46E-01	-6.14E-02	-4.20E-02	-1.13E-02	-2.05E-01	-1.24E-01	-3.15E-02	-4.87E-03	-1.33E-02	-2.19E-02	-6.15E-02	-1.68E-01	-4.35E-02	-1.26E-02	-3.69E-02
118	-1.46E-01	-6.14E-02	-4.20E-02	-1.13E-02	-2.05E-01	-1.24E-01	-3.15E-02	-4.87E-03	-1.33E-02	-2.19E-02	-6.15E-02	-1.68E-01	-4.35E-02	-1.26E-02	-3.69E-02
119	-1.46E-01	-6.14E-02	-4.20E-02	-1.13E-02	-2.05E-01	-1.24E-01	-3.15E-02	-4.87E-03	-1.33E-02	-2.19E-02	-6.15E-02	-1.68E-01	-4.35E-02	-1.26E-02	-3.69E-02
120	-1.46E-01	-6.14E-02	-4.20E-02	-1.13E-02	-2.05E-01	-1.24E-01	-3.15E-02	-4.87E-03	-1.33E-02	-2.19E-02	-6.15E-02	-1.68E-01	-4.35E-02	-1.26E-02	-3.69E-02

Appendix B - Results of undrained analysis using the ”original mesh” properties

number	1	2	3	4	5	6	7	8	9	10	11
model	R3_OB50_P23_E1_C0.1_sat	R3_OB50_P29_E3_C1.5_sat	R3_OB100_P29_E3_C1.5_sat	R3_OB200_P29_E3_C1.5_sat	R3_OB500_P29_E3_C3_sat	R3_OB500_P35_E10_C3_sat	R3_OB1000_P29_E3_C1.5_sat	R3_OB1000_P35_E10_C3_sat	R5_OB100_P29_E3_C0.5_sat	R5_OB200_P29_E3_C0.5_sat	R5_OB200_P29_E3_C1.5_sat
pl. Radius	9.3	3.9	4.2	4.6	5	4.9	13.9	7.7	8.9	14.1	7.3
shear strength c' [Mpa]	0.1	1.5	1.5	1.5	3	3	1.5	3	0.5	0.5	1.5
friction angle	23	29	29	29	29	35	29	35	29	29	29
Young's Modulus [Mpa]	1000	3000	3000	3000	3000	10000	3000	10000	3000	3000	3000
UCS [Mpa]	0.302167	5.092989	5.092989	5.092989	10.18598	11.52589	5.092989	11.52589	1.697663	1.697663	5.092989
Overburden [m]	50	50	100	200	500	500	1000	1000	100	200	200
Sigma 0 effective [Mpa]	0.75	0.75	1.5	3	7.5	7.5	15	15	1.5	3	3
UCS / Sigma 0,eff	0.402889	6.790652	3.395326	1.697663	1.35813	1.536786	0.339533	0.768393	1.131775	0.565888	1.697663
tunnelradius	3	3	3	3	3	3	3	3	5	5	5
rpl/rt	3.1	1.3	1.4	1.533333	1.666667	1.633333	4.633333	2.566667	1.78	2.82	1.46
u0/umax	0.299912	0.263336	0.26903	0.282072	0.213051	0.221785	0.228891	0.231781	0.287752	0.291356	0.277788
Station	z_disp	z_disp	z_disp	z_disp	z_disp	z_disp	z_disp	z_disp	z_disp	z_disp	z_disp
1	6.98E-08	-9.78E-09	-1.06E-08	-2.85E-08	-1.55E-07	-4.00E-08	-1.29E-06	-1.34E-07	-1.03E-06	-2.39E-06	-1.77E-06
2	1.36E-07	-1.91E-09	-6.81E-08	-1.60E-07	-4.75E-07	-1.10E-07	-3.06E-06	-3.78E-07	-1.37E-06	-3.34E-06	-2.28E-06
3	1.64E-07	8.05E-09	-9.32E-08	-1.89E-07	-5.29E-07	-1.57E-07	-3.49E-06	-5.15E-07	-1.43E-06	-3.66E-06	-2.34E-06
4	8.69E-08	1.90E-08	-8.18E-08	-1.75E-07	-5.12E-07	-1.76E-07	-3.35E-06	-5.36E-07	-1.47E-06	-3.63E-06	-2.41E-06
5	1.72E-07	2.26E-08	-7.88E-08	-1.71E-07	-5.04E-07	-1.85E-07	-3.00E-06	-5.12E-07	-1.46E-06	-3.48E-06	-2.43E-06
6	2.93E-07	1.75E-08	-7.08E-08	-1.53E-07	-4.76E-07	-1.95E-07	-2.05E-06	-4.33E-07	-1.42E-06	-3.21E-06	-2.45E-06
7	3.43E-07	2.75E-08	-5.47E-08	-1.36E-07	-4.54E-07	-2.01E-07	-8.14E-07	-3.23E-07	-1.39E-06	-2.86E-06	-2.46E-06
8	4.91E-07	2.86E-08	-4.68E-08	-1.15E-07	-4.06E-07	-2.04E-07	6.69E-07	-1.98E-07	-1.37E-06	-2.41E-06	-2.53E-06
9	6.94E-07	4.96E-08	-4.00E-08	-1.03E-07	-3.77E-07	-2.24E-07	2.26E-06	-9.11E-08	-1.33E-06	-1.92E-06	-2.55E-06
10	9.07E-07	5.04E-08	-3.71E-08	-9.79E-08	-3.57E-07	-2.27E-07	4.14E-06	6.95E-09	-1.34E-06	-1.44E-06	-2.63E-06
11	1.08E-06	5.86E-08	-3.40E-08	-8.61E-08	-3.03E-07	-2.49E-07	5.74E-06	1.17E-07	-1.31E-06	-9.76E-07	-2.70E-06
12	1.34E-06	6.97E-08	-3.19E-08	-8.06E-08	-2.82E-07	-2.68E-07	7.44E-06	2.06E-07	-1.33E-06	-5.04E-07	-2.82E-06
13	1.54E-06	7.44E-08	-2.93E-08	-7.30E-08	-3.12E-07	-2.89E-07	9.06E-06	3.19E-07	-1.35E-06	-7.58E-08	-2.95E-06
14	1.67E-06	8.94E-08	-3.12E-08	-7.75E-08	-2.98E-07	-3.21E-07	1.07E-05	3.89E-07	-1.39E-06	2.80E-07	-3.13E-06
15	1.93E-06	9.79E-08	-4.26E-08	-8.52E-08	-3.46E-07	-3.55E-07	1.22E-05	4.66E-07	-1.46E-06	6.01E-07	-3.32E-06
16	2.13E-06	1.10E-07	-5.20E-08	-1.02E-07	-3.86E-07	-3.95E-07	1.37E-05	5.25E-07	-1.53E-06	8.60E-07	-3.58E-06
17	2.31E-06	1.10E-07	-6.64E-08	-1.21E-07	-4.51E-07	-4.44E-07	1.51E-05	5.51E-07	-1.62E-06	1.03E-06	-3.85E-06
18	2.53E-06	1.16E-07	-8.10E-08	-1.47E-07	-5.65E-07	-4.99E-07	1.65E-05	5.63E-07	-1.76E-06	1.13E-06	-4.15E-06
19	2.74E-06	1.22E-07	-9.99E-08	-1.92E-07	-6.44E-07	-5.60E-07	1.77E-05	5.75E-07	-1.91E-06	1.17E-06	-4.60E-06
20	2.95E-06	1.30E-07	-1.22E-07	-2.35E-07	-8.17E-07	-6.34E-07	1.89E-05	5.35E-07	-2.11E-06	1.11E-06	-5.03E-06
21	3.17E-06	1.34E-07	-1.52E-07	-2.88E-07	-9.64E-07	-7.18E-07	1.99E-05	4.77E-07	-2.37E-06	9.51E-07	-5.59E-06
22	3.33E-06	1.36E-07	-1.82E-07	-3.65E-07	-1.21E-06	-8.17E-07	2.05E-05	3.78E-07	-2.65E-06	6.35E-07	-6.19E-06
23	3.51E-06	1.36E-07	-2.26E-07	-4.45E-07	-1.45E-06	-9.33E-07	2.11E-05	2.39E-07	-2.99E-06	1.60E-07	-6.91E-06
24	3.65E-06	1.33E-07	-2.76E-07	-5.50E-07	-1.77E-06	-1.06E-06	2.16E-05	5.53E-08	-3.41E-06	-4.50E-07	-7.73E-06
25	3.84E-06	1.29E-07	-3.35E-07	-6.73E-07	-2.12E-06	-1.20E-06	2.17E-05	-1.85E-07	-3.88E-06	-1.25E-06	-8.68E-06
26	3.97E-06	1.20E-07	-4.00E-07	-8.06E-07	-2.52E-06	-1.36E-06	2.16E-05	-4.77E-07	-4.43E-06	-2.24E-06	-9.75E-06
27	4.07E-06	1.11E-07	-4.79E-07	-9.72E-07	-3.01E-06	-1.55E-06	2.11E-05	-8.17E-07	-5.08E-06	-3.49E-06	-1.10E-05
28	4.19E-06	9.95E-08	-5.74E-07	-1.16E-06	-3.57E-06	-1.77E-06	2.03E-05	-1.27E-06	-5.80E-06	-5.02E-06	-1.24E-05
29	4.26E-06	7.99E-08	-6.76E-07	-1.38E-06	-4.25E-06	-2.02E-06	1.92E-05	-1.83E-06	-6.65E-06	-6.89E-06	-1.40E-05
30	4.32E-06	5.40E-08	-7.99E-07	-1.63E-06	-5.07E-06	-2.31E-06	1.75E-05	-2.45E-06	-7.66E-06	-9.13E-06	-1.59E-05
31	4.36E-06	2.10E-08	-9.46E-07	-1.93E-06	-5.91E-06	-2.64E-06	1.50E-05	-3.23E-06	-8.81E-06	-1.18E-05	-1.80E-05
32	4.36E-06	-1.20E-08	-1.11E-06	-2.29E-06	-6.97E-06	-3.02E-06	1.20E-05	-4.18E-06	-1.01E-05	-1.50E-05	-2.04E-05
33	4.26E-06	-5.78E-08	-1.31E-06	-2.69E-06	-8.15E-06	-3.45E-06	8.13E-06	-5.27E-06	-1.17E-05	-1.89E-05	-2.32E-05
34	4.30E-06	-1.19E-07	-1.53E-06	-3.19E-06	-9.60E-06	-3.96E-06	3.05E-06	-6.61E-06	-1.34E-05	-2.34E-05	-2.64E-05
35	4.11E-06	-1.82E-07	-1.80E-06	-3.75E-06	-1.13E-05	-4.55E-06	-3.06E-06	-8.13E-06	-1.55E-05	-2.88E-05	-3.01E-05
36	3.99E-06	-2.73E-07	-2.13E-06	-4.39E-06	-1.32E-05	-5.22E-06	-1.09E-05	-9.96E-06	-1.79E-05	-3.53E-05	-3.44E-05
37	3.62E-06	-3.59E-07	-2.50E-06	-5.20E-06	-1.56E-05	-6.03E-06	-2.02E-05	-1.22E-05	-2.07E-05	-4.29E-05	-3.94E-05
38	3.25E-06	-4.79E-07	-2.93E-06	-6.12E-06	-1.83E-05	-6.98E-06	-3.21E-05	-1.48E-05	-2.40E-05	-5.21E-05	-4.53E-05
39	2.49E-06	-6.26E-07	-3.46E-06	-7.23E-06	-2.16E-05	-8.06E-06	-4.64E-05	-1.78E-05	-2.80E-05	-6.31E-05	-5.21E-05
40	1.82E-06	-7.93E-07	-4.08E-06	-8.57E-06	-2.55E-05	-9.40E-06	-6.42E-05	-2.16E-05	-3.26E-05	-7.63E-05	-6.01E-05
41	5.61E-07	-1.02E-06	-4.82E-06	-1.02E-05	-3.02E-05	-1.10E-05	-8.61E-05	-2.61E-05	-3.81E-05	-9.23E-05	-6.97E-05
42	-6.63E-07	-1.26E-06	-5.75E-06	-1.21E-05	-3.60E-05	-1.29E-05	-1.13E-04	-3.16E-05	-4.46E-05	-1.12E-04	-8.09E-05
43	-2.66E-06	-1.59E-06	-6.84E-06	-1.45E-05	-4.31E-05	-1.53E-05	-1.47E-04	-3.84E-05	-5.24E-05	-1.36E-04	-9.43E-05
44	-4.93E-06	-1.98E-06	-8.21E-06	-1.75E-05	-5.13E-05	-1.80E-05	-1.90E-04	-4.67E-05	-6.20E-05	-1.65E-04	-1.11E-04
45	-8.03E-06	-2.51E-06	-9.96E-06	-2.11E-05	-6.20E-05	-2.16E-05	-2.45E-04	-5.70E-05	-7.35E-05	-2.02E-04	-1.30E-04
46	-1.33E-05	-3.14E-06	-1.20E-05	-2.57E-05	-7.54E-05	-2.59E-05	-3.14E-04	-7.02E-05	-8.76E-05	-2.48E-04	-1.54E-04
47	-1.83E-05	-3.97E-06	-1.48E-05	-3.18E-05	-9.29E-05	-3.13E-05	-4.06E-04	-8.69E-05	-1.05E-04	-3.08E-04	-1.83E-04
48	-2.86E-05	-5.06E-06	-1.83E-05	-3.95E-05	-1.15E-04	-3.84E-05	-5.27E-04	-1.09E-04	-1.27E-04	-3.85E-04	-2.19E-04
49	-3.78E-05	-6.60E-06	-2.30E-05	-4.95E-05	-1.44E-04	-4.76E-05	-6.92E-04	-1.37E-04	-1.54E-04	-4.86E-04	-2.64E-04
50	-6.08E-05	-8.63E-06	-2.92E-05	-6.31E-05	-1.83E-04	-5.95E-05	-9.22E-04	-1.76E-04	-1.88E-04	-6.21E-04	-3.20E-04
51	-7.65E-05	-1.17E-05	-3.76E-05	-8.13E-05	-2.35E-04	-7.59E-05	-1.25E-03	-2.29E-04	-2.31E-04	-8.05E-04	-3.90E-04
52	-1.31E-04	-1.57E-05	-4.91E-05	-1.07E-04	-3.07E-04	-9.86E-05	-1.75E-03	-3.04E-04	-2.85E-04	-1.06E-03	-4.79E-04
53	-1.67E-04	-2.19E-05	-6.54E-05	-1.43E-04	-4.08E-04	-1.30E-04	-2.54E-03	-4.11E-04	-3.55E-04	-1.41E-03	-5.91E-04
54	-2.95E-04	-3.18E-05	-8.91E-05	-1.94E-04	-5.54E-04	-1.77E-04	-3.82E-03	-5.70E-04	-4.45E-04	-1.89E-03	-7.34E-04
55	-3.96E-04	-4.72E-05	-1.24E-04	-2.70E-04	-7.67E-04	-2.45E-04	-6.09E-03	-8.14E-04	-5.59E-04	-2.54E-03	-9.15E-04
56	-7.63E-04	-7.14E-05	-1.76E-04	-3.82E-04	-1.08E-03	-3.49E-04	-9.63E-03	-1.20E-03	-7.07E-04	-3.39E-03	-1.14E-03
57	-1.03E-03	-1.11E-04	-2.54E-04	-5.47E-04	-1.55E-03	-5.11E-04	-1.55E-02	-1.85E-03	-8.99E-04	-4.39E-03	-1.42E-03
58	-1.84E-03	-1.72E-04	-3.75E-04	-7.92E-04	-2.23E-03	-7.75E-04	-2.27E-02	-2.87E-03	-1.15E-03	-5.42E-03	-1.77E-03
59	-2.30E-03	-2.67E-04	-5.63E-04	-1.15E-03	-3.36E-03	-1.27E-03	-3.15E-02	-4.73E-03	-1.43E-03	-6.46E-03	-2.23E-03
60	-3.77E-03	-4.17E-04	-8.44E-04	-1.91E-03	-4.86E-03	-2.04E-03	-4.30E-02	-7.73E-03	-1.94E-03	-8.11E-03	-3.01E-03
61	-5.75E-03	-1.09E-03	-2.15E-03	-4.60E-03	-1.62E-02	-7.07E-03	-7.11E-02	-1.79E-02	-3.69E-03	-1.20E-02	-6.50E-03
62	-7.01E-03	-1.26E-03	-2.52E-03	-5.37E-03	-1.88E-02	-8.07E-03	-8.75E-02	-2.16E-02	-4.40E-03	-1.42E-02	-7.73E-03
63	-7.77E-03	-1.36E-03	-2.74E-03	-5.84E-03	-2.00E-02	-8.50E-03	-1.01E-01	-2.40E-02	-4.87E-03	-1.60E-02	-8.51E-03
64	-8.59E-03	-1.42E-03	-2.85E-03	-6.08E-03	-2.07E-02	-8.71E-03	-1.12E-01	-2.58E-02	-5.20E-03	-1.76E-02	-9.00E-03
65	-9.02E-03	-1.46E-03	-2.93E-03	-6.25E-03	-2.12E-02	-8.83E-03	-1.21E-01	-2.72E-02	-5.45E-03	-1.88E-02	-9.35E-03
66	-9.60E-03	-1.49E-03	-2.98E-03	-6.37E-03	-2.15E-02	-8.92E-03	-1.30E-01	-2.82E-02	-5.64E-03	-1.99E-02	-9.61E-03
67	-9.86E-03	-1.51E-03	-3.02E-03	-6.45E-03	-2.18E-02	-8.97E-03	-1.37E-01	-2.90E-02	-5.80E-03	-2.09E-02	-9.81E-03
68	-1.03E-02	-1.52E-03	-3.04E-03	-6.52E-03	-2.20E-02	-9.02E-03	-1.43E-01	-2.97E-02	-5.93E-03	-2.17E-02	-9.98E-03
69	-1.05E-02	-1.53E-03	-3.07E-03	-6.57E-03	-2.21E-02	-9.05E-03	-1.48E-01	-3.03E-02	-6.04E-03	-2.24E-02	-1.01E-02
70	-1.08E-02	-1.54E-03	-3.08E-03	-6.61E-03	-2.22E-02	-9.08E-03	-1.53E-01	-3.07E-02	-6.13E-03	-2.30E-02	-1.02E-02
71	-1.09E-02	-1.55E-03	-3.09E-03	-6.64E-03	-2.23E-02	-9.10E-03	-1.57E-01	-3.11E-02	-6.21E-03	-2.36E-02	-1.03E-02
72	-1.11E-02	-1.55E-03	-3.10E-03	-6.66E-03	-2.24E-02	-9.11E-03	-1.60E-01	-3.14E-02	-6.28E-03	-2.41E-02	-1.04E-02
73	-1.12E-02	-1.55E-03	-3.11E-03	-6.68E-03	-2.25E-02	-9.12E-03	-1.64E-01	-3.17E-02	-6.34E-03	-2.45E-02	-1.05E-02
74	-1.14E-02	-1.56E-03	-3.11E-03	-6.70E-03	-2.25E-02	-9.13E-03	-1.66E-01	-3.19E-02	-6.39E-03	-2.49E-02	-1.05E-02
75	-1.15E-02	-1.56E-03	-3.12E-03	-6.71E-03	-2.26E-02	-9.14E-03	-1.69E-01	-3.21E-02	-6.44E-03	-2.52E-02	-1.06E-02
76	-1.16E-02	-1.56E-03	-3.12E-03	-6.72E-03	-2.26E-02	-9.15E-03	-1.71E-01	-3.22E-02	-6.48E-03	-2.55E-02	-1.06E-02
77	-1.17E-02	-1.56E-03	-3.13E-03	-6.73E-03	-2.27E-02	-9.16E-03	-1.73E-01	-3.24E-02	-6.51E-03	-2.58E-02	-1.07E-02
78	-1.18E-02	-1.57E-03	-3.13E-03	-6.74E-03	-2.27E-02	-9.16E-03	-1.75E-01	-3.25E-02	-6.54E-03	-2.60E-02	-1.07E-02
79	-1.18E-02	-1.57E-03	-3.13E-03	-6.75E-03	-2.27E-02	-9.16E-03	-1.76E-01	-3.26E-02	-6.57E-03	-2.62E-02	-1.07E-02
80	-1.19E-02	-1.57E-03	-3.13E-03	-6.75E-03	-2.27E-02	-9.17E-03	-1.77E-01	-3.27E-02	-6.59E-03	-2.64E-02	-1.07E-02
81	-1.20E-02	-1.57E-03	-3.13E-03	-6.76E-03	-2.28E-02	-9.17E-03	-1.79E-01	-3.28E-02	-6.61E-03	-2.66E-02	-1.08E-02
82	-1.20E-02	-1.57E-03	-3.13E-03	-6.76E-03	-2.28E-02	-9.17E-03	-1.80E-01	-3.28E-02	-6.63E-03	-2.67E-02	-1.08E-02
83	-1.21E-02	-1.57E-03	-3.13E-03	-6.76E-03	-2.28E-02	-9.17E-03	-1.81E-01	-3.29E-02	-6.65E-03	-2.69E-02	-1.08E-02
84	-1.21E-02	-1.57E-03	-3.14E-03	-6.77E-03	-2.28E-02	-9.18E-03	-1.82E-01	-3.30E-02	-6.66E-03	-2.70E-02	-1.08E-02
85	-1.21E-02	-1.57E-03	-3.14E-03	-6.77E-03	-2.28E-02	-9.18E-03	-1.82E-01	-3.30E-02	-6.68E-03	-2.71E-02	-1.08E-02
86	-1.22E-02	-1.57E-03	-3.14E-03	-6.77E-03	-2.28E-02	-9.18E-03	-1.83E-01	-3.31E-02	-6.69E-03	-2.72E-02	-1.08E-02
87	-1.22E-02	-1.57E-03	-3.14E-03	-6.77E-03	-2.28E-02	-9.18E-03	-1.84E-01	-3.31E-02	-6.70E-03	-2.73E-02	-1.08E-02
88	-1.22E-02	-1.57E-03	-3.14E-03	-6.77E-03	-2.28E-02	-9.18E-03	-1.84E-01	-3.31E-02	-6.70E-03	-2.74E-02	-1.08E-02
89	-1.22E-02	-1.57E-03	-3.14E-03	-6.77E-03	-2.28E-02	-9.18E-03	-1.85E-01	-3.32E-02	-6.71E-03	-2.74E-02	-1.08E-02
90	-1.23E-02	-1.57E-03	-3.14E-03	-6.77E-03	-2.28E-02	-9.18E-03	-1.85E-01	-3.32E-02	-6.72E-03	-2.75E-02	-1.08E-02
91	-1.23E-02	-1.57E-03	-3.14E-03	-6.78E-03	-2.28E-02	-9.18E-03	-1.86E-01	-3.32E-02	-6.72E-03	-2.76E-02	-1.09E-02
92	-1.23E-02	-1.58E-03	-3.14E-03	-6.78E-03	-2.28E-02	-9.18E-03	-1.86E-01	-3.32E-02	-6.73E-03	-2.76E-02	-1.09E-02
93	-1.23E-02	-1.58E-03	-3.14E-03	-6.78E-03	-2.28E-02	-9.18E-03	-1.86E-01	-3.32E-02	-6.73E-03	-2.77E-02	-1.09E-02
94	-1.23E-02	-1.58E-03	-3.14E-03	-6.78E-03	-2.28E-02	-9.18E-03	-1.86E-01	-3.33E-02	-6.74E-03	-2.77E-02	-1.09E-02
95	-1.23E-02	-1.58E-03	-3.14E-03	-6.78E-03	-2.28E-02	-9.18E-03	-1.87E-01	-3.33E-02	-6.74E-03	-2.77E-02	-1.09E-02
96	-1.24E-02	-1.58E-03	-3.14E-03	-6.78E-03	-2.28E-02	-9.19E-03	-1.87E-01	-3.33E-02	-6.74E-03	-2.78E-02	-1.09E-02
97	-1.24E-02	-1.58E-03	-3.14E-03	-6.78E-03	-2.28E-02	-9.19E-03	-1.87E-01	-3.33E-02	-6.74E-03	-2.78E-02	-1.09E-02
98	-1.24E-02	-1.58E-03	-3.14E-03	-6.78E-03	-2.28E-02	-9.19E-03	-1.87E-01	-3.33E-02	-6.74E-03	-2.78E-02	-1.09E-02
99	-1.24E-02	-1.58E-03	-3.14E-03	-6.78E-03	-2.28E-02	-9.19E-03	-1.87E-01	-3.33E-02	-6.74E-03	-2.78E-02	-1.09E-02
100	-1.24E-02	-1.58E-03	-3.14E-03	-6.78E-03	-2.28E-02	-9.19E-03	-1.87E-01	-3.33E-02	-6.75E-03	-2.78E-02	-1.09E-02
101	-1.24E-02	-1.58E-03	-3.14E-03	-6.78E-03	-2.28E-02	-9.19E-03	-1.88E-01	-3.33E-02	-6.75E-03	-2.78E-02	-1.09E-02
102	-1.24E-02	-1.58E-03	-3.14E-03	-6.78E-03	-2.28E-02	-9.19E-03	-1.88E-01	-3.33E-02	-6.75E-03	-2.79E-02	-1.09E-02
103	-1.24E-02	-1.58E-03	-3.14E-03	-6.78E-03	-2.28E-02	-9.19E-03	-1.88E-01	-3.33E-02	-6.75E-03	-2.79E-02	-1.09E-02
104	-1.24E-02	-1.58E-03	-3.14E-03	-6.78E-03	-2.28E-02	-9.19E-03	-1.88E-01	-3.34E-02	-6.75E-03	-2.79E-02	-1.09E-02
105	-1.24E-02	-1.58E-03	-3.14E-03	-6.78E-03	-2.28E-02	-9.19E-03	-1.88E-01	-3.34E-02	-6.75E-03	-2.79E-02	-1.09E-02
106	-1.25E-02	-1.58E-03	-3.14E-03	-6.78E-03	-2.28E-02	-9.19E-03	-1.88E-01	-3.34E-02	-6.75E-03	-2.79E-02	-1.09E-02
107	-1.25E-02	-1.58E-03	-3.14E-03	-6.78E-03	-2.28E-02	-9.19E-03	-1.88E-01	-3.34E-02	-6.75E-03	-2.79E-02	-1.09E-02
108	-1.25E-02	-1.58E-03	-3.14E-03	-6.78E-03	-2.28E-02	-9.19E-03	-1.88E-01	-3.34E-02	-6.75E-03	-2.79E-02	-1.09E-02
109	-1.25E-02	-1.58E-03	-3.14E-03	-6.78E-03	-2.28E-02	-9.19E-03	-1.88E-01	-3.34E-02	-6.74E-03	-2.79E-02	-1.09E-02
110	-1.25E-02	-1.58E-03	-3.14E-03	-6.78E-03	-2.28E-02	-9.19E-03	-1.88E-01	-3.34E-02	-6.74E-03	-2.79E-02	-1.09E-02
111	-1.25E-02	-1.58E-03	-3.14E-03	-6.78E-03	-2.28E-02	-9.19E-03	-1.88E-01	-3.34E-02	-6.74E-03	-2.79E-02	-1.09E-02
112	-1.25E-02	-1.58E-03	-3.14E-03	-6.78E-03	-2.28E-02	-9.19E-03	-1.88E-01	-3.34E-02	-6.74E-03	-2.79E-02	-1.09E-02
113	-1.25E-02	-1.58E-03	-3.14E-03	-6.78E-03	-2.28E-02	-9.19E-03	-1.88E-01	-3.34E-02	-6.74E-03	-2.79E-02	-1.09E-02
114	-1.25E-02	-1.58E-03	-3.14E-03	-6.77E-03	-2.28E-02	-9.19E-03	-1.88E-01	-3.34E-02	-6.74E-03	-2.79E-02	-1.09E-02
115	-1.25E-02	-1.58E-03	-3.14E-03	-6.77E-03	-2.28E-02	-9.19E-03	-1.88E-01	-3.34E-02	-6.74E-03	-2.79E-02	-1.09E-02
116	-1.25E-02	-1.58E-03	-3.14E-03	-6.77E-03	-2.28E-02	-9.18E-03	-1.88E-01	-3.34E-02	-6.74E-03	-2.79E-02	-1.09E-02
117	-1.25E-02	-1.58E-03	-3.14E-03	-6.77E-03	-2.28E-02	-9.18E-03	-1.88E-01	-3.34E-02	-6.74E-03	-2.79E-02	-1.09E-02
118	-1.25E-02	-1.58E-03	-3.14E-03	-6.77E-03	-2.28E-02	-9.18E-03	-1.88E-01	-3.34E-02	-6.74E-03	-2.79E-02	-1.09E-02
119	-1.26E-02	-1.58E-03	-3.14E-03	-6.77E-03	-2.28E-02	-9.18E-03	-1.88E-01	-3.34E-02	-6.74E-03	-2.79E-02	-1.09E-02
120	-1.26E-02	-1.58E-03	-3.14E-03	-6.77E-03	-2.28E-02	-9.18E-03	-1.88E-01	-3.34E-02	-6.74E-03	-2.79E-02	-1.08E-02

													additional models	
number	12	13	14	15	16	17	18	19	20	21	22	23	24	25	26
model	R5_OB500_P29_E3_C0.5_sat	R5_OB500_P29_E3_C1.5_sat	R5_OB500_P29_E3_C3_sat	R5_OB500_P35_E10_C3_sat	R5_OB1000_P29_E3_C1.5_sat	R5_OB1000_P29_E3_C3_sat	R5_OB1000_P35_E10_C3_sat	R7_OB50_P29_E3_C0.5_sat	R7_OB100_P29_E3_C0.5_sat	R7_OB200_P29_E3_C1.5_sat	R7_OB500_P29_E3_C3_sat	R7_OB1000_P29_E3_C3_sat	R7_OB1000_P35_E10_C3_sat	R5_OB500_P29_E10_C3_sat	R5_OB1000_P29_E10_C3_sat
pl. Radius	24.6	13	8.3	7.8	20.2	13	13	8.8	12	10.1	11.3	18.3	18.3	8.9	15.4
shear strength c' [Mpa]	0.5	1.5	3	3	1.5	3	3	0.5	0.5	1.5	3	3	3	3	3
friction angle	29	29	29	35	29	29	35	29	29	29	29	29	35	29	29
Young's Modulus [Mpa]	3000	3000	3000	10000	3000	3000	10000	3000	3000	3000	3000	3000	10000	10000	10000
UCS [Mpa]	1.697663	5.092989	10.18598	11.52589	5.092989	10.18598	11.52589	1.697663	1.697663	5.092989	10.18598	10.18598	11.52589	10.18598	10.18598
Overburden [m]	500	500	500	500	1000	1000	1000	50	100	200	500	1000	1000	500	500
Sigma 0 effective [Mpa]	7.5	7.5	7.5	7.5	15	15	15	0.75	1.5	3	7.5	15	15	7.5	7.5
UCS / Sigma 0,eff	0.226355	0.679065	1.35813	1.536786	0.339533	0.679065	0.768393	2.263551	1.131775	1.697663	1.35813	0.679065	0.768393	1.35813	1.35813
tunnelradius	5	5	5	5	5	5	5	7	7	7	7	7	7	5	5
rpl/rt	4.92	2.6	1.66	1.56	4.04	2.6	2.6	1.257143	1.714286	1.442857	1.614286	2.614286	2.614286	1.78	3.08
u0/umax	0.27402	0.265866	0.212983	0.226412	0.252826	0.261809	0.223719	0.285976	0.293435	0.262489	0.210734	0.269586	0.228201	0.238441	0.220741
Station	z_disp	z_disp	z_disp	z_disp	z_disp	z_disp	z_disp	z_disp	z_disp	z_disp	z_disp	z_disp	z_disp	z_disp	z_disp
1	-7.77E-06	-5.97E-06	-4.77E-06	-1.14E-06	-1.52E-05	-1.19E-05	-2.74E-06	-8.20E-07	-2.56E-06	-3.96E-06	-1.08E-05	-2.55E-05	-5.48E-06	-1.22E-06	-3.01E-06
2	-1.34E-05	-8.35E-06	-6.70E-06	-1.67E-06	-2.20E-05	-1.62E-05	-4.12E-06	-1.38E-06	-3.35E-06	-5.83E-06	-1.58E-05	-5.02E-05	-1.06E-05	-1.71E-06	-4.83E-06
3	-1.63E-05	-8.96E-06	-6.91E-06	-1.80E-06	-2.62E-05	-1.80E-05	-5.16E-06	-1.81E-06	-4.62E-06	-7.75E-06	-2.17E-05	-6.10E-05	-1.50E-05	-1.91E-06	-5.73E-06
4	-1.91E-05	-9.05E-06	-7.48E-06	-1.97E-06	-2.95E-05	-1.81E-05	-5.52E-06	-1.92E-06	-5.08E-06	-8.37E-06	-2.42E-05	-6.48E-05	-1.78E-05	-2.10E-06	-6.18E-06
5	-2.13E-05	-8.74E-06	-7.44E-06	-2.02E-06	-3.17E-05	-1.73E-05	-5.69E-06	-2.04E-06	-5.47E-06	-9.05E-06	-2.66E-05	-6.88E-05	-1.94E-05	-2.15E-06	-6.53E-06
6	-2.27E-05	-8.18E-06	-7.57E-06	-2.12E-06	-3.24E-05	-1.61E-05	-5.75E-06	-2.07E-06	-5.62E-06	-9.30E-06	-2.77E-05	-7.08E-05	-2.05E-05	-2.25E-06	-6.67E-06
7	-2.32E-05	-7.41E-06	-7.56E-06	-2.16E-06	-3.17E-05	-1.47E-05	-5.69E-06	-2.10E-06	-5.69E-06	-9.63E-06	-2.87E-05	-7.16E-05	-2.16E-05	-2.24E-06	-6.66E-06
8	-2.32E-05	-6.58E-06	-7.56E-06	-2.27E-06	-3.01E-05	-1.30E-05	-5.63E-06	-2.14E-06	-5.72E-06	-9.81E-06	-2.92E-05	-7.06E-05	-2.24E-05	-2.35E-06	-6.51E-06
9	-2.28E-05	-5.77E-06	-7.78E-06	-2.36E-06	-2.76E-05	-1.13E-05	-5.47E-06	-2.21E-06	-5.81E-06	-1.02E-05	-3.02E-05	-6.93E-05	-2.32E-05	-2.42E-06	-6.19E-06
10	-2.19E-05	-4.82E-06	-7.92E-06	-2.47E-06	-2.42E-05	-9.29E-06	-5.34E-06	-2.26E-06	-5.82E-06	-1.05E-05	-3.09E-05	-6.64E-05	-2.36E-05	-2.53E-06	-5.92E-06
11	-2.08E-05	-4.00E-06	-8.07E-06	-2.62E-06	-2.04E-05	-7.59E-06	-5.17E-06	-2.31E-06	-5.94E-06	-1.10E-05	-3.21E-05	-6.44E-05	-2.43E-05	-2.64E-06	-5.59E-06
12	-1.94E-05	-3.21E-06	-8.42E-06	-2.76E-06	-1.67E-05	-5.91E-06	-5.07E-06	-2.40E-06	-6.05E-06	-1.15E-05	-3.34E-05	-6.36E-05	-2.48E-05	-2.77E-06	-5.27E-06
13	-1.77E-05	-2.51E-06	-8.66E-06	-2.95E-06	-1.34E-05	-4.36E-06	-5.00E-06	-2.51E-06	-6.26E-06	-1.21E-05	-3.46E-05	-6.25E-05	-2.57E-05	-2.94E-06	-5.04E-06
14	-1.63E-05	-1.91E-06	-9.12E-06	-3.16E-06	-1.02E-05	-3.19E-06	-5.05E-06	-2.61E-06	-6.46E-06	-1.28E-05	-3.64E-05	-6.24E-05	-2.65E-05	-3.16E-06	-4.89E-06
15	-1.52E-05	-1.51E-06	-9.68E-06	-3.41E-06	-7.53E-06	-2.35E-06	-5.20E-06	-2.81E-06	-6.81E-06	-1.36E-05	-3.85E-05	-6.28E-05	-2.75E-05	-3.38E-06	-4.80E-06
16	-1.42E-05	-1.18E-06	-1.05E-05	-3.70E-06	-5.41E-06	-1.74E-06	-5.44E-06	-2.98E-06	-7.16E-06	-1.46E-05	-4.11E-05	-6.53E-05	-2.90E-05	-3.66E-06	-4.87E-06
17	-1.39E-05	-1.03E-06	-1.12E-05	-3.99E-06	-4.12E-06	-1.23E-06	-5.82E-06	-3.19E-06	-7.71E-06	-1.57E-05	-4.39E-05	-6.81E-05	-3.09E-05	-3.95E-06	-5.09E-06
18	-1.41E-05	-1.09E-06	-1.22E-05	-4.35E-06	-3.26E-06	-1.24E-06	-6.28E-06	-3.46E-06	-8.27E-06	-1.68E-05	-4.75E-05	-7.18E-05	-3.32E-05	-4.31E-06	-5.45E-06
19	-1.46E-05	-1.37E-06	-1.33E-05	-4.77E-06	-3.06E-06	-1.50E-06	-6.93E-06	-3.74E-06	-9.12E-06	-1.84E-05	-5.20E-05	-7.68E-05	-3.60E-05	-4.71E-06	-6.04E-06
20	-1.57E-05	-1.77E-06	-1.46E-05	-5.28E-06	-3.55E-06	-2.19E-06	-7.73E-06	-4.10E-06	-9.94E-06	-2.01E-05	-5.65E-05	-8.30E-05	-3.93E-05	-5.18E-06	-6.79E-06
21	-1.76E-05	-2.39E-06	-1.62E-05	-5.82E-06	-5.01E-06	-3.43E-06	-8.71E-06	-4.48E-06	-1.08E-05	-2.20E-05	-6.18E-05	-9.15E-05	-4.32E-05	-5.71E-06	-7.76E-06
22	-2.01E-05	-3.31E-06	-1.79E-05	-6.42E-06	-7.90E-06	-5.28E-06	-9.90E-06	-4.90E-06	-1.19E-05	-2.44E-05	-6.75E-05	-1.02E-04	-4.77E-05	-6.35E-06	-8.96E-06
23	-2.36E-05	-4.58E-06	-1.99E-05	-7.15E-06	-1.17E-05	-7.64E-06	-1.13E-05	-5.43E-06	-1.31E-05	-2.68E-05	-7.36E-05	-1.14E-04	-5.29E-05	-7.06E-06	-1.05E-05
24	-2.77E-05	-6.28E-06	-2.22E-05	-7.92E-06	-1.70E-05	-1.11E-05	-1.30E-05	-6.07E-06	-1.45E-05	-2.96E-05	-8.19E-05	-1.29E-04	-5.86E-05	-7.87E-06	-1.23E-05
25	-3.29E-05	-8.37E-06	-2.48E-05	-8.82E-06	-2.40E-05	-1.52E-05	-1.50E-05	-6.74E-06	-1.60E-05	-3.28E-05	-9.01E-05	-1.47E-04	-6.53E-05	-8.77E-06	-1.45E-05
26	-3.94E-05	-1.10E-05	-2.79E-05	-9.83E-06	-3.27E-05	-2.05E-05	-1.74E-05	-7.46E-06	-1.79E-05	-3.60E-05	-9.96E-05	-1.68E-04	-7.34E-05	-9.82E-06	-1.72E-05
27	-4.74E-05	-1.42E-05	-3.13E-05	-1.10E-05	-4.33E-05	-2.68E-05	-2.02E-05	-8.37E-06	-2.00E-05	-4.02E-05	-1.11E-04	-1.92E-04	-8.28E-05	-1.10E-05	-2.03E-05
28	-5.67E-05	-1.80E-05	-3.53E-05	-1.23E-05	-5.63E-05	-3.45E-05	-2.34E-05	-9.37E-06	-2.24E-05	-4.44E-05	-1.23E-04	-2.20E-04	-9.31E-05	-1.24E-05	-2.39E-05
29	-6.81E-05	-2.26E-05	-3.99E-05	-1.38E-05	-7.20E-05	-4.35E-05	-2.72E-05	-1.05E-05	-2.51E-05	-4.94E-05	-1.37E-04	-2.54E-04	-1.05E-04	-1.39E-05	-2.82E-05
30	-8.12E-05	-2.81E-05	-4.51E-05	-1.55E-05	-9.08E-05	-5.44E-05	-3.15E-05	-1.17E-05	-2.82E-05	-5.52E-05	-1.53E-04	-2.91E-04	-1.19E-04	-1.56E-05	-3.33E-05
31	-9.71E-05	-3.47E-05	-5.11E-05	-1.74E-05	-1.13E-04	-6.73E-05	-3.66E-05	-1.32E-05	-3.19E-05	-6.16E-05	-1.70E-04	-3.37E-04	-1.35E-04	-1.76E-05	-3.92E-05
32	-1.15E-04	-4.23E-05	-5.78E-05	-1.96E-05	-1.40E-04	-8.26E-05	-4.25E-05	-1.48E-05	-3.60E-05	-6.92E-05	-1.91E-04	-3.88E-04	-1.53E-04	-1.99E-05	-4.61E-05
33	-1.38E-04	-5.13E-05	-6.57E-05	-2.21E-05	-1.71E-04	-1.01E-04	-4.94E-05	-1.67E-05	-4.07E-05	-7.75E-05	-2.14E-04	-4.47E-04	-1.74E-04	-2.25E-05	-5.41E-05
34	-1.63E-04	-6.21E-05	-7.49E-05	-2.50E-05	-2.09E-04	-1.22E-04	-5.74E-05	-1.89E-05	-4.62E-05	-8.70E-05	-2.42E-04	-5.16E-04	-1.98E-04	-2.56E-05	-6.34E-05
35	-1.94E-04	-7.47E-05	-8.54E-05	-2.83E-05	-2.53E-04	-1.47E-04	-6.66E-05	-2.13E-05	-5.23E-05	-9.81E-05	-2.72E-04	-5.98E-04	-2.26E-04	-2.90E-05	-7.44E-05
36	-2.29E-04	-8.96E-05	-9.77E-05	-3.22E-05	-3.06E-04	-1.77E-04	-7.75E-05	-2.41E-05	-5.95E-05	-1.11E-04	-3.06E-04	-6.91E-04	-2.59E-04	-3.30E-05	-8.72E-05
37	-2.72E-04	-1.07E-04	-1.12E-04	-3.66E-05	-3.68E-04	-2.12E-04	-9.03E-05	-2.73E-05	-6.78E-05	-1.25E-04	-3.47E-04	-8.01E-04	-2.96E-04	-3.77E-05	-1.02E-04
38	-3.22E-04	-1.28E-04	-1.28E-04	-4.17E-05	-4.42E-04	-2.54E-04	-1.05E-04	-3.11E-05	-7.74E-05	-1.42E-04	-3.94E-04	-9.29E-04	-3.40E-04	-4.30E-05	-1.20E-04
39	-3.84E-04	-1.53E-04	-1.48E-04	-4.77E-05	-5.31E-04	-3.04E-04	-1.23E-04	-3.55E-05	-8.83E-05	-1.61E-04	-4.47E-04	-1.08E-03	-3.91E-04	-4.93E-05	-1.41E-04
40	-4.56E-04	-1.83E-04	-1.71E-04	-5.47E-05	-6.39E-04	-3.64E-04	-1.44E-04	-4.05E-05	-1.01E-04	-1.83E-04	-5.09E-04	-1.26E-03	-4.51E-04	-5.66E-05	-1.66E-04
41	-5.45E-04	-2.19E-04	-1.98E-04	-6.29E-05	-7.69E-04	-4.36E-04	-1.69E-04	-4.63E-05	-1.16E-04	-2.09E-04	-5.81E-04	-1.47E-03	-5.22E-04	-6.53E-05	-1.96E-04
42	-6.53E-04	-2.63E-04	-2.30E-04	-7.26E-05	-9.29E-04	-5.24E-04	-1.98E-04	-5.32E-05	-1.34E-04	-2.39E-04	-6.63E-04	-1.73E-03	-6.06E-04	-7.56E-05	-2.32E-04
43	-7.88E-04	-3.16E-04	-2.69E-04	-8.43E-05	-1.13E-03	-6.30E-04	-2.34E-04	-6.12E-05	-1.54E-04	-2.74E-04	-7.59E-04	-2.03E-03	-7.05E-04	-8.79E-05	-2.76E-04
44	-9.55E-04	-3.81E-04	-3.15E-04	-9.83E-05	-1.37E-03	-7.61E-04	-2.78E-04	-7.06E-05	-1.78E-04	-3.14E-04	-8.74E-04	-2.40E-03	-8.23E-04	-1.03E-04	-3.29E-04
45	-1.17E-03	-4.61E-04	-3.70E-04	-1.15E-04	-1.68E-03	-9.22E-04	-3.31E-04	-8.16E-05	-2.07E-04	-3.62E-04	-1.01E-03	-2.85E-03	-9.66E-04	-1.21E-04	-3.96E-04
46	-1.44E-03	-5.62E-04	-4.37E-04	-1.35E-04	-2.07E-03	-1.12E-03	-3.97E-04	-9.47E-05	-2.41E-04	-4.18E-04	-1.16E-03	-3.39E-03	-1.14E-03	-1.42E-04	-4.78E-04
47	-1.80E-03	-6.89E-04	-5.20E-04	-1.61E-04	-2.58E-03	-1.38E-03	-4.80E-04	-1.10E-04	-2.81E-04	-4.84E-04	-1.35E-03	-4.06E-03	-1.35E-03	-1.69E-04	-5.83E-04
48	-2.27E-03	-8.52E-04	-6.21E-04	-1.92E-04	-3.26E-03	-1.71E-03	-5.85E-04	-1.28E-04	-3.29E-04	-5.62E-04	-1.57E-03	-4.90E-03	-1.61E-03	-2.02E-04	-7.17E-04
49	-2.91E-03	-1.06E-03	-7.48E-04	-2.30E-04	-4.16E-03	-2.13E-03	-7.17E-04	-1.50E-04	-3.87E-04	-6.54E-04	-1.82E-03	-5.94E-03	-1.94E-03	-2.44E-04	-8.92E-04
50	-3.78E-03	-1.34E-03	-9.04E-04	-2.79E-04	-5.40E-03	-2.69E-03	-8.90E-04	-1.76E-04	-4.54E-04	-7.64E-04	-2.13E-03	-7.25E-03	-2.34E-03	-2.96E-04	-1.12E-03
51	-4.95E-03	-1.71E-03	-1.10E-03	-3.41E-04	-7.11E-03	-3.43E-03	-1.12E-03	-2.07E-04	-5.36E-04	-8.94E-04	-2.49E-03	-8.89E-03	-2.85E-03	-3.64E-04	-1.43E-03
52	-6.64E-03	-2.22E-03	-1.35E-03	-4.21E-04	-9.50E-03	-4.45E-03	-1.42E-03	-2.44E-04	-6.33E-04	-1.05E-03	-2.91E-03	-1.09E-02	-3.49E-03	-4.51E-04	-1.86E-03
53	-9.07E-03	-2.91E-03	-1.66E-03	-5.25E-04	-1.26E-02	-5.83E-03	-1.83E-03	-2.88E-04	-7.47E-04	-1.23E-03	-3.40E-03	-1.35E-02	-4.29E-03	-5.64E-04	-2.45E-03
54	-1.24E-02	-3.86E-03	-2.05E-03	-6.61E-04	-1.71E-02	-7.75E-03	-2.39E-03	-3.39E-04	-8.85E-04	-1.44E-03	-3.98E-03	-1.65E-02	-5.29E-03	-7.15E-04	-3.26E-03
55	-1.65E-02	-5.17E-03	-2.55E-03	-8.41E-04	-2.23E-02	-1.04E-02	-3.17E-03	-4.00E-04	-1.05E-03	-1.69E-03	-4.65E-03	-2.01E-02	-6.53E-03	-9.16E-04	-4.33E-03
56	-2.11E-02	-6.82E-03	-3.17E-03	-1.09E-03	-2.84E-02	-1.37E-02	-4.20E-03	-4.71E-04	-1.24E-03	-1.98E-03	-5.44E-03	-2.41E-02	-8.03E-03	-1.19E-03	-5.83E-03
57	-2.57E-02	-8.91E-03	-3.96E-03	-1.42E-03	-3.56E-02	-1.79E-02	-5.61E-03	-5.51E-04	-1.47E-03	-2.31E-03	-6.37E-03	-2.83E-02	-9.56E-03	-1.57E-03	-7.54E-03
58	-3.03E-02	-1.11E-02	-4.98E-03	-1.89E-03	-4.31E-02	-2.23E-02	-7.26E-03	-6.41E-04	-1.74E-03	-2.68E-03	-7.48E-03	-3.25E-02	-1.11E-02	-2.09E-03	-9.49E-03
59	-3.51E-02	-1.35E-02	-6.36E-03	-2.46E-03	-5.15E-02	-2.72E-02	-9.15E-03	-7.34E-04	-2.00E-03	-3.12E-03	-8.83E-03	-3.70E-02	-1.29E-02	-2.68E-03	-1.17E-02
60	-4.10E-02	-1.67E-02	-7.85E-03	-3.03E-03	-6.12E-02	-3.37E-02	-1.18E-02	-9.19E-04	-2.56E-03	-3.82E-03	-1.05E-02	-4.28E-02	-1.54E-02	-3.36E-03	-1.50E-02
61	-5.43E-02	-2.86E-02	-2.17E-02	-8.95E-03	-8.85E-02	-5.79E-02	-2.38E-02	-1.82E-03	-4.45E-03	-8.31E-03	-2.62E-02	-7.04E-02	-2.82E-02	-9.19E-03	-2.73E-02
62	-6.35E-02	-3.41E-02	-2.63E-02	-1.07E-02	-1.06E-01	-6.91E-02	-2.86E-02	-2.17E-03	-5.30E-03	-9.81E-03	-3.25E-02	-8.48E-02	-3.42E-02	-1.10E-02	-3.30E-02
63	-7.20E-02	-3.83E-02	-2.90E-02	-1.16E-02	-1.20E-01	-7.77E-02	-3.22E-02	-2.41E-03	-5.90E-03	-1.08E-02	-3.64E-02	-9.47E-02	-3.84E-02	-1.19E-02	-3.75E-02
64	-7.93E-02	-4.17E-02	-3.07E-02	-1.21E-02	-1.33E-01	-8.48E-02	-3.51E-02	-2.57E-03	-6.33E-03	-1.15E-02	-3.91E-02	-1.03E-01	-4.20E-02	-1.24E-02	-4.14E-02
65	-8.60E-02	-4.45E-02	-3.19E-02	-1.24E-02	-1.44E-01	-9.06E-02	-3.76E-02	-2.68E-03	-6.68E-03	-1.20E-02	-4.10E-02	-1.09E-01	-4.51E-02	-1.28E-02	-4.46E-02
66	-9.19E-02	-4.68E-02	-3.27E-02	-1.26E-02	-1.54E-01	-9.55E-02	-3.96E-02	-2.77E-03	-6.95E-03	-1.24E-02	-4.25E-02	-1.15E-01	-4.78E-02	-1.30E-02	-4.74E-02
67	-9.74E-02	-4.88E-02	-3.33E-02	-1.27E-02	-1.63E-01	-9.97E-02	-4.13E-02	-2.84E-03	-7.18E-03	-1.27E-02	-4.35E-02	-1.20E-01	-5.01E-02	-1.32E-02	-4.98E-02
68	-1.02E-01	-5.06E-02	-3.39E-02	-1.29E-02	-1.71E-01	-1.03E-01	-4.28E-02	-2.90E-03	-7.37E-03	-1.29E-02	-4.44E-02	-1.25E-01	-5.21E-02	-1.33E-02	-5.19E-02
69	-1.07E-01	-5.20E-02	-3.43E-02	-1.29E-02	-1.78E-01	-1.06E-01	-4.40E-02	-2.95E-03	-7.53E-03	-1.31E-02	-4.51E-02	-1.28E-01	-5.38E-02	-1.34E-02	-5.37E-02
70	-1.11E-01	-5.33E-02	-3.47E-02	-1.30E-02	-1.85E-01	-1.09E-01	-4.51E-02	-2.99E-03	-7.67E-03	-1.33E-02	-4.57E-02	-1.32E-01	-5.54E-02	-1.35E-02	-5.53E-02
71	-1.14E-01	-5.44E-02	-3.50E-02	-1.31E-02	-1.91E-01	-1.11E-01	-4.60E-02	-3.02E-03	-7.80E-03	-1.34E-02	-4.63E-02	-1.35E-01	-5.67E-02	-1.36E-02	-5.67E-02
72	-1.18E-01	-5.54E-02	-3.53E-02	-1.31E-02	-1.96E-01	-1.13E-01	-4.68E-02	-3.05E-03	-7.90E-03	-1.36E-02	-4.67E-02	-1.38E-01	-5.79E-02	-1.37E-02	-5.80E-02
73	-1.21E-01	-5.63E-02	-3.55E-02	-1.32E-02	-2.01E-01	-1.15E-01	-4.75E-02	-3.08E-03	-8.00E-03	-1.37E-02	-4.71E-02	-1.40E-01	-5.89E-02	-1.37E-02	-5.90E-02
74	-1.24E-01	-5.70E-02	-3.57E-02	-1.32E-02	-2.05E-01	-1.17E-01	-4.81E-02	-3.10E-03	-8.08E-03	-1.38E-02	-4.75E-02	-1.42E-01	-5.99E-02	-1.38E-02	-6.00E-02
75	-1.26E-01	-5.77E-02	-3.59E-02	-1.32E-02	-2.09E-01	-1.18E-01	-4.87E-02	-3.11E-03	-8.15E-03	-1.39E-02	-4.78E-02	-1.44E-01	-6.07E-02	-1.38E-02	-6.09E-02
76	-1.29E-01	-5.83E-02	-3.60E-02	-1.32E-02	-2.12E-01	-1.19E-01	-4.91E-02	-3.13E-03	-8.22E-03	-1.40E-02	-4.81E-02	-1.46E-01	-6.14E-02	-1.38E-02	-6.16E-02
77	-1.31E-01	-5.88E-02	-3.62E-02	-1.33E-02	-2.15E-01	-1.20E-01	-4.96E-02	-3.14E-03	-8.28E-03	-1.40E-02	-4.83E-02	-1.47E-01	-6.21E-02	-1.39E-02	-6.23E-02
78	-1.33E-01	-5.93E-02	-3.63E-02	-1.33E-02	-2.18E-01	-1.21E-01	-4.99E-02	-3.15E-03	-8.33E-03	-1.41E-02	-4.85E-02	-1.49E-01	-6.27E-02	-1.39E-02	-6.29E-02
79	-1.34E-01	-5.97E-02	-3.64E-02	-1.33E-02	-2.21E-01	-1.22E-01	-5.03E-02	-3.16E-03	-8.38E-03	-1.41E-02	-4.87E-02	-1.50E-01	-6.32E-02	-1.39E-02	-6.34E-02
80	-1.36E-01	-6.01E-02	-3.64E-02	-1.33E-02	-2.23E-01	-1.23E-01	-5.05E-02	-3.17E-03	-8.43E-03	-1.42E-02	-4.89E-02	-1.51E-01	-6.37E-02	-1.40E-02	-6.39E-02
81	-1.38E-01	-6.04E-02	-3.65E-02	-1.33E-02	-2.25E-01	-1.24E-01	-5.08E-02	-3.18E-03	-8.46E-03	-1.42E-02	-4.90E-02	-1.52E-01	-6.41E-02	-1.40E-02	-6.43E-02
82	-1.39E-01	-6.07E-02	-3.66E-02	-1.33E-02	-2.27E-01	-1.24E-01	-5.10E-02	-3.19E-03	-8.50E-03	-1.43E-02	-4.92E-02	-1.53E-01	-6.45E-02	-1.40E-02	-6.47E-02
83	-1.40E-01	-6.09E-02	-3.66E-02	-1.33E-02	-2.29E-01	-1.25E-01	-5.12E-02	-3.19E-03	-8.53E-03	-1.43E-02	-4.93E-02	-1.54E-01	-6.48E-02	-1.40E-02	-6.51E-02
84	-1.41E-01	-6.12E-02	-3.67E-02	-1.33E-02	-2.31E-01	-1.25E-01	-5.14E-02	-3.20E-03	-8.56E-03	-1.43E-02	-4.94E-02	-1.54E-01	-6.51E-02	-1.40E-02	-6.54E-02
85	-1.42E-01	-6.14E-02	-3.67E-02	-1.34E-02	-2.32E-01	-1.26E-01	-5.16E-02	-3.20E-03	-8.58E-03	-1.43E-02	-4.95E-02	-1.55E-01	-6.54E-02	-1.40E-02	-6.57E-02
86	-1.43E-01	-6.16E-02	-3.67E-02	-1.34E-02	-2.33E-01	-1.26E-01	-5.17E-02	-3.21E-03	-8.60E-03	-1.44E-02	-4.96E-02	-1.55E-01	-6.57E-02	-1.40E-02	-6.59E-02
87	-1.44E-01	-6.17E-02	-3.68E-02	-1.34E-02	-2.34E-01	-1.27E-01	-5.19E-02	-3.21E-03	-8.62E-03	-1.44E-02	-4.96E-02	-1.56E-01	-6.59E-02	-1.40E-02	-6.61E-02
88	-1.45E-01	-6.19E-02	-3.68E-02	-1.34E-02	-2.35E-01	-1.27E-01	-5.20E-02	-3.21E-03	-8.64E-03	-1.44E-02	-4.97E-02	-1.56E-01	-6.61E-02	-1.41E-02	-6.63E-02
89	-1.45E-01	-6.20E-02	-3.68E-02	-1.34E-02	-2.36E-01	-1.27E-01	-5.21E-02	-3.21E-03	-8.65E-03	-1.44E-02	-4.97E-02	-1.57E-01	-6.62E-02	-1.41E-02	-6.65E-02
90	-1.46E-01	-6.21E-02	-3.68E-02	-1.34E-02	-2.37E-01	-1.27E-01	-5.22E-02	-3.22E-03	-8.67E-03	-1.44E-02	-4.98E-02	-1.57E-01	-6.64E-02	-1.41E-02	-6.67E-02
91	-1.46E-01	-6.22E-02	-3.69E-02	-1.34E-02	-2.38E-01	-1.28E-01	-5.23E-02	-3.22E-03	-8.68E-03	-1.45E-02	-4.98E-02	-1.57E-01	-6.65E-02	-1.41E-02	-6.68E-02
92	-1.47E-01	-6.23E-02	-3.69E-02	-1.34E-02	-2.39E-01	-1.28E-01	-5.24E-02	-3.22E-03	-8.69E-03	-1.45E-02	-4.99E-02	-1.58E-01	-6.67E-02	-1.41E-02	-6.69E-02
93	-1.47E-01	-6.24E-02	-3.69E-02	-1.34E-02	-2.39E-01	-1.28E-01	-5.24E-02	-3.22E-03	-8.70E-03	-1.45E-02	-4.99E-02	-1.58E-01	-6.68E-02	-1.41E-02	-6.70E-02
94	-1.48E-01	-6.25E-02	-3.69E-02	-1.34E-02	-2.40E-01	-1.28E-01	-5.25E-02	-3.22E-03	-8.71E-03	-1.45E-02	-4.99E-02	-1.58E-01	-6.69E-02	-1.41E-02	-6.71E-02
95	-1.48E-01	-6.25E-02	-3.69E-02	-1.34E-02	-2.40E-01	-1.28E-01	-5.25E-02	-3.22E-03	-8.71E-03	-1.45E-02	-4.99E-02	-1.58E-01	-6.70E-02	-1.41E-02	-6.72E-02
96	-1.48E-01	-6.26E-02	-3.69E-02	-1.34E-02	-2.40E-01	-1.28E-01	-5.26E-02	-3.22E-03	-8.72E-03	-1.45E-02	-4.99E-02	-1.58E-01	-6.71E-02	-1.41E-02	-6.73E-02
97	-1.48E-01	-6.26E-02	-3.69E-02	-1.34E-02	-2.41E-01	-1.28E-01	-5.26E-02	-3.22E-03	-8.72E-03	-1.45E-02	-5.00E-02	-1.59E-01	-6.71E-02	-1.41E-02	-6.74E-02
98	-1.49E-01	-6.27E-02	-3.69E-02	-1.34E-02	-2.41E-01	-1.29E-01	-5.27E-02	-3.22E-03	-8.73E-03	-1.45E-02	-5.00E-02	-1.59E-01	-6.72E-02	-1.41E-02	-6.74E-02
99	-1.49E-01	-6.27E-02	-3.69E-02	-1.34E-02	-2.41E-01	-1.29E-01	-5.27E-02	-3.22E-03	-8.73E-03	-1.45E-02	-5.00E-02	-1.59E-01	-6.73E-02	-1.41E-02	-6.75E-02
100	-1.49E-01	-6.27E-02	-3.69E-02	-1.34E-02	-2.41E-01	-1.29E-01	-5.27E-02	-3.22E-03	-8.73E-03	-1.45E-02	-5.00E-02	-1.59E-01	-6.73E-02	-1.41E-02	-6.75E-02
101	-1.49E-01	-6.28E-02	-3.69E-02	-1.34E-02	-2.42E-01	-1.29E-01	-5.27E-02	-3.22E-03	-8.74E-03	-1.45E-02	-5.00E-02	-1.59E-01	-6.73E-02	-1.41E-02	-6.76E-02
102	-1.49E-01	-6.28E-02	-3.69E-02	-1.34E-02	-2.42E-01	-1.29E-01	-5.28E-02	-3.22E-03	-8.74E-03	-1.45E-02	-5.00E-02	-1.59E-01	-6.74E-02	-1.41E-02	-6.76E-02
103	-1.49E-01	-6.28E-02	-3.69E-02	-1.34E-02	-2.42E-01	-1.29E-01	-5.28E-02	-3.22E-03	-8.74E-03	-1.45E-02	-5.00E-02	-1.59E-01	-6.74E-02	-1.41E-02	-6.77E-02
104	-1.49E-01	-6.28E-02	-3.69E-02	-1.34E-02	-2.42E-01	-1.29E-01	-5.28E-02	-3.22E-03	-8.74E-03	-1.45E-02	-5.00E-02	-1.59E-01	-6.74E-02	-1.41E-02	-6.77E-02
105	-1.49E-01	-6.28E-02	-3.69E-02	-1.34E-02	-2.42E-01	-1.29E-01	-5.28E-02	-3.22E-03	-8.74E-03	-1.45E-02	-5.00E-02	-1.59E-01	-6.75E-02	-1.41E-02	-6.77E-02
106	-1.49E-01	-6.28E-02	-3.69E-02	-1.34E-02	-2.42E-01	-1.29E-01	-5.28E-02	-3.22E-03	-8.74E-03	-1.45E-02	-5.00E-02	-1.59E-01	-6.75E-02	-1.41E-02	-6.77E-02
107	-1.50E-01	-6.28E-02	-3.69E-02	-1.34E-02	-2.42E-01	-1.29E-01	-5.28E-02	-3.22E-03	-8.74E-03	-1.45E-02	-5.00E-02	-1.59E-01	-6.75E-02	-1.41E-02	-6.77E-02
108	-1.50E-01	-6.28E-02	-3.69E-02	-1.34E-02	-2.42E-01	-1.29E-01	-5.28E-02	-3.22E-03	-8.74E-03	-1.45E-02	-5.00E-02	-1.59E-01	-6.75E-02	-1.41E-02	-6.78E-02
109	-1.50E-01	-6.28E-02	-3.69E-02	-1.34E-02	-2.42E-01	-1.29E-01	-5.29E-02	-3.22E-03	-8.74E-03	-1.45E-02	-5.00E-02	-1.59E-01	-6.75E-02	-1.41E-02	-6.78E-02
110	-1.50E-01	-6.28E-02	-3.69E-02	-1.34E-02	-2.42E-01	-1.29E-01	-5.29E-02	-3.22E-03	-8.74E-03	-1.45E-02	-5.00E-02	-1.59E-01	-6.75E-02	-1.41E-02	-6.78E-02
111	-1.50E-01	-6.28E-02	-3.69E-02	-1.34E-02	-2.42E-01	-1.29E-01	-5.29E-02	-3.22E-03	-8.74E-03	-1.46E-02	-5.00E-02	-1.59E-01	-6.75E-02	-1.41E-02	-6.78E-02
112	-1.50E-01	-6.28E-02	-3.69E-02	-1.34E-02	-2.42E-01	-1.29E-01	-5.29E-02	-3.22E-03	-8.74E-03	-1.45E-02	-5.00E-02	-1.59E-01	-6.75E-02	-1.41E-02	-6.78E-02
113	-1.50E-01	-6.28E-02	-3.69E-02	-1.34E-02	-2.42E-01	-1.29E-01	-5.29E-02	-3.22E-03	-8.74E-03	-1.45E-02	-4.99E-02	-1.59E-01	-6.75E-02	-1.41E-02	-6.78E-02
114	-1.50E-01	-6.28E-02	-3.69E-02	-1.34E-02	-2.42E-01	-1.29E-01	-5.29E-02	-3.22E-03	-8.74E-03	-1.45E-02	-4.99E-02	-1.59E-01	-6.75E-02	-1.41E-02	-6.78E-02
115	-1.50E-01	-6.28E-02	-3.69E-02	-1.34E-02	-2.42E-01	-1.29E-01	-5.29E-02	-3.22E-03	-8.74E-03	-1.46E-02	-4.99E-02	-1.59E-01	-6.75E-02	-1.41E-02	-6.78E-02
116	-1.50E-01	-6.28E-02	-3.69E-02	-1.34E-02	-2.42E-01	-1.29E-01	-5.29E-02	-3.22E-03	-8.73E-03	-1.46E-02	-4.99E-02	-1.59E-01	-6.75E-02	-1.41E-02	-6.78E-02
117	-1.50E-01	-6.28E-02	-3.69E-02	-1.34E-02	-2.42E-01	-1.29E-01	-5.29E-02	-3.22E-03	-8.73E-03	-1.46E-02	-4.99E-02	-1.59E-01	-6.76E-02	-1.41E-02	-6.78E-02
118	-1.50E-01	-6.28E-02	-3.69E-02	-1.34E-02	-2.42E-01	-1.29E-01	-5.29E-02	-3.22E-03	-8.73E-03	-1.46E-02	-4.99E-02	-1.59E-01	-6.76E-02	-1.41E-02	-6.78E-02
119	-1.50E-01	-6.27E-02	-3.69E-02	-1.34E-02	-2.42E-01	-1.29E-01	-5.29E-02	-3.22E-03	-8.73E-03	-1.46E-02	-4.99E-02	-1.59E-01	-6.76E-02	-1.41E-02	-6.78E-02
120	-1.50E-01	-6.27E-02	-3.69E-02	-1.34E-02	-2.42E-01	-1.29E-01	-5.29E-02	-3.21E-03	-8.73E-03	-1.46E-02	-4.99E-02	-1.59E-01	-6.76E-02	-1.41E-02	-6.78E-02

Appendix C - Results of dry and undrained analysis using the ”treated mesh” properties

number	14	14		17	17
	dry	undrained		dry	undrained
model	RS_OB500_P29_E3_C3	RS_OB500_P29_E3_C3_sat		RS_OB1000_P29_E3_C3	RS_OB1000_P29_E3_C3_sat
pl. Radius [m]	6.5	8.3		8.9	13
pl. Rad._analytical [m]	6.6	-		8.8	-
shear strength c' [Mpa]	3	3		3	3
friction angle	29	29		29	29
Young's Modulus [Mpa]	3000	3000		3000	3000
UCS [Mpa]	10.19	10.19		10.19	10.19
Overburden [m]	500	500		1000	1000
Sigma 0 effective [Mpa]	12.5	7.5		25	15
UCS / Sigma 0,eff	0.815	1.358		0.407	0.679
tunnelradius [m]	5	5		5	5
rpl/rt	1.3	1.66		1.78	2.6
u0/umax	0.240	0.340		0.260	0.367
Station	z_disp	z_disp		z_disp	z_disp
1	-5.86E-06	-7.65E-06		-1.21E-05	-1.92E-05
2	-6.71E-06	-9.09E-06		-1.37E-05	-2.23E-05
3	-7.20E-06	-9.68E-06		-1.48E-05	-2.32E-05
4	-7.42E-06	-9.87E-06		-1.52E-05	-2.24E-05
5	-7.55E-06	-9.87E-06		-1.52E-05	-2.10E-05
6	-7.67E-06	-9.75E-06		-1.51E-05	-1.90E-05
7	-7.76E-06	-9.55E-06		-1.49E-05	-1.69E-05
8	-7.93E-06	-9.35E-06		-1.48E-05	-1.46E-05
9	-8.13E-06	-9.11E-06		-1.47E-05	-1.26E-05
10	-8.36E-06	-8.97E-06		-1.48E-05	-1.06E-05
11	-8.67E-06	-8.85E-06		-1.50E-05	-8.70E-06
12	-9.06E-06	-8.84E-06		-1.53E-05	-6.88E-06
13	-9.56E-06	-8.87E-06		-1.59E-05	-5.27E-06
14	-1.01E-05	-9.04E-06		-1.66E-05	-3.91E-06
15	-1.08E-05	-9.32E-06		-1.77E-05	-2.75E-06
16	-1.17E-05	-9.73E-06		-1.91E-05	-1.75E-06
17	-1.26E-05	-1.03E-05		-2.07E-05	-1.13E-06
18	-1.38E-05	-1.10E-05		-2.28E-05	-7.70E-07
19	-1.51E-05	-1.19E-05		-2.53E-05	-8.00E-07
20	-1.67E-05	-1.30E-05		-2.82E-05	-1.34E-06
21	-1.84E-05	-1.44E-05		-3.17E-05	-2.32E-06
22	-2.04E-05	-1.60E-05		-3.58E-05	-3.84E-06
23	-2.27E-05	-1.79E-05		-4.05E-05	-6.00E-06
24	-2.54E-05	-2.01E-05		-4.60E-05	-8.91E-06
25	-2.83E-05	-2.28E-05		-5.24E-05	-1.25E-05
26	-3.17E-05	-2.59E-05		-5.98E-05	-1.73E-05
27	-3.56E-05	-2.95E-05		-6.83E-05	-2.29E-05
28	-4.01E-05	-3.37E-05		-7.81E-05	-2.99E-05
29	-4.52E-05	-3.85E-05		-8.94E-05	-3.85E-05
30	-5.10E-05	-4.41E-05		-1.02E-04	-4.85E-05
31	-5.76E-05	-5.06E-05		-1.17E-04	-6.08E-05
32	-6.52E-05	-5.82E-05		-1.35E-04	-7.55E-05
33	-7.40E-05	-6.70E-05		-1.55E-04	-9.25E-05
34	-8.40E-05	-7.73E-05		-1.78E-04	-1.13E-04
35	-9.56E-05	-8.92E-05		-2.05E-04	-1.37E-04
36	-1.09E-04	-1.03E-04		-2.36E-04	-1.66E-04
37	-1.25E-04	-1.20E-04		-2.72E-04	-2.00E-04
38	-1.43E-04	-1.39E-04		-3.15E-04	-2.42E-04
39	-1.64E-04	-1.61E-04		-3.64E-04	-2.90E-04
40	-1.89E-04	-1.88E-04		-4.23E-04	-3.49E-04
41	-2.18E-04	-2.20E-04		-4.93E-04	-4.20E-04
42	-2.53E-04	-2.58E-04		-5.75E-04	-5.05E-04
43	-2.94E-04	-3.04E-04		-6.74E-04	-6.09E-04
44	-3.44E-04	-3.59E-04		-7.94E-04	-7.37E-04
45	-4.03E-04	-4.26E-04		-9.39E-04	-8.94E-04
46	-4.75E-04	-5.08E-04		-1.12E-03	-1.09E-03
47	-5.63E-04	-6.09E-04		-1.33E-03	-1.33E-03
48	-6.72E-04	-7.34E-04		-1.60E-03	-1.64E-03
49	-8.05E-04	-8.88E-04		-1.94E-03	-2.03E-03
50	-9.69E-04	-1.08E-03		-2.37E-03	-2.53E-03
51	-1.17E-03	-1.32E-03		-2.91E-03	-3.18E-03
52	-1.43E-03	-1.62E-03		-3.61E-03	-4.02E-03
53	-1.74E-03	-2.00E-03		-4.51E-03	-5.12E-03
54	-2.13E-03	-2.46E-03		-5.69E-03	-6.56E-03
55	-2.61E-03	-3.03E-03		-7.24E-03	-8.48E-03
56	-3.17E-03	-3.71E-03		-9.27E-03	-1.10E-02
57	-3.81E-03	-4.52E-03		-1.19E-02	-1.45E-02
58	-4.52E-03	-5.51E-03		-1.54E-02	-1.88E-02
59	-5.35E-03	-7.01E-03		-2.03E-02	-2.41E-02
60	-7.74E-03	-1.00E-02		-2.69E-02	-3.26E-02
61	-1.62E-02	-1.68E-02		-4.74E-02	-4.66E-02
62	-2.01E-02	-1.99E-02		-5.92E-02	-5.53E-02
63	-2.28E-02	-2.19E-02		-6.75E-02	-6.17E-02
64	-2.47E-02	-2.34E-02		-7.38E-02	-6.66E-02
65	-2.62E-02	-2.46E-02		-7.87E-02	-7.04E-02
66	-2.73E-02	-2.55E-02		-8.27E-02	-7.36E-02
67	-2.82E-02	-2.62E-02		-8.59E-02	-7.61E-02
68	-2.89E-02	-2.68E-02		-8.86E-02	-7.82E-02
69	-2.94E-02	-2.73E-02		-9.08E-02	-8.00E-02
70	-2.99E-02	-2.77E-02		-9.27E-02	-8.15E-02
71	-3.02E-02	-2.80E-02		-9.42E-02	-8.28E-02
72	-3.05E-02	-2.83E-02		-9.55E-02	-8.39E-02
73	-3.08E-02	-2.86E-02		-9.66E-02	-8.48E-02
74	-3.10E-02	-2.88E-02		-9.75E-02	-8.56E-02
75	-3.12E-02	-2.90E-02		-9.83E-02	-8.63E-02
76	-3.13E-02	-2.91E-02		-9.90E-02	-8.69E-02
77	-3.14E-02	-2.93E-02		-9.96E-02	-8.74E-02
78	-3.16E-02	-2.94E-02		-1.00E-01	-8.78E-02
79	-3.17E-02	-2.95E-02		-1.01E-01	-8.82E-02
80	-3.17E-02	-2.95E-02		-1.01E-01	-8.85E-02
81	-3.18E-02	-2.96E-02		-1.01E-01	-8.87E-02
82	-3.19E-02	-2.96E-02		-1.02E-01	-8.90E-02
83	-3.19E-02	-2.97E-02		-1.02E-01	-8.91E-02
84	-3.20E-02	-2.97E-02		-1.02E-01	-8.93E-02
85	-3.20E-02	-2.98E-02		-1.02E-01	-8.94E-02
86	-3.20E-02	-2.98E-02		-1.02E-01	-8.95E-02
87	-3.21E-02	-2.98E-02		-1.03E-01	-8.96E-02
88	-3.21E-02	-2.98E-02		-1.03E-01	-8.96E-02
89	-3.21E-02	-2.98E-02		-1.03E-01	-8.97E-02
90	-3.21E-02	-2.98E-02		-1.03E-01	-8.97E-02
91	-3.22E-02	-2.98E-02		-1.03E-01	-8.97E-02
92	-3.22E-02	-2.98E-02		-1.03E-01	-8.97E-02
93	-3.22E-02	-2.98E-02		-1.03E-01	-8.97E-02
94	-3.22E-02	-2.98E-02		-1.03E-01	-8.97E-02
95	-3.22E-02	-2.98E-02		-1.03E-01	-8.97E-02
96	-3.22E-02	-2.98E-02		-1.03E-01	-8.97E-02
97	-3.22E-02	-2.98E-02		-1.03E-01	-8.96E-02
98	-3.22E-02	-2.98E-02		-1.03E-01	-8.96E-02
99	-3.22E-02	-2.98E-02		-1.03E-01	-8.96E-02
100	-3.22E-02	-2.98E-02		-1.03E-01	-8.96E-02
101	-3.22E-02	-2.97E-02		-1.03E-01	-8.95E-02
102	-3.22E-02	-2.97E-02		-1.03E-01	-8.95E-02
103	-3.22E-02	-2.97E-02		-1.03E-01	-8.95E-02
104	-3.22E-02	-2.97E-02		-1.03E-01	-8.94E-02
105	-3.22E-02	-2.97E-02		-1.03E-01	-8.94E-02
106	-3.22E-02	-2.97E-02		-1.03E-01	-8.94E-02
107	-3.22E-02	-2.97E-02		-1.03E-01	-8.93E-02
108	-3.22E-02	-2.96E-02		-1.03E-01	-8.93E-02
109	-3.22E-02	-2.96E-02		-1.03E-01	-8.92E-02
110	-3.22E-02	-2.96E-02		-1.03E-01	-8.92E-02
111	-3.22E-02	-2.96E-02		-1.03E-01	-8.92E-02
112	-3.22E-02	-2.96E-02		-1.03E-01	-8.92E-02
113	-3.22E-02	-2.96E-02		-1.03E-01	-8.91E-02
114	-3.22E-02	-2.96E-02		-1.03E-01	-8.91E-02
115	-3.22E-02	-2.95E-02		-1.03E-01	-8.91E-02
116	-3.22E-02	-2.95E-02		-1.03E-01	-8.90E-02
117	-3.22E-02	-2.95E-02		-1.03E-01	-8.90E-02
118	-3.22E-02	-2.95E-02		-1.03E-01	-8.89E-02
119	-3.22E-02	-2.95E-02		-1.03E-01	-8.89E-02
120	-3.22E-02	-2.94E-02		-1.03E-01	-8.88E-02